N73 25140

NASA CR-112324

CO_2 REMOVAL BY SOLID AMINE SORBENTS:

1. Experimental Studies of Amine Resin IR-45 With Regard to Spacecraft Applications

2. Computer Program for Predicting the Transient Performance of Solid Amine Sorbent Systems

R.M. Wright
K.C. Hwang

73-9091

June 1, 1973

Prepared Under

Contract No. NAS 1-8559

by

AIRESEARCH MANUFACTURING COMPANY
Los Angeles, California

for

National Aeronautics and Space Administration

Langley Research Center

Hampton, Virginia

NASA CR-112324

CO_2 REMOVAL BY SOLID AMINE SORBENTS:

1. Experimental Studies of Amine Resin IR-45 With Regard to Spacecraft Applications

2. Computer Program for Predicting the Transient Performance of Solid Amine Sorbent Systems

R.M. Wright
K.C. Hwang

73-9091

June 1, 1973

Prepared Under

Contract No. NAS 1-8559

by

AIRESEARCH MANUFACTURING COMPANY
Los Angeles, California

for

National Aeronautics and Space Administration

Langley Research Center

Hampton, Virginia

FOREWORD

This report presents the results of experimental studies conducted by the AiResearch Manufacturing Company on the sorbent behavior of solid amine resin IR-45 with regard to potential use in regenerative CO_2-removal systems for manned spacecraft. The experiments included the measurement of equilibrium sorption capacity of IR-45 for water and for CO_2. The dynamic mass-transfer behavior of IR-45 beds was studied under conditions representative of those expected in a manned spacecraft.

The experiments reported here were conducted as part of Task 3.1 - Basic Chemisorption Data, under NASA Langley Research Center Contract NAS1-8559, "Development of Regenerative CO_2-Removal-System Design Techniques." Mr. Rex B. Martin was technical monitor of the contract. At AiResearch, Mr. Calvin Browning was program manager; Dr. Roger Wright was principal investigator.

Under Task 3.2 - Analytical Model Development, of this contract, a digital computer program was written for the transient performance prediction of CO_2-removal systems comprised of solid amine beds. This program is documented in Appendix A of this document. Dr. K. C. Hwang was the author of this program.

Other tasks of this contract, which concerned regenerative CO_2-removal systems employing inorganic molecular-sieve sorbents, are documented in the following two reports: "A Transient Performance Method for CO_2 Removal with Regenerable Adsorbents" NASA CR-112098 (Reference 1) and "Development of Design Information for Molecular Sieve Type Regenerative CO_2-Removal Systems", AiResearch Report 72-8417 (Reference 2), which will be a low-numbered NASA CR-document.

CONTENTS

Section		Page
1	INTRODUCTION	1-1
	Sorbents for CO_2 Removal	1-1
	Lithium Hydroxide	1-1
	Molecular-Sieves	1-1
	Recent Specifications for CO_2 Level in Spacecraft Cabins	1-2
	Investigation of Other CO_2-Removal Sorbents	1-3
	Characteristics of IR-45 Resin	1-4
2	EQUILIBRIUM DATA	2-1
	Equipment and Procedures	2-1
	Observations of the Mass-Transfer Rate with IR-45 from Equilibrium Experiments	2-3
	Sorbent Pretreatment Procedures and Sorbent Degradation	2-4
	Equilibruim Absorption Capacity of IR-45 for Water	2-9
	Equilibrium Absorption Capacity of IR-45 for CO_2 with Various Preloads of Water	2-11
3	DYNAMIC MASS-TRANSFER EXPERIMENTS	3-1
	Test Objectives and Approach	3-1
	Experimental Equipment	3-1
	Isothermal CO_2 Absorption Breakthrough Tests	3-6
	Adiabatic CO_2 Absorption Breakthrough Tests on Steam-Desorbed IR-45	3-12
	Steam Desorption Procedures	3-12
	Adiabatic CO_2 Absorption Breakthrough Following Steam Desorptions	3-13
4.	SUMMARY AND CONCLUSIONS	4-1
	APPENDIX A - Computer Program for Predicting the Transient Performance of Solid Sorbents for CO_2 Removal	A-1
	APPENDIX B - AMINE Fortran V Listings	B-1
	REFERENCES	R-1

ILLUSTRATIONS

Figure		Page
1-1	Particle Size Distribution, Air-Dried Rohm and Haas IR-45	1-5
2-1	Equilibrium Test Apparatus	2-2
2-2	Degradation of the Sorbent Capacity of IR-45 for CO_2 after Exposure to Low Pressure Conditions--Mallinckrodt IR-45, 75°F	2-7
2-3	Effect of Vacuum-Bakeout Pretreatment on IR-45--Mallinckrodt IR-45, 75°F	2-8
2-4	Equilibrium Absorption Capacity of IR-45 for Water, 75°F	2-10
2-5	Equilibrium Absorption Capacity of IR-45 for CO_2, Parametric with Water Preload, 75°F Sorbent Temperature	2-12
3-1	Schematic of Dynamic Mass-Transfer Apparatus	3-3
3-2	Test Bed for Isothermal Dynamic Adsorption Tests with IR-45 1/2-in.-Fin Bed	3-4
3-3	Cylindrical Test Bed for Dynamic Absorption with IR-45	3-5
3-4	Isothermal Water Preload on IR-45 in 1/2-in.-Fin Bed Prior to CO_2 Absorption at 6.9 mm Hg P_{CO_2}	3-7
3-5	Isothermal CO_2 Absorption by IR-45 in 1/2-in.-Fin Bed; 6.9 mm Hg P_{CO_2}	3-8
3-6	Isothermal Water Preload on IR-45 in 1/2-in.-Fin Bed Prior to CO_2 Absorption at 2.9 mm Hg P_{CO_2}	3-9
3-7	CO_2 Absorption by IR-45 in 1/2-in.-Fin Bed; 2.9 mm P_{CO_2}	3-10
3-8	CO_2 Breakthrough on Steam Desorbed IR-45, 0.43 lb/hr Flow Rate	3-14
3-9	CO_2 Breakthrough on Steam Desorbed IR-45, 0.80 lb/hr Flow Rate	3-15

ILLUSTRATIONS (Continued)

Figure		Page
3-10	CO_2 Breakthrough on Desorbed IR-45, 1.60 lb/hr Flow Rate	3-16
3-11	CO_2 Breakthrough on Steam Desorbed IR-45, 3.2 lb/hr Flow Rate	3-17
3-12	CO_2 Breakthrough on Steam Desorbed IR-45, Bed Cooling Before Absorption	3-18

TABLES

Table		Page
2-1	Test Sequence on the Second Sample of IR-45 in the Equilibrium Apparatus	2-6

SECTION 1

INTRODUCTION

SORBENTS FOR CO_2 REMOVAL

Lithium Hydroxide

Until recently, the task of CO_2 removal from manned spacecraft atmospheres was accomplished by using lithium hydroxide (LiOH); Mercury, Gemini, Apollo command module, lunar module, and PLSS all employed lithium hydroxide. The reaction of CO_2 and lithium hydroxide occurs readily and is not reversible. When properly sized, a lithium hydroxide system can limit the levels of carbon dioxide to a low level (under 3 mm Hg P_{CO2}). However, since the reaction is not reversible, such systems are not regenerative, and the proper amount of lithium hydroxide as an expendable must be carried on board the spacecraft.

For long duration missions, the amount of lithium hydroxide that must be carried can become very large. This is the obvious drawback to LiOH. For a number of years there have been concentrated efforts to develop regenerative CO_2-removal systems which would give a lower weight penalty to the vehicle. An additional incentive for the development of regenerative systems is the possible reclamation of oxygen carried in the separated CO_2 product.

Molecular-Sieves

One of the first concepts of a regenerative CO_2-removal system to receive considerable attention involved the use of molecular-sieve adsorbents. Molecular sieves are inorganic synthetic materials which are classed with the naturally-occurring zeolites. Molecular sieves have high affinity for polar molecules (including CO_2) and yet with lowering of pressure or increase in temperature they can be made to desorb the previously adsorbed gases. Since they are inorganic, they are highly stable, both chemically and geometrically. In many diverse adsorption applications, millions of pounds of these materials are in daily use in the chemical industry. The most significant characteristic of molecular sieves is their extreme affinity for water. This affinity is so pronounced that for even very low concentrations of water (for example, 10 parts per million) passing through a molecular sieve bed, eventually the bed will reach a point where it adsorbs only water and has a no capacity for any other sorbate. Even previously adsorbed gases are driven off and replaced by water. The bed is said to be poisoned by water when this occurs. In practice, this characteristic is overcome by providing a drier bed upstream of the CO_2-removal molecular-sieve bed. The drier sorbate can be either silica gel or one of the molecular sieves.

Molecular sieve systems have been built for a number of applications. For the Apollo Applications Program, AiResearch provided a prototype system.

The Air Force Manned Orbiting Laboratory was to have had a molecular-sieve CO_2-removal system. At present, AiResearch is supplying the Regenerative Carbon Dioxide Removal System (RCRS) for the Skylab vehicle; this system uses molecular sieve types 5A and 13X. Also under development at AiResearch is the application of adsorbent type system for Space Shuttle (Dessicant Humidity Control System) in which both water vapor and CO_2 levels would be controlled with molecular sieve and silica gel sorbents.

The Skylab RCRS uses molecular sieve type 5A as a CO_2 sorbent and molecular sieve 13X as the drier sorbent. The system is a two-bed system, designed for three crew members, with each bed containing 7.5 lb of molecular sieve 13X and 9.9 lb of molecular sieve 5A. The flow rate is 15 lb per hour; cycle time is 30 minutes. The system specification requires the system to provide continuous CO_2 removal for 28 days. After this time interval, electric heaters can be employed to bake out adsorbed water. In effect, the specification requires a design that will function to specified conditions in the face of the poisoning effect of water for a period of 28 days. In actuality, the RCRS has demonstrated proper performance for over 120 days. This demonstrated that it was possible to provide a reliable design in spite of the hydrophyllic-nature of molecular sieves, and that the poisoning effect of water can be provided for with a properly designed predrier. A penalty occurs due to the existence of the predrier bed. This penalty consists of bed weight, power used in overcoming flow resistance of the bed, and the small loss of atmospheric gases absorbed on the drier sorbent. (This latter item is discussed later.)

Recent Specifications for CO_2 Level in Spacecraft Cabins

For the original US manned-spacecraft missions, the cabin level of CO_2 was set at 7 mm Hg P_{CO_2}. Generally, at normal metabolic loads, the LiOH systems are able to maintain levels well below this; approximately 3 to 4 mm Hg. Early molecular-sieve systems were designed to meet the 7 mm Hg P_{CO_2} level; this was the case with the AAP system. More recently, it has become evident that it is physiologically desirable to have the cabin p_{CO_2} as low as possible. Consequently, specifications have been lowered on new systems. For example, the Skylab RCRS was originally designed to maintain 7 mm Hg p_{CO_2}; it was later modified to achieve 4 to 5 mm Hg. The Space Shuttle Desiccant Humidity Control System has a nominal 5 mm Hg specification, with a desired cabin level of 3 mm Hg.

The requirement for lower CO_2 levels has a pronounced effect on the design of CO_2-removal systems. First, since the cabin partial pressure is lower, the driving force for mass-transfer is thus lower. In one manner or another, more surface area would be required for the lower cabin levels. Second, for any

sorption process (or a chemical reaction that does not go to completion), the equilibrium sorption capacity for CO_2 depends upon the cabin level. For molecular-sieve type 5A, the equilibrium capacity at 7 mm Hg is about 0.068 lb CO_2 per lb of sorbent at 70°F; at 3 mm Hg the capacity is less than half of this value. Therefore this aspect of lower cabin partial pressure would have to be considered; more sorbent in the beds, or shorter absorption/desorption cycle times, or both, would have to be employed.

The lower cabin CO_2 specifications result in generally larger, heavier beds; and the net penalty to the vehicle becomes greater. With molecular sieves there is another compounding problem. Even though molecular sieves on a relative basis have a much greater capacity for water and CO_2 than for the atmosphere gases of oxygen and nitrogen--thus a separation is possible--they do have a finite capacity to adsorb O_2 and N_2. For example at 500 mm Hg, a typical equilibrium capacity for N_2 is 0.009 lb N_2/lb sorbent. The result of this adsorption is a loss of cabin gases. The total penalty to the vehicle depends upon the particular application. Gas losses can be on the order of several pounds per day. Since the gas loss is proportional to bed size, lower P_{CO_2} levels result in even higher losses of O_2 and N_2.

From the above discussion it is easy to conclude that molecular sieves are not the "ideal" sorbents for spacecraft CO_2-removal systems. It would be desirable to have a sorbent that has more capacity for CO_2, and of course less capacity for O_2 and N_2. Also, it would be desirable that the sorbent would not be affected by water, so that drier beds or preconditioning apparatus would not be needed.

Investigation of Other CO_2-Removal Sorbents

With regard to regenerable CO_2 sorbents, the alkano-amines (monoethanol amine $NH_2C_2H_4OH$ and diethanol amine $NH(C_2H_4OH)_2$) are in heavy use in the chemical process industry and in U.S. submarines. These amines possess high capacity for CO_2 while having low capacity for O_2 and N_2. They are also easily regenerated; that is, upon heating they easily give up the adsorbed CO_2; and since they are used in water solution, they are not affected by water vapor in the process gas. However, as liquids their use would introduce significant problems of phase contact and phase separation into the design of zero-g spacecraft systems. Thus, the use of the proven alkanoamines cannot be strongly supported for an immediate development leading to a near-term application in spacecraft.

The choice of a CO_2 sorbent for space systems is not clear cut. There have been a number of investigations by several organizations to find or produce a better CO_2-removal sorbent. One such study, under contract to NASA Langley Research Center (Reference 3), considered a number of solid materials which included amine groups in their molecular structure. One particular

material, an aminated ion exchange resin, Amberlite IR-45, emerged as being superior to other sorbents tested in the study, and as a result various exploratory tests were conducted on the material. Equilibrium capacity of the resin for CO_2 was indicated to be as high as 5 to 10 percent.

In the summer of 1970, a demonstration CO_2-removal system employing amine resin IR-45 was produced and used in a 90-day manned chamber test (References 4 and 5). In 1971, Tasks 3.1 and 3.2 were added to contract NAS1-8559 with AiResearch for the purpose of (1) producing basic equilibrium and dynamic data for IR-45, which were not available from the previous contracts, and 2) to produce a computer program for the design and transient performance prediction of systems which employ solid absorbents such as aminated resins.

This report describes the tests and results of Task 3.1. The equilibrium and dynamic data presented in this report were produced on basically the same test facilities that were used to produce similar molecular-sieve data in Reference 2.

CHARACTERISTICS OF IR-45 RESIN

Amberlite IR-45 is a commercial, weak-base type ion exchange resin manufactured by Rohm and Haas. It is a chlormethylated polystyrenedivinyl benzene copolymer aminated with diethylenetriamine.

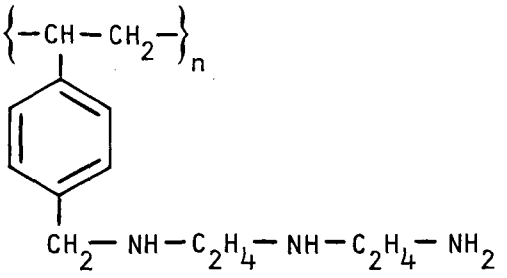

It is produced in a spherical bead form of approximately 20 to 50 mesh. It is light yellow in color. According to tests of Reference 3 the material swells considerably with water content: from very dry resin to 45 percent water, the bulk volumetric swelling of a bed of resin beads is about 45 percent. Figure 1-1 presents the particle size distribution obtained from a sample of air dried Rohm and Haas IR-45. According to water equilibrium data presented in the next section, the air-dried material contains approximately 5.5 weight percent water. IR-45 resin is also available in a purified form (reagent grade) from Mallinckrodt Chemical Co. The cost of this material is about six times that of the bulk material obtained from Rohm and Haas.

According to Reference 3, both the CO_2 absorption capacity and the rate of absorption are dependent upon water being present; although at very high water contents, CO_2 absorption starts to decline with increasing water loading. Early tests of the previous study indicated vacuum regeneration (i.e., vacuum desorption of CO_2) was not practical as too much water was lost, rates were slow, and the sorbent started out the absorption cycle far too dry for

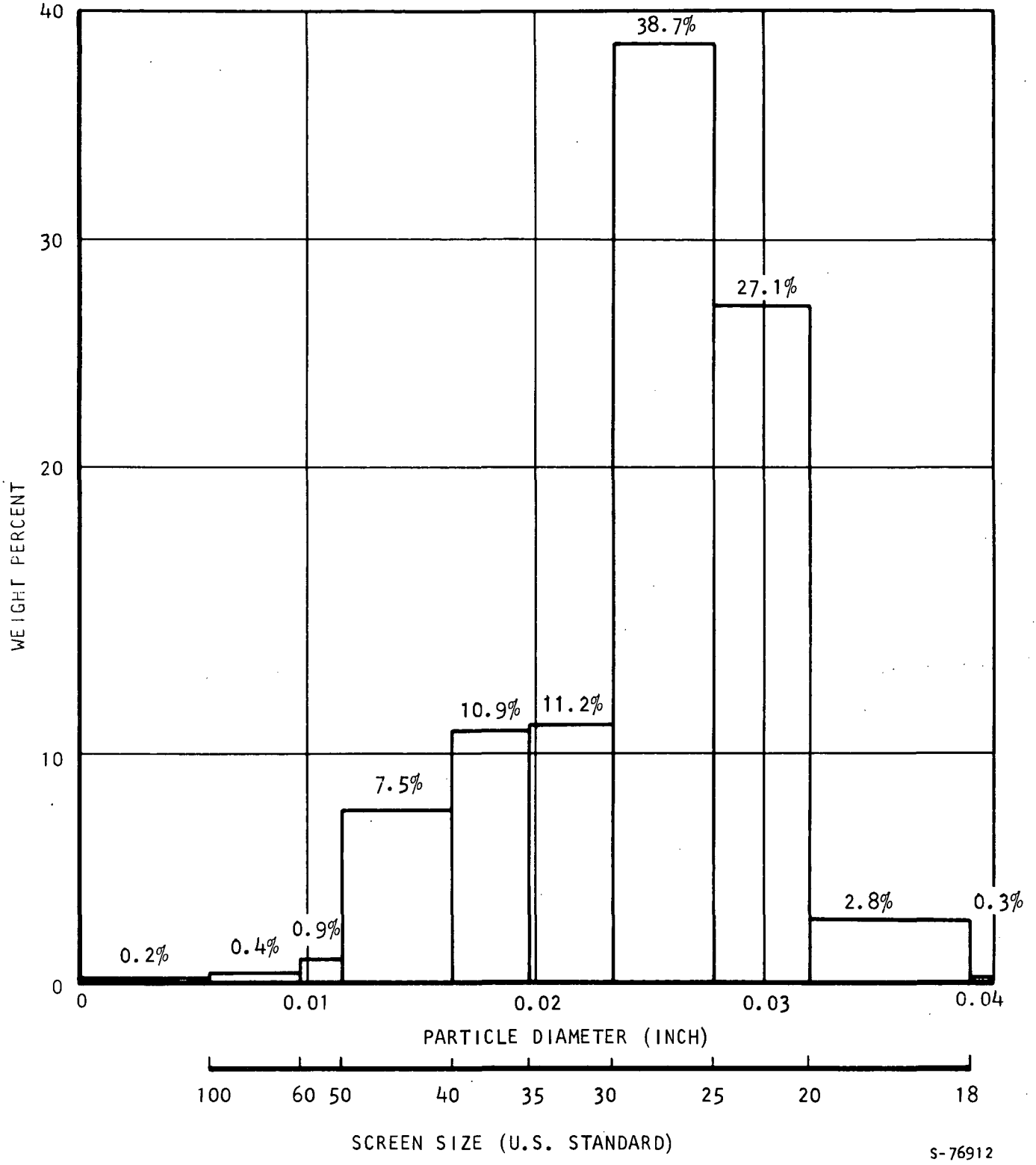

Figure 1-1. Particle Size Distribution, Air-Dried Rohm and Haas IR-45

efficient CO_2 absorption. Thus, steam desorption was considered to be the preferred method of desorption. This is especially so if CO_2 collection is desired for oxygen reclamation. In this arrangement the CO_2 can be delivered at relatively high pressure without pumps. Steam desorption also leaves the bed in the reasonably favorable condition for absorption; although the most favorable conditions for CO_2 absorption do not occur until some cooling and and drying of the bed takes place.

Because of the preference for steam desorption of the IR-45, it was desirable in this study to provide equilibrium and mass-transfer data for a wide range of water loadings (approaching saturated resin) and up to moderately high temperatures (up to about 212°F).

SECTION 2

EQUILIBRIUM DATA

EQUIPMENT AND PROCEDURES

The apparatus used to obtain water and CO_2 absorption equilibria on IR-45 was the same as that used for molecular-sieve equilibria obtained in Task 1 of the contract. Figure 2-1 presents a photograph of the apparatus. A full description of the equipment is contained in Reference 2. The heart of the apparatus is a Cahn Model RG electrobalance that is situated entirely within the gas-tight glass envelope of the apparatus and is capable of very accurate weighings regardless of the pressure within the enclosed volume. There are two weighing pans suspended from opposite ends of the balance beam of the Cahn electrobalance. One weigh pan (the sample pan) contains the sorbent particles which are to be tested; about 65 mg of sorbent is normally used. The other weigh pan (the reference pan) contains precision weights which are used to initially zero the output of the device. Thereafter, the difference between sorbent weight and reference weight is automatically readout on a strip chart recorder adjacent to the apparatus.

The apparatus is setup with appropriate manifolding to allow the introduction of one or more sorbate gases into the test volume. Also, with the aid of vacuum pumps, gases can be withdrawn from the test volume. Pressure in the apparatus is measured directly with a MKS Baratron pressure indicator.

The basic procedure in producing equilibrium data is as follows. First the test sorbent undergoes some sort of a vacuum bakeout operation to remove sorbate gases down to a low, reproducible level. The sorbent in this vacuum-bakeout condition is considered to have zero sorbate loading; the weight reading upon cooling to the desired temperature is used to obtain the dry sorbent weight. Then the sorbate gas is introduced into the electrobalance chamber. The pressure is adjusted to the desired value, and held there as well as possible until no further changes are noticed in the sorbent weight. Temperature of the sorbent is held constant during this time by means of a jacket around the glass tube surrounding the sample weigh pan. Readings of pressure, temperature, and weight are taken. From these data an equilibrium loading value in terms of mass of sorbate per unit mass of dry sorbent is obtained. Conditions can then be adjusted; sorbate pressure can be increased or reduced, or another sorbate gas introduced.

Two equipment modifications were made specifically for tests performed with IR-45. The first modification involved enclosing the entire apparatus (transparent acrylic plastic was used) and installing heaters within the enclosure. This was done to prohibit condensation within the test volume by insuring that all parts of the apparatus would be above the dewpoint of the contained water vapor. Previously, with molecular sieves, the maximum dew points for which tests were made were no more than would be obtained in a spacecraft cabin. In almost all cases, the test conditions involved relative humidities below 80 percent and dewpoints were always less than the laboratory room temperature to which the apparatus was exposed. With IR-45, since the material would be steam desorbed in an actual system, testing at high sorbent temperatures and high relative humidities (approaching saturation) is desired. This leads to dewpoints within the apparatus which are above the room ambient

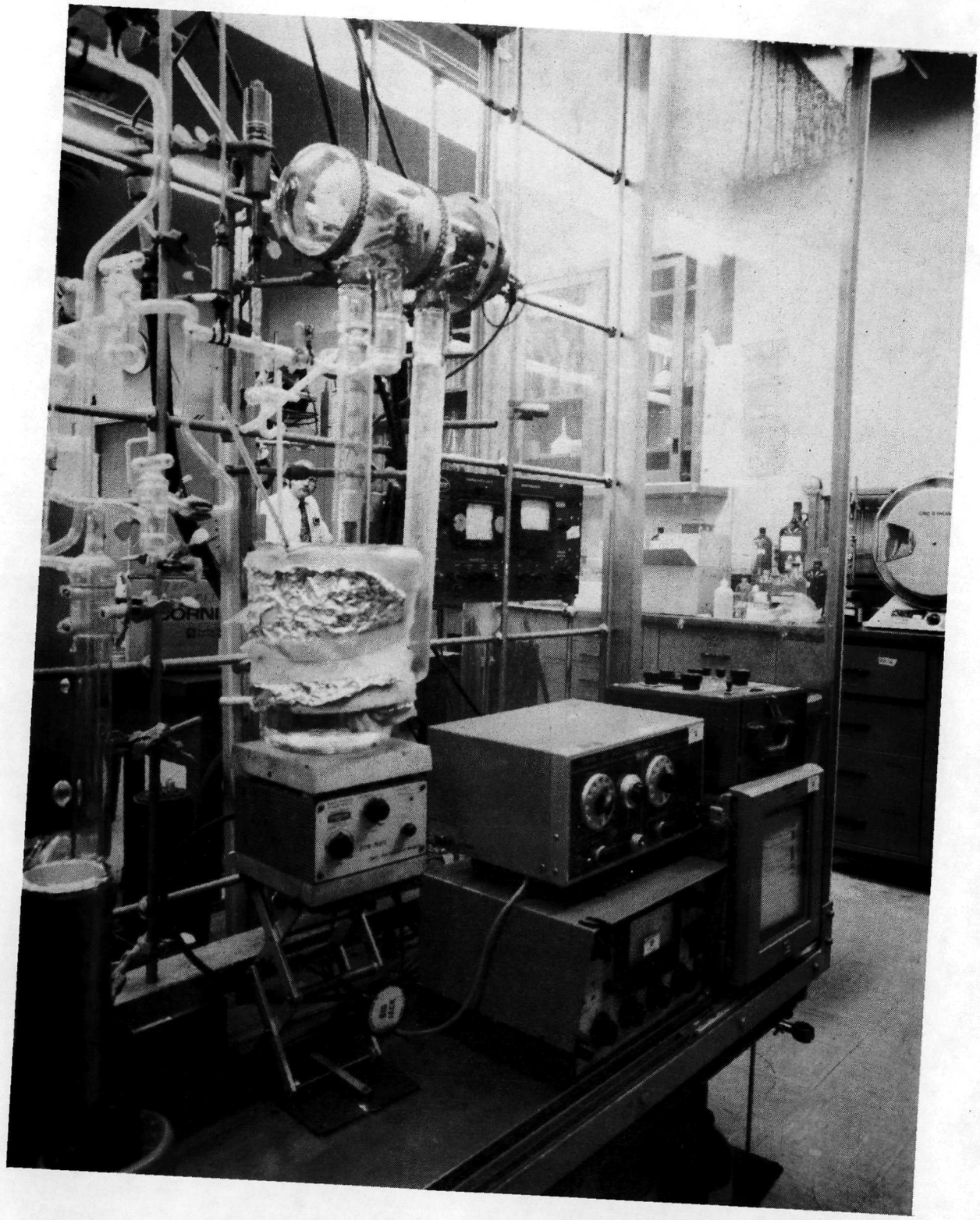

F-17661

Figure 2-1. Equilibrium Test Apparatus

temperature. Since condensation within the apparatus would invalidate all results and must therefore be avoided, it was necessary to provide a means to heat the apparatus enclosure.

The second equipment modification was the installation of an automatic temperature control system for the sorbent sample. A Rosemount Engineering Co. bath was used for this application. Previously, all molecular-sieve equilibrium data was obtained with simple, manually-regulated baths for sample temperature control. The need for the automatic temperature control system is discussed in the following paragraph. The Rosemount device obtains temperature control by modulating the output of electric heaters immersed in the bath. For bath temperatures at or below room temperature, a cold sink must be supplied by the user. The cold sink is usually ice, or for lower temperatures, dry ice in an organic solvent such as acetone. Normally the ice is supplied to a small chamber which contains the temperature-controlled liquid. Normally only about a pound of ice can be placed in the chamber; this charge of ice may last one or two hours. In order to provide overnight, unattended operation, a special cooling arrangement was devised. In this arrangement the cold sink for the temperature-controlled bath was provided by cooling coils immersed directly in the bath. Cold water was circulated through these coils and then through a set of coils immersed in an external 75-liter Dewar filled with crushed ice. This arrangement allowed temperature control within about $\pm 0.3^{o}F$ for at least a 16-hour period.

OBSERVATIONS OF THE MASS-TRANSFER RATE WITH IR-45 FROM EQUILIBRIUM EXPERIMENTS

From the general behavior of the equilibrium apparatus during the period when conditions are being changed and stabilized, it is possible to obtain a relative judgment of the mass-transfer rate of a sorbent for a particular sorbate. This judgment primarily relates to the internal diffusivity of the sorbent particles. From the equilibrium tests with IR-45 with either water or CO_2, it was quite clear that the mass-transfer rates with IR-45 were much slower than had been observed with any of the molecular-sieve materials previously tested. It was estimated that the IR-45 rates were 10 times slower. This slowness was not expected, and it had a tremendous impact on the experimental program. As a result, much less data were taken than had been expected.

Originally, it was expected that equilibrium isotherms would be obtained much faster than with molecular sieves. The background information upon which this expectation was based are described as follows. First, it should be noted that IR-45/CO_2 equilibria are widely variant with water content. Thus, the goal of this task was to produce CO_2 equilibria parametric with water loading. Thus water coabsorbtion is involved in all equilibrium isotherms (except the few CO_2 isotherms for dry sorbent). Similar coadsorption equilibrium data had been obtained earlier with molecular sieves. The important characteristic of molecular sieves is that water loadings in the range of interest--up to 12 percent--are obtained at extremely low water partial pressures. For instance, at $-80^{o}F$ dewpoint corresponding to water partial pressure of 0.006 mm Hg, molecular sieve 5A at $70^{o}F$ has an equilibrium water capacity of 0.085 lb water/lb sorbent (or 8.5 percent). To obtain an 8.5 percent water preload requires that water vapor at 0.006 mm Hg be introduced into the apparatus and held at essentially this pressure until equilibrium is achieved. Even with the hydrophyllic nature of molecular sieves, the rate of adsorption of water is slow. This is because the partial pressure driving force for adsorption is so low (approximately 0.006 mm Hg). Also, even a small amount of adsorption tends to deplete the water supply and alter the partial pressure above the sample. Thus, it is fairly

difficult to control the pressure at this level; it requires continual diligence by the operating technician. Frequently, there are overshoots which must be corrected.

On the other hand, with higher partial pressure (from 0.1 mm Hg and up), adsorption of both CO_2 and water by molecular sieves is very fast. This in part is a direct consequence of the higher partial-pressure driving force. From the data of Reference 3 on IR-45, it was obvious that very low water partial pressures would not be encountered in the new series of tests. This is because significant water loads on IR-45 are not obtained until p_{H_2O} reaches the range of at least 1 mm Hg; at this level it was throught that mass-transfer rates would be fairly rapid. It was not expected that the rates would be as fast as for molecular sieves in this range, but they were expected to be reasonable. Normally about three working days (one shift per day) would be required to obtain one molecular-sieve coadsorption equilibrium isotherm. For IR-45, working at much higher water vapor pressures, it was expected that three working days would also be quite sufficient for each isotherm. As will be discussed below, the final procedure of round-the-clock adsorption testing (with technician attendance for one shift) requires 7 to 8 days, and sometimes more, to complete an IR-45 isotherm.

Because of the unexpected slowness of water and CO_2 uptake by IR-45, the test procedure was significantly altered. With molecular sieves, in a single 8-1/2 hour period it was possible to establish temperature control of the sample, provide the desired partial pressure in the system, and produce a number of equilibrium data points. As a result it was not really necessary to provide precise sample temperature control overnight. Sample temperature could be adjusted early in a morning, and soon thereafter equilibrium would be established. On the other hand, with IR-45, mass-transfer stabilization was so slow that after the initial temperature adjustment in the morning, no more than one data point could be obtained in one shift; and all too frequently stabilization had not occurred at the end of the shift. Generally, the higher the water loading, and thus the higher the CO_2 capacity of the sorbent, the longer the stabilization times would be. As a result with this procedure, as the test sequence progressed encountering higher and higher water loadings, the time required to obtain a data point became longer.

Finally, it was necessary to suspend testing and devise an automatic temperature control system. Even with continuous temperature control it often required two days for stabilization to occur. This long stabilization period was unprecedented with molecular-sieve materials. The sum total of the observation of IR-45 during equilibrium testing indicated a serious deficiency in the internal diffusion mass transfer of the material.

SORBENT PRETREATMENT PROCEDURES AND SORBENT DEGRADATION

IR-45 is a complex chemical material designed to be used in aqueous solutions as an ion exchange resin. As it comes from the manufacturer, it is quite moist and gives off a strong odor of ammonia. Previous testing (References 3 and 5) indicates that a number of organic solvents may be present in the bulk materials. Also, in the study of Reference 3, various pretreatments (washes with water or solvents, heating, etc.) seemed to give slightly different sorbent behavior. It was hoped that in the present study that the problems of pretreatment could be avoided. To this end, it was decided to use the purified,

reagent grade Mallinckrodt IR-45 material for equilibrium tests, and later on to make spot checks with water-washed Rohm and Haas IR-45. Unfortunately, due to the slowness of the CO_2 and water absorption of the material, and due to other problems which are discussed below, only one check isotherm was obtained with the Rohm and Haas material. This check isotherm was for CO_2 on dry resin; it will be discussed later.

With molecular-sieve sorbents, the normal procedure was to obtain all necessary isotherms with one sample in the apparatus. Hundreds of hours of vacuum exposure, with numerous bakeouts at temperatures as high as 600°F, had shown that molecular sieves exhibit virtually no degradation. Thus, keeping one sample in the equilibrium apparatus for all tests on that type material was judged to be proper from the point of view of data quality, and to be the most economical way to produce the data.

For IR-45 testing, it was intended to follow this procedure and run at least several isotherms on one sample. The original pretreatment would be a vacuum bakeout at 150°C (302°F). From previous work of others it seemed that IR-45 could stand this temperature without degradation. The first test sequence involved two water isotherms for the IR-45 at 75°F.; two 150°C vacuum-bakeouts were involved. Then a new sample was placed in the apparatus; this second test sequence is illustrated in Table 2-1. A total of 12 vacuum bakeouts were made on this second sample; total time in the apparatus was 68 days.

The data up through the 3.00-percent-water isotherm looked good. The CO_2 isotherms (dry, 1-percent and 3-percent water) showed significantly increased CO_2 loading with increasing water content. Then, however, after the 8th bakeout, the 5.97-percent-water isotherm was shown to be only slightly above the 3-percent-water isotherm. In fact at low p_{CO_2} (0.5 mm Hg) one data point was below the 3-percent isotherm. Later, the 12.71-percent-water isotherm was seen to have no significant difference in CO_2 loading from the 5.97-percent isotherm. These results were contrary to that which had been expected, and that which had been indicated by the tests of Reference 3. At this point it was suspected that the sample had degraded. Therefore 6- and 3-percent-water isotherms were repeated. Then a new sample was loaded into the apparatus and, after just one bakeout, a new 6-percent isotherm was taken. It was significantly higher than other 6-percent isotherms.

Figure 2-2 shows data from the above tests on the degradation effect of prolonged exposure to the low pressure in the equilibrium apparatus (the total pressure is just the sum of the CO_2 and water partial pressures) and to a number of vacuum bakeouts at 150°C. It was concluded that such prolonged exposure to low pressure was detrimental to the sorbent capacity of IR-45. Therefore, it was decided that only one isotherm would be obtained on a sample. Also, each new sample would be subjected to only one vacuum bakeout. However, the question arose as to whether the 150°C bakeout temperature itself was detrimental. Therefore, various vacuum-bakeout temperatures were tried on three fresh samples of IR-45.

Figure 2-3 shows the results of the tests with various vacuum-bakeout temperatures. The black, filled-in data points are for 150°C bakeouts; the open data points are for 100°C and room-temperature vacuum bakeouts. These data show appreciable scatter. Some of the scatter is considered to be due to experimental equipment difficulties. From observations of the numerous

TABLE 2-1

TEST SEQUENCE ON THE SECOND SAMPLE OF IR-45 IN THE EQUILIBRIUM APPARATUS

Pretreatment		Equilibrium Isotherm at 75°F	
Bakeout No.	Bakeout Temperature (°C)	Water Loading (%)	Comment
1	150	0 to 11.8	Water Isotherm--First isotherm on this sample; third total water isotherm.
2	150	0	CO_2 Isotherm on dry sorbent
3	150 Partial Bakeout	0	CO_2 Isotherm on dry sorbent--recheck
4	150	0	2nd CO_2 Isotherm on dry sorbent
5	150 Partial Bakeout	0	2nd CO_2 Isotherm on dry sorbent--recheck
6	150	1.16	CO_2 Isotherm with 1% water preload
7	150	3.00	CO_2 Isotherm with 3% water preload
8	150	5.98	CO_2 Isotherm with 6% water preload
9	150	---	Test Interrupted
10	150	12.71	CO_2 Isotherm with 12% water preload
11	150	6.21	Rerun of CO_2 Isotherm with 6% water preload
12	150	2.97	Rerun of CO_2 Isotherm with 3% water preload

Total Duration in Equilibrium Apparatus: 68 Days

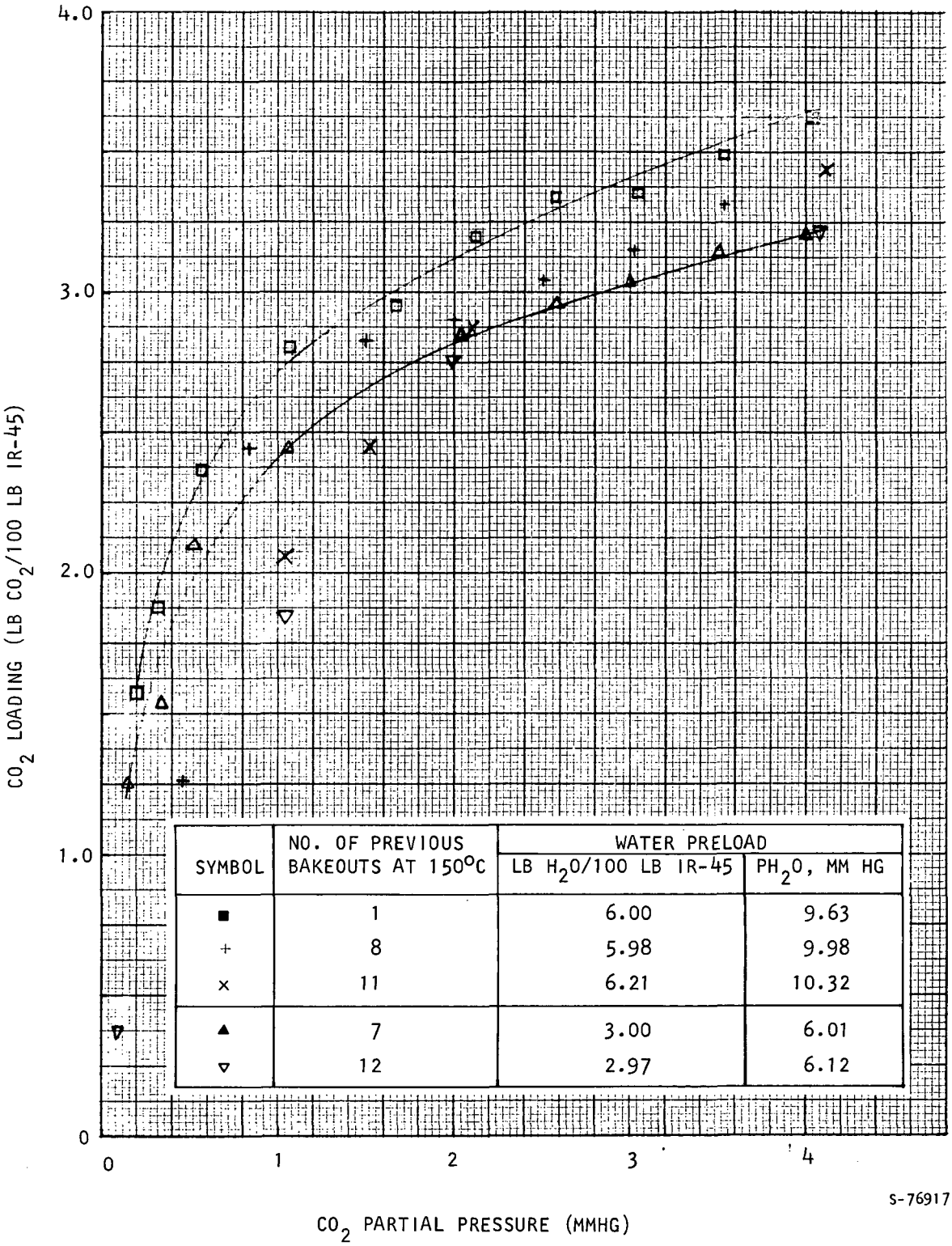

SYMBOL	NO. OF PREVIOUS BAKEOUTS AT 150°C	WATER PRELOAD	
		LB H_2O/100 LB IR-45	PH_2O, MM HG
■	1	6.00	9.63
+	8	5.98	9.98
×	11	6.21	10.32
▲	7	3.00	6.01
▽	12	2.97	6.12

Figure 2-2. Degradation of the Sorbent Capacity of IR-45 for CO_2 after Exposure to Low Pressure Conditions -- Mallinckrodt IR-45, 75°F.

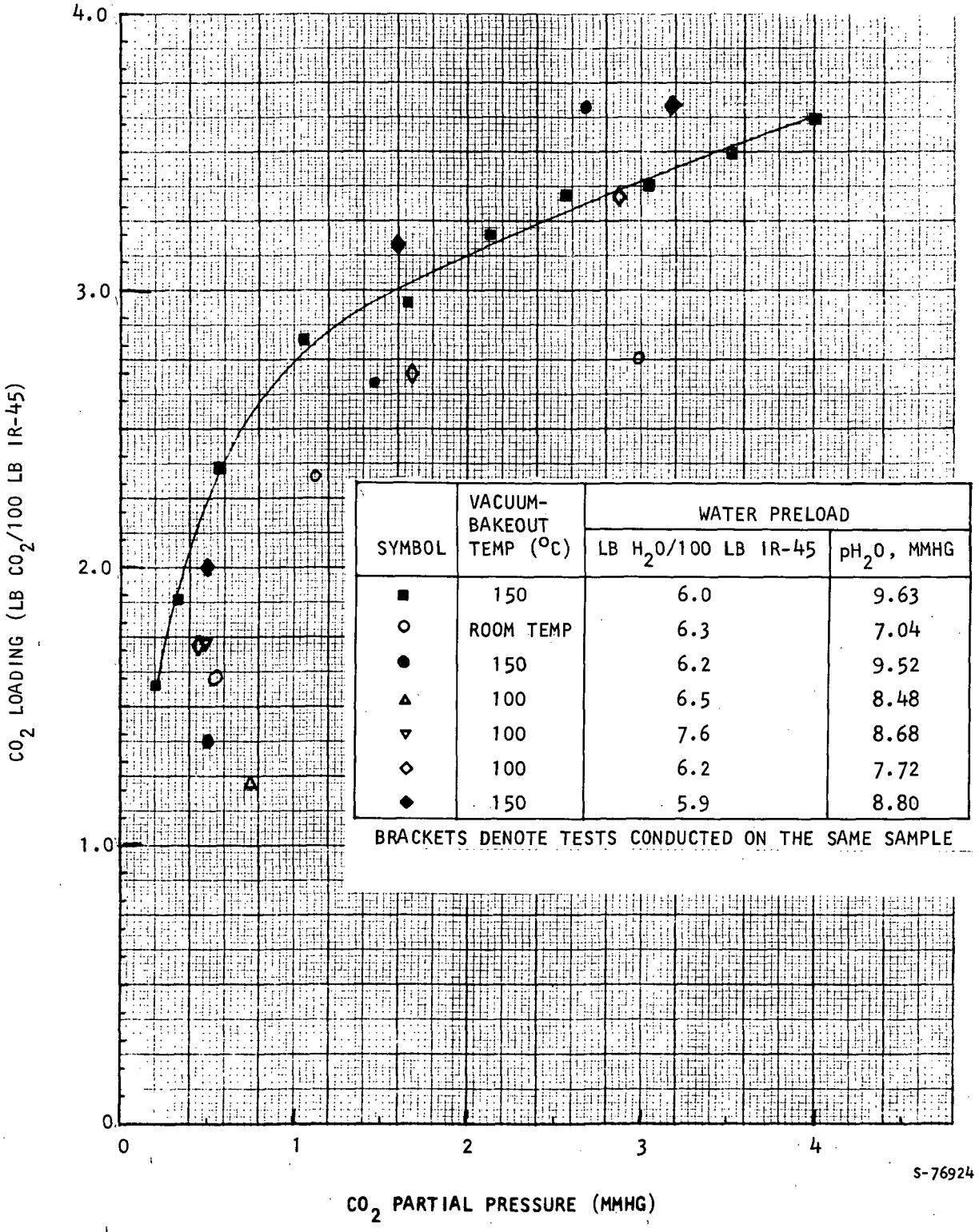

SYMBOL	VACUUM-BAKEOUT TEMP (°C)	WATER PRELOAD	
		LB H_2O/100 LB IR-45	pH_2O, MMHG
■	150	6.0	9.63
○	ROOM TEMP	6.3	7.04
●	150	6.2	9.52
▲	100	6.5	8.48
▽	100	7.6	8.68
◇	100	6.2	7.72
◆	150	5.9	8.80

BRACKETS DENOTE TESTS CONDUCTED ON THE SAME SAMPLE

Figure 2-3. Effect of Vacuum-Bakeout Pretreatment on IR-45 -- Mallinckrodt IR-45, 75°F.

tests with IR-45, it is considered that some of the scatter is inherent with the material itself. In spite of the scatter some general conclusions about bakeout temperature can be drawn from the figure. Generally, in comparison to lower bakeout temperatures, the 150°C bakeout pretreatment somewhat enhances CO_2 absorption, but slightly hinders water absorption. The data from the last sample, denoted by diamond-shaped data points, indicates that even after some vacuum exposure, a single 150°C vacuum bakeout is not harmful to CO_2 absorption, and seems to enhance it. It was judged that previous data for 150°C bakeouts was not invalid because of the level of the bakeout temperature.

Essentially all of the data presented in this report is for vacuum bakeouts of 150°C. For dynamic breakthrough tests which used Rohm and Haas resin, the material was water washed until ammonia was no longer detected in the wash water. Some of the dynamic absorption tests were preceded by 100°F vacuum bakeouts; others were preceded by steam desorptions.

EQUILIBRIUM ABSORPTION CAPACITY OF IR-45 FOR WATER

Figure 2-4 presents data and the recommended curve for the absorption capacity of IR-45 for water at 75°F sorbent temperature. The figure contains data from several types of tests and for both the purified Mallinckrodt IR-45 and for the bulk-supplied Rohm and Haas resin. The consistency of the various data is reasonably good. Most of the data are those taken in the AiResearch equilibrium apparatus on Mallinckrodt IR-45. Three full isotherms on two different samples were originally obtained. In addition to these isotherms are a number of individual data points which resulted from the water-preloading sequences which preceded CO_2 absorption isotherms.

Four data points seem anomolously high in the range of 12 to 16 mm Hg p_{H_2O}. These data points were for bakeout pretreatments less than 150°C (e.g. 100°C and room temperature). It is not known why lower temperature bakeouts should promote water absorption, and yet, as mentioned earlier, inhibit CO_2 absorption Possibly some hydrophillic impurity is removed at the higher-temperature vacuum bakeout.

There are two data points at approximately 15.8 mm Hg which are known to be somewhat low. These two data points come from water preloading sequences on Rohm and Haas IR-45 in the dynamic (packed-bed) mass-transfer apparatus. In these tests it was desired to saturate the IR-45 bed with water at 65°F dewpoint (P_{H_2O} = 15.8 mm Hg) by passing a stream of nitrogen and water vapor through the bed. These tests are discussed more fully in the next section. The primary result of these tests was that saturation was not achieved--that is, the water breakthrough was not completed--due to the slowness of absorption. Thus the data points are known to be low; it is estimated that if the breakthroughs were completed, the water loadings would have been 15.3 and 13.9 lb H_2O/100 lb IR-45.

The two data points for Mallinkrodt IR-45 at 15.8 mm Hg p_{H_2O} are considered to be low. It is considered that equilibrium was not fully achieved in the apparatus when the data were taken. With the slowness of absorption as equilibrium is approached, it is difficult to know when to take data and terminate

Symbol	No. of Bakeouts On Sample	Bakeout Temperature (°C)	Comments
●	-	-	MSA Data, Rohm and Haas IR-45 70°F (Ref. 3)
○	1	150	
△	2	150	
□	1	150	
⊕	6	150	
⊗	7	150	
⊜	8	150	
⊙	10	150	
+		150	New Sample for Each Data Point
×		100	New Sample for Each Data Point
∓		Room Temp	New Sample for Each Data Point
*		100	From Incomplete Dynamic Tests, Rohm and Haas IR-45

Mallinckrodt IR-45, 75°F, unless otherwise specified.
Brackets denote all such data taken on one sample

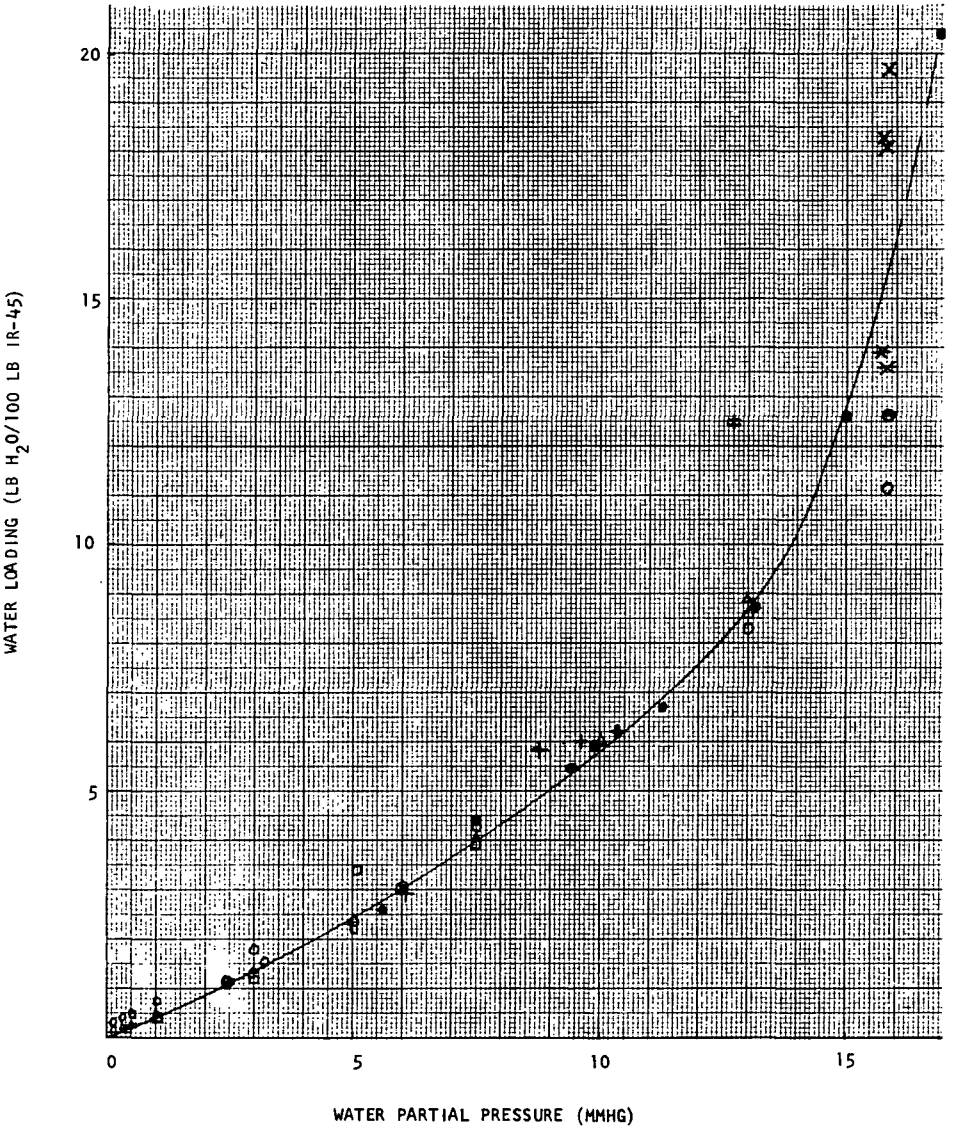

Figure 2-4. Equilibrium Absorption Capacity of IR-45 for Water, 75°F.

testing. Also plotted on Figure 2-4 are data points derived from tests conducted by MSAR. The original presentation of the data in Reference 3 was in terms of relative humidity at room temperature. Room temperature was not specified; to obtain the values given in Figure 2-4, room temperature was assumed to have been 70°F.

EQULIBRIUM ABSORPTION CAPACITY OF IR-45 FOR CO_2 WITH VARIOUS PRELOADS OF WATER

Figure 2-5 presents the equilibrium absorption capacity data taken in this study on IR-45 for CO_2 with various water preloads. Most of the data in the figure were for Mallinckrodt IR-45 with 150°C bakeouts. The 12.5 and 19.7 percent water preloads are for room-temperature and 100°C bakeouts. Judging by the previous tests involving 6-percent water preloads, these latter two sets of data are probably low with respect to that which could be obtained after 150°C bakeouts.

Also shown on the figure are the data points for the one isotherm (dry sorbent) taken on IR-45 resin obtained in bulk from the manufacturer, Rohm and Haas. These data are somewhat lower than the data on Mallinckrodt material. It is not known why the data are lower.

It was originally intended in the study to obtain data for much higher water preloads, and for various sorbent temperatures. Unfortunately, because of the extreme slowness of the absorption of water and CO_2, it was not possible to obtain more data. To the extent that equilibrium testing advanced, no appreciable increase in the rate of CO_2 absorption with increasing water preload was noticed.

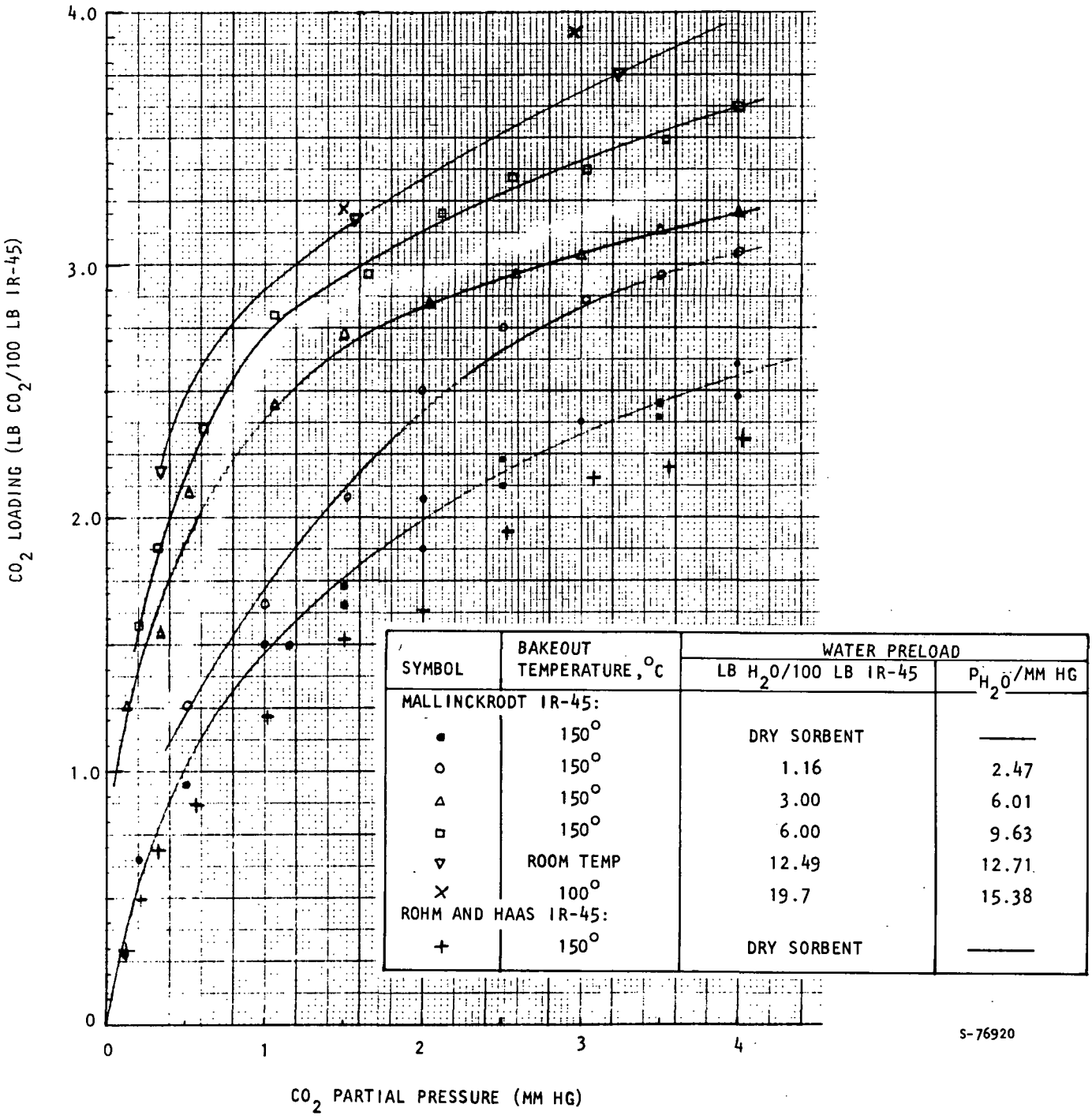

SYMBOL	BAKEOUT TEMPERATURE, °C	WATER PRELOAD LB H_2O/100 LB IR-45	WATER PRELOAD P_{H_2O}/MM HG
MALLINCKRODT IR-45:			
●	150°	DRY SORBENT	———
○	150°	1.16	2.47
△	150°	3.00	6.01
□	150°	6.00	9.63
▽	ROOM TEMP	12.49	12.71
×	100°	19.7	15.38
ROHM AND HAAS IR-45:			
+	150°	DRY SORBENT	———

Figure 2-5. Equilibrium Absorption Capacity of IR-45 for CO_2, Parametric with Water Preload, 75°F Sorbent Temperature.

SECTION 3

DYNAMIC MASS-TRANSFER EXPERIMENTS

TEST OBJECTIVES AND APPROACH

The primary objective of the dynamic mass-transfer experiments was to provide a quantitative evaluation of IR-45 as a fixed-bed sorbent for CO_2 under conditions representative of those that might actually be encountered in a spacecraft CO_2-removal system. Ultimately, using the computer program developed under this contract (Appendix A), the mass-transfer experiments could be used to predict pertinent mass-transfer parameters (gas-phase mass-transfer coefficient, intra-particle diffusivity, etc.). The general approach that was followed in this area was to conduct CO_2 breakthrough tests on packed beds of IR-45 resin; prior to each breakthrough the beds were subjected to a desorption pretreatment. The dynamic mass-transfer tests were conducted in the same facility that had been used extensively for molecular-sieve and silica-gel tests presented in Reference 2.

Actually, two types of CO_2 breakthrough tests were conducted. The first series involved isothermal breakthroughs on IR-45 beds. For each test, the bed was desorbed with a vacuum bakeout and then given a known water preload. These tests used the same physical bed test section and procedures as the coad-sorption experiments of Reference 2. The test bed contained coolant passages, and sorbent was intimately in contact with copper heat-transfer fins. The second test series involved adiabatic adsorption breakthroughs, each of which had been immediately preceded by a steam desorption of the bed. These tests required some test apparatus modifications: a new cylindrical test bed was constructed; and a steam generator was installed just upstream of the new bed. The second series of tests are representative of the actual operating conditions that would prevail for a flight-type IR-45 CO_2-removal system. The first series of isothermal tests are valuable in comparing the mass-transfer performance of IR-45 with other sorbents.

Total pressure for the breakthroughs was generally 10 psia. The inlet P_{CO_2} was nominally 3 mm Hg; inlet concentration was nominally 0.010 lb CO_2/lb N_2. Inlet dewpoint for all tests was 50°F. The dry sorbent mass for the isothermal tests was 0.836 lb; for the adiabatic, steam-desorbed tests, the bed mass was 0.731 lb. Flow rate of the nitrogen carrier gas was varied over the range 0.4 to 3.2 lb per hr. These flows, at 100 percent removal efficiency, are roughly equivalent to the man-ratings of 0.04 and 0.35, respectively (CO_2 production is considered to be 2.2 lb CO_2/man-day). For perfect adsorption conditions, breakthroughs would require approximately 0.8 hr for the 3.2 lb/hr flow, and 6.4 hr at the 0.4 lb/hr flow.

Rohm and Haas IR-45 was used in all tests. The resin was water washed and then air dried. It was then screened at approximately 80 mesh to remove fines. 100-mesh screens were used in the beds to retain the resin.

EXPERIMENTAL EQUIPMENT

The schematic of the dynamic mass-transfer test apparatus is shown in Figure 3-1. The schematic depicts the apparatus in the configuration used when the internally-finned test beds are in place. Figure 3-2 shows a sketch of the internally-finned bed used for the isothermal absorptions with IR-45. This bed is rectangular, 3 in. by 3 in. at the face, with a 6 in. flow length. It contains a matrix of copper fins. These rectangular, offset plate fins are 1/2 in. high and spaced 1/2 in. apart. They are offset (or interrupted) every 1/2 in.; their thickness is 0.008 in. Only one modification was required to use this bed with IR-45. The 24-mesh screens that were originally used to hold molecular sieve and silica gel sorbents in the bed were replaced with 100-mesh screens.

Full descriptions of the test apparatus, internally-finned beds, and experimental procedures are given in Reference 2. For the isothermal tests, the procedures used with IR-45 are exactly the same as those used in the coadsorption test series on molecular sieves. Generally, the sorbent first undergoes a vacuum bakeout. Then a moisture-containing nitrogen stream is passed through the bed until the sorbent has absorbed the desired amount of water. Then the CO_2-absorption breakthrough is made.

This procedure, as mentioned earlier, is useful for comparing one sorbent to another. However, it is not representative of the conditions that would be employed with actual amine-resin systems. To more fully similate these conditions, a number of test equipment modifications were made. These centered around a new cylindrical test bed specifically designed for IR-45. This bed was 13.59 in. in overall length; its inside diameter was 2.88 in. Referring to Figure 3-1, the new bed replaced the internally-finned test bed and the outlet flow section; when installed, it spanned from the inlet flow section to the right-hand vacuum valve. An outlet flow section was incorporated within the test bed itself. Figure 3-3 shows the cylindrical test bed. This bed contained no coolant passages; after installation it was heavily insulated.

The unique feature of the cylindrical test bed is that one of the sorbent retaining screens (100 mesh) is moveable to allow for swelling and contraction of the resin. The screen is bonded to a metallic ring which was machined to be slightly smaller than the bed inside diameter. In the region of travel of this moveable screen, the cylinder was specially honed. A helical spring was used to maintain the screen against the packed resin. The spring was anchored at the bed-end flange. The spring constant was approximately 5 lb/in. The packed length of bed was approximately 6 in.

To permit steam desorptions of the IR-45 resin within the bed, a steam generator system was installed in the apparatus. Since it was desired to generate the steam as close to the bed entrance as possible, the steam generator was installed in the inlet flow section. A cylindrical well was fitted to the bottom part of the inlet section. A Chromolax immersion heater

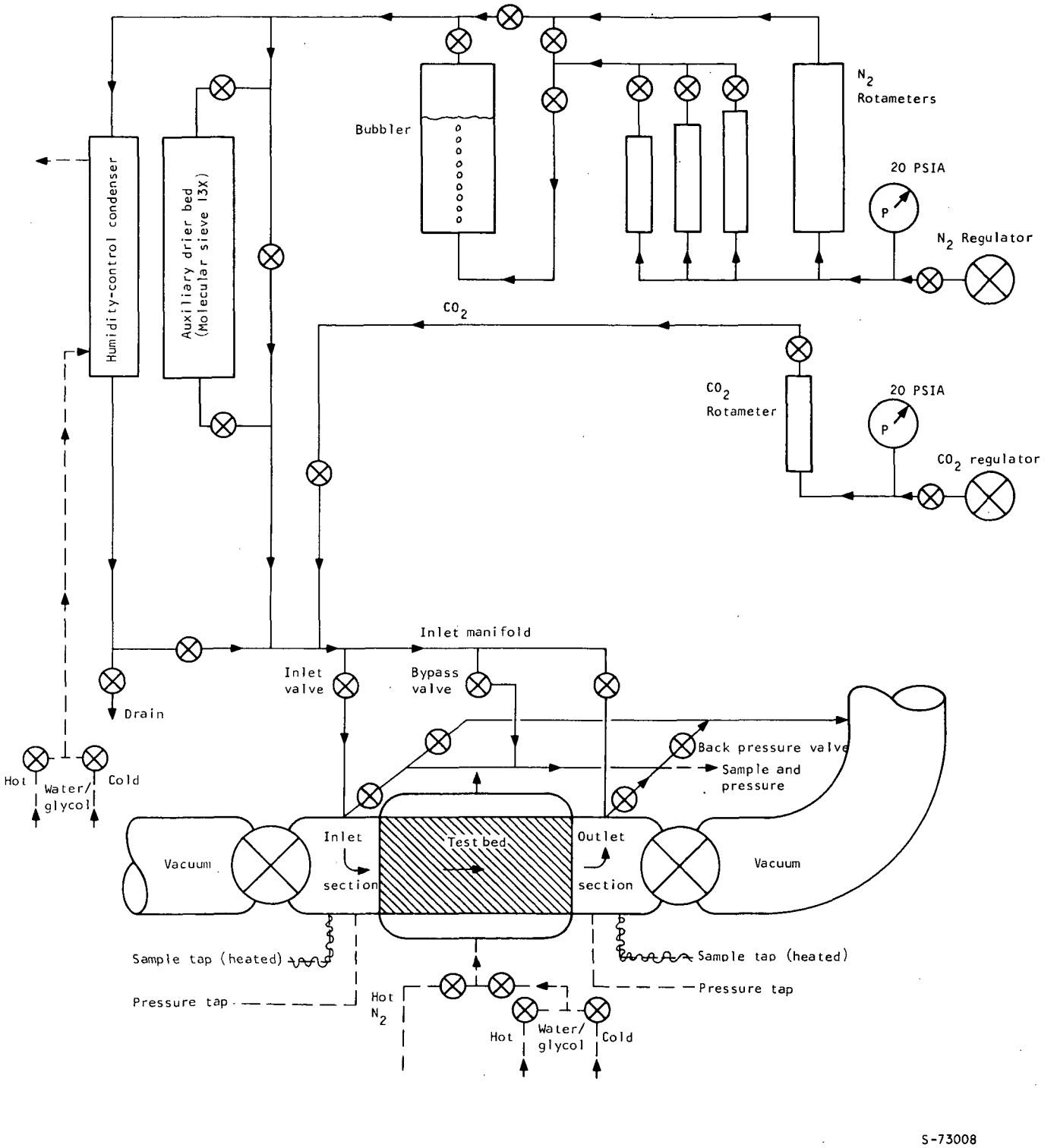

Figure 3-1. Schematic of Dynamic Mass-Transfer Apparatus

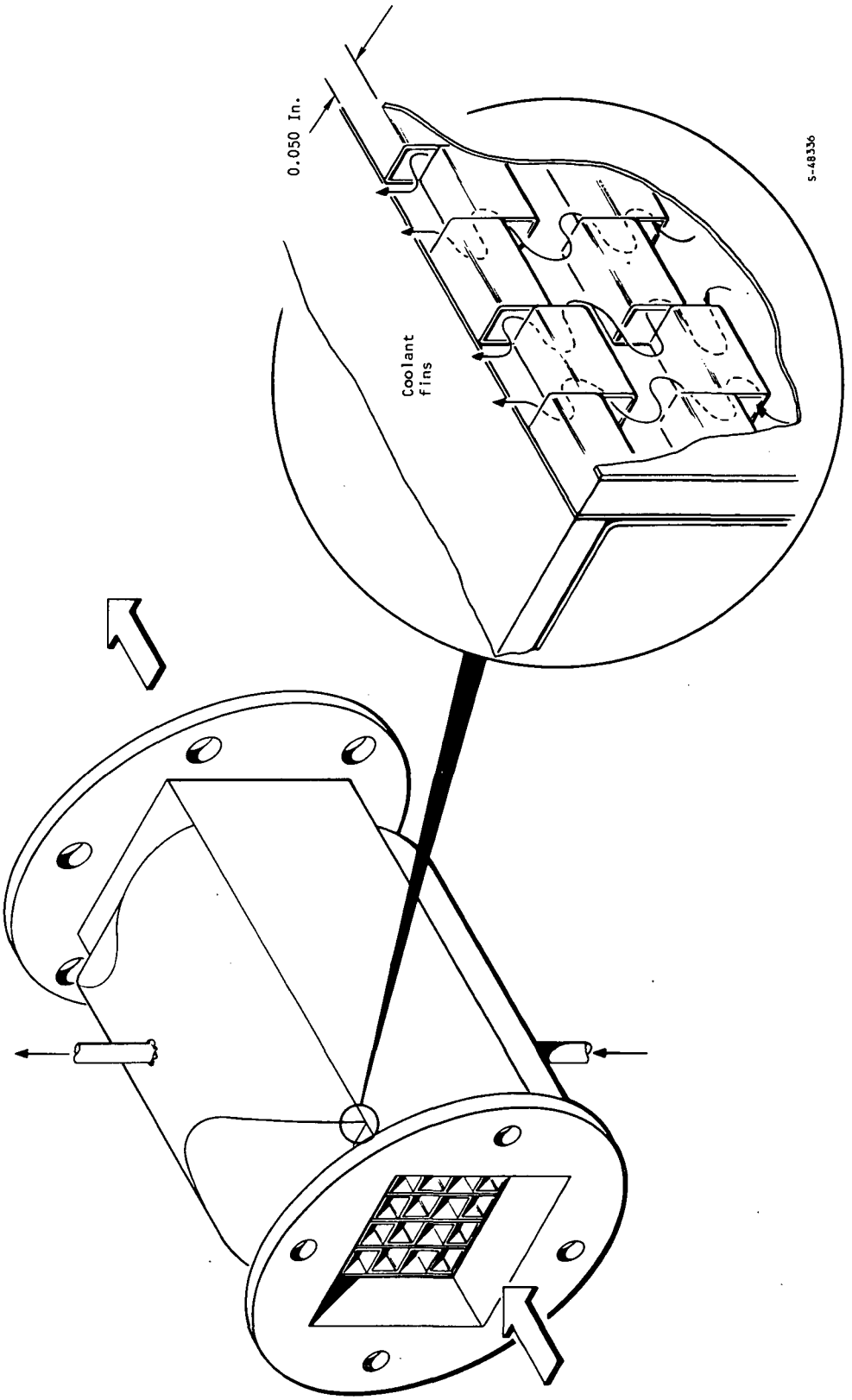

Figure 3-2. Test Bed for Isothermal Dynamic Absorption Tests with IR-45; 1/2-in.-Fin Bed.

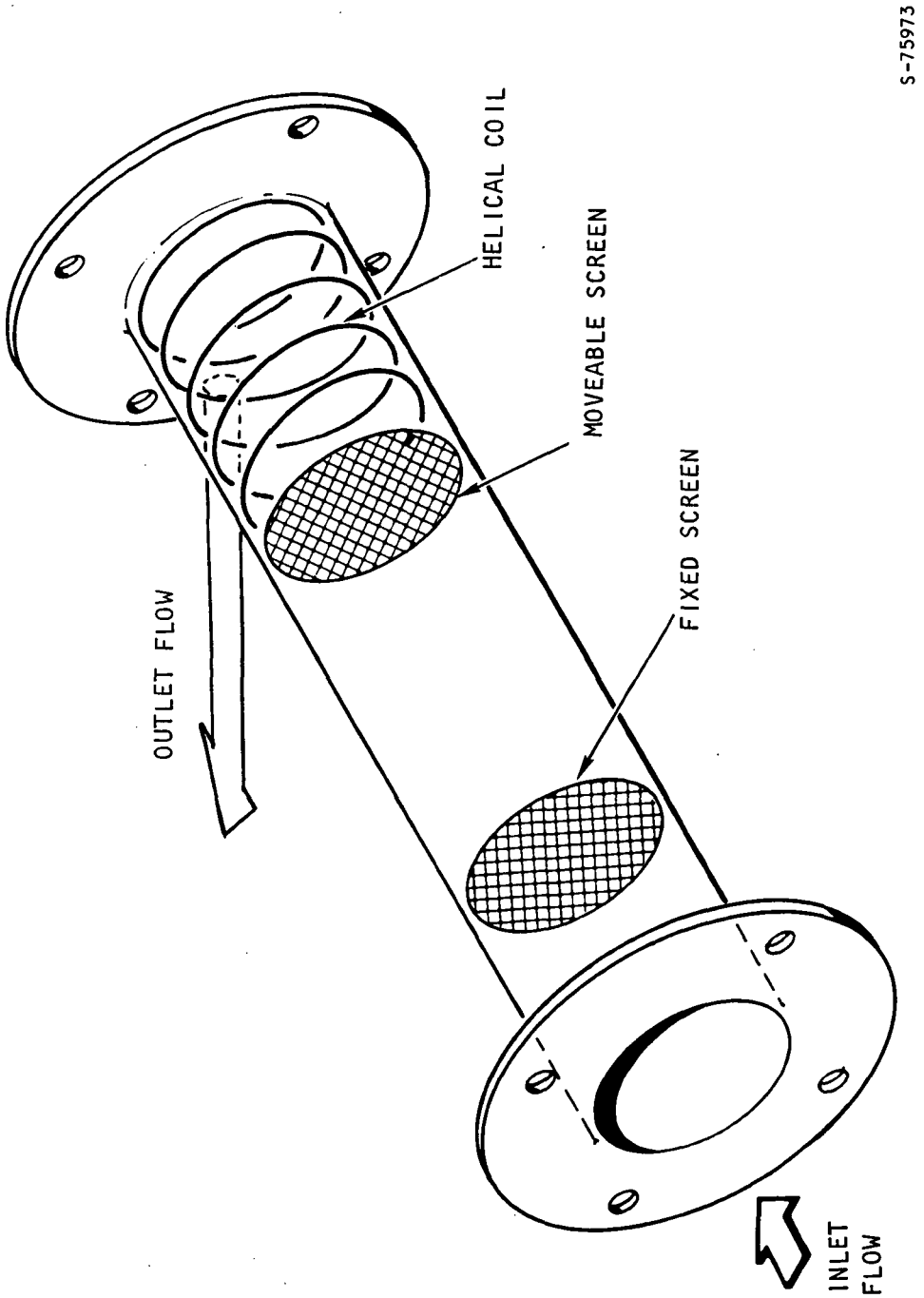

Figure 3-3. Cylindrical Test Bed for Dynamic Absorption Tests with IR-45.

(Model RB) was installed in this well with the upper surface of the heater just extending into the main cylindrical portion of the inlet section. A small-diameter water stream was directed onto the heater upper surface by means of a 1/8-in. OD tube which was suspended about 1/4 in. above the heater. Water flow to the steam generator was controlled by a needle valve and water flow rate was measured by a rotameter. A Micro Thermac temperature controller was used to maintain heater temperature. Stable steam generation was achieved for flow rates up through 2 lb/hr. The stability of the steam evolution was verified by visual observations--the generator was first operated without the bed in place--and by noting that flow, pressure, and temperature measurements remained steady.

ISOTHERMAL CO_2 ABSORPTION BREAKTHROUGH TESTS

The first dynamic tests conducted on IR-45 were made with one of the internally-finned beds used previously for molecular-sieve tests. There were two reasons for this series of tests. First, they allowed immediate comparisons to previous tests with molecular sieves. Second, because the only equipment modifications necessary were the replacement of the bed screens (with 100-mesh screens), these tests could be conducted immediately after Task 1 tests were completed.

At the beginning of these tests, there was some concern that swelling of the packed resin upon absorption of water might damage the bed. In order to evaluate the effect of swelling, immediately after packing the bed, water was poured through it. Swelling of the IR-45 caused the end screens to bulge about 1/4 to 3/8 inch. Since there seemed to be no detrimental effect due to the swelling, it was decided to use the bed as packed. (If swelling had seemed to be severe enough to damage the bed, it would have been emptied and repacked with wet, previously swollen resin.)

It was noticed that the water which was poured through the bed to cause the swelling came out a brillant blue. This was in spite of a water wash and drying before packing. Analysis indicated that the blue color was copper ions complexed with residual ammonia from the resin. Several water washings removed all traces of color from the effluent. (It is noted the fins within the bed are copper.) The bed was then installed in the apparatus, and while heated to 100°F was opened to vacuum. The exposure to vacuum was continued until bed pressure dropped to 12 μ/Hg. At this point the resin was considered to be dry.

Each CO_2 absorption was preceded by a water absorption at 65°F dew point. Figures 3-4 and 3-6 show the two water adsorptions. Figures 3-5 and 3-7 show the CO_2 adsorptions which followed the water absorptions. The first CO_2 absorption run was conducted at 7 psia, 7 mm Hg p_{CO_2}; the second run was conducted at 10 psia and 2.9 mm Hg p_{CO_2}.

The two water absorptions were quite similar. Both show a poor-quality breakthrough; in fact, after running 12 and 13.5 hr respectively, full breakthroughs had not been obtained. The calculated water loadings at the end of

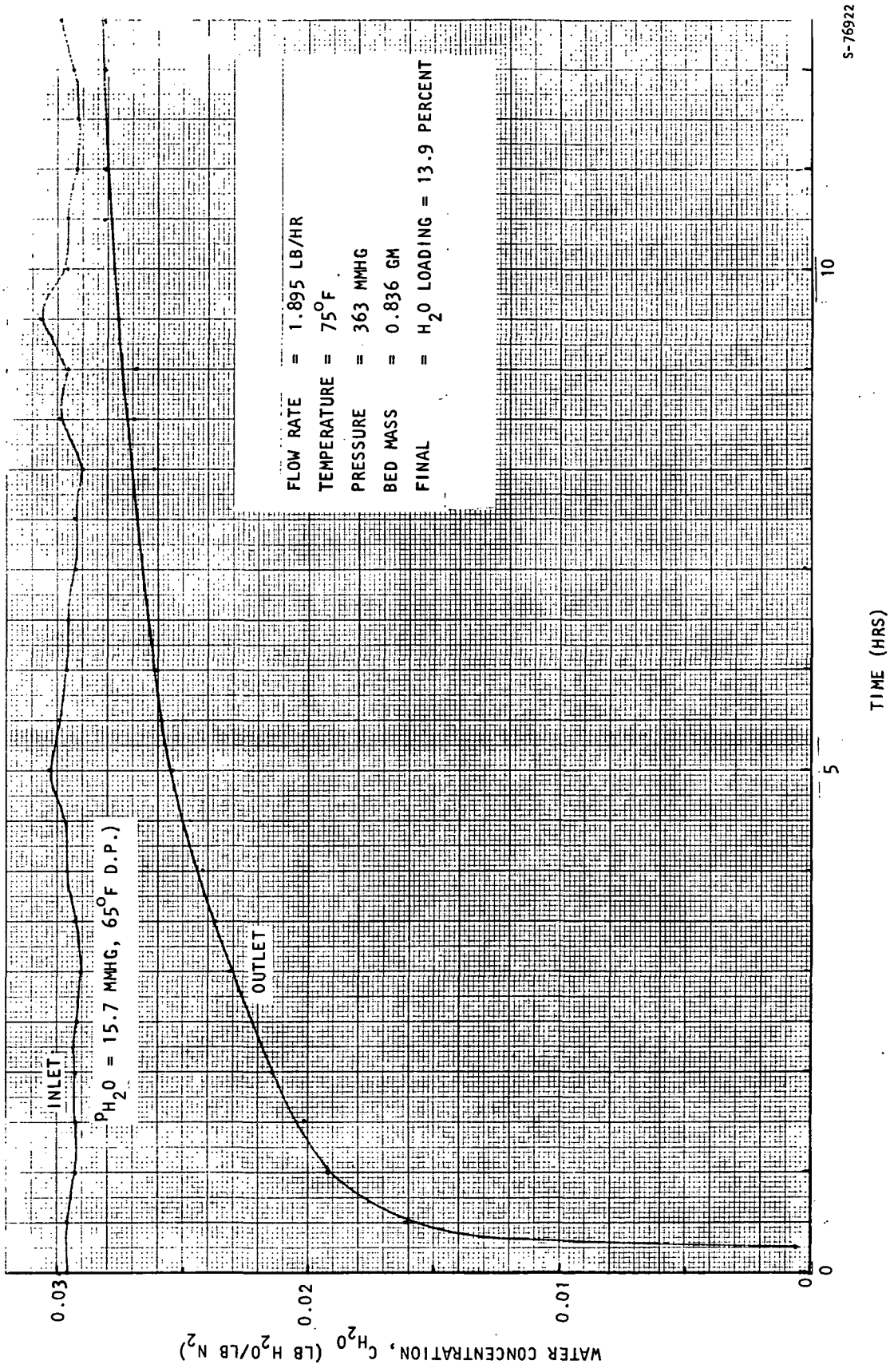

Figure 3-4. Isothermal Water Preload on IR-45 in 1/2 in.-Fin Bed Prior to CO_2 Absorption at 6.9 mm P_{CO_2}.

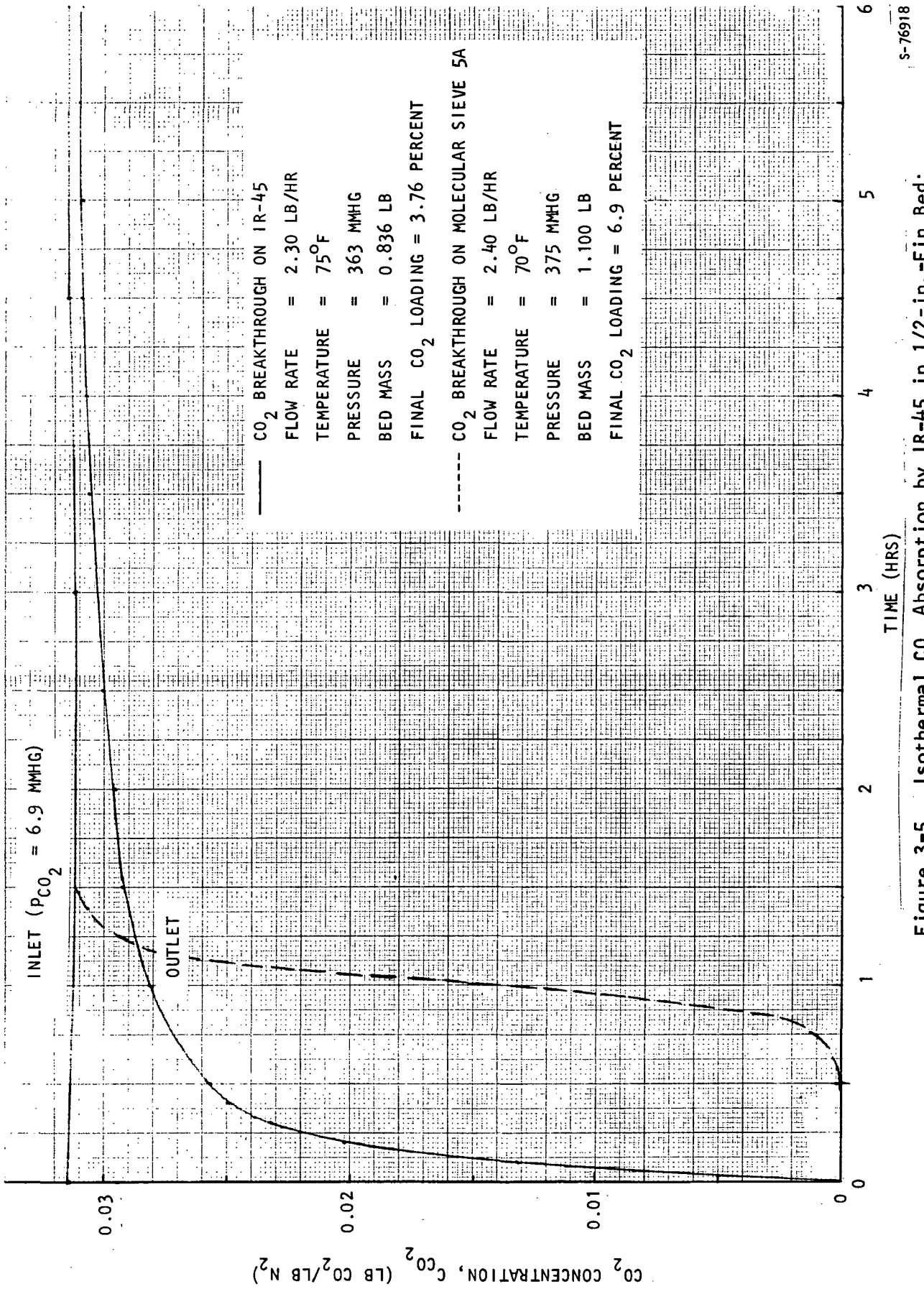

Figure 3-5. Isothermal CO_2 Absorption by IR-45 in 1/2-in.-Fin Bed; 6.9 mm Hg P_{CO_2}.

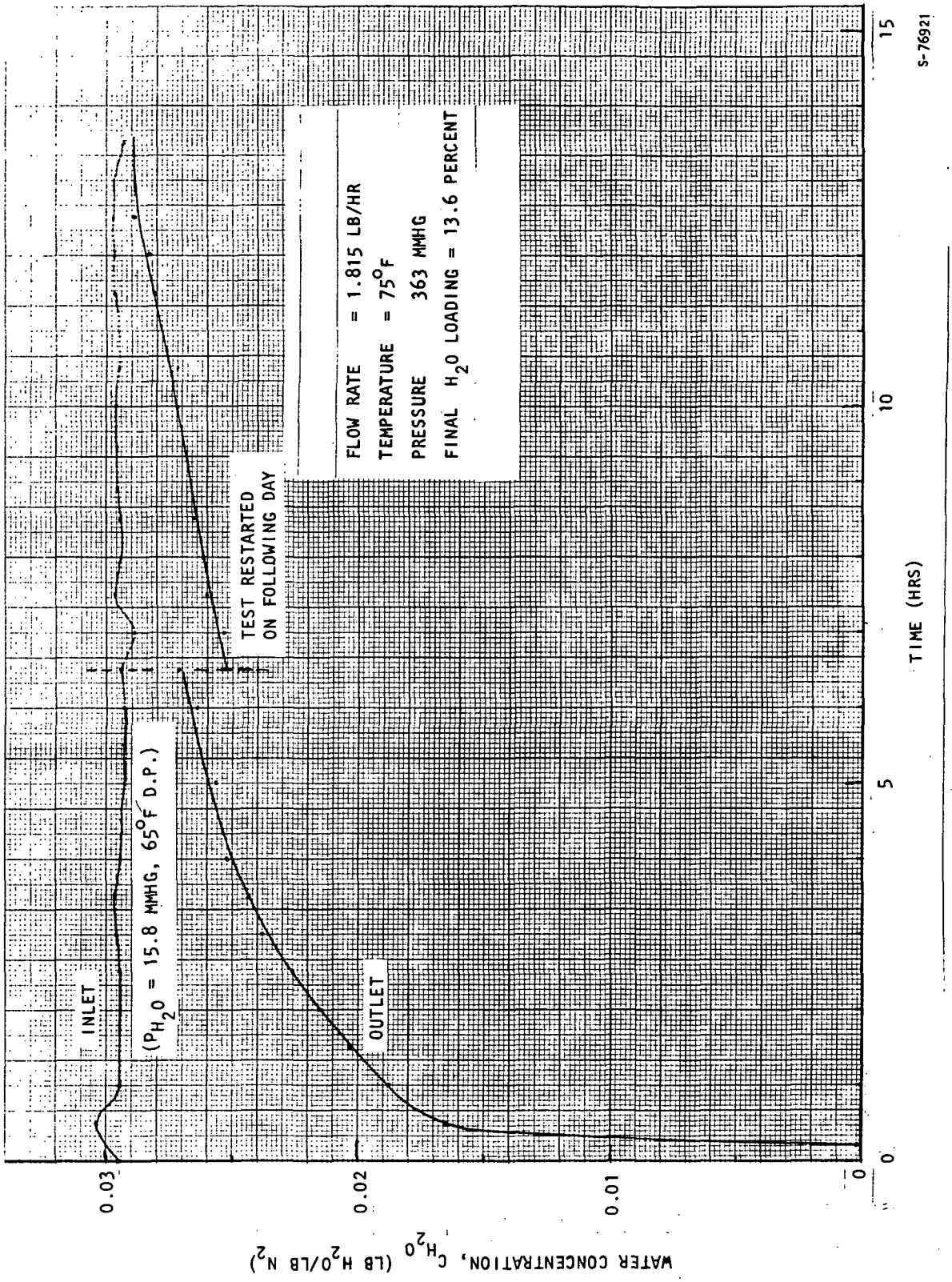

Figure 3-6. Isothermal Water Preload on IR-45 in 1/2-in.-Fin Bed Prior to CO_2 Absorption at 2.9 mm Hg P_{CO_2}.

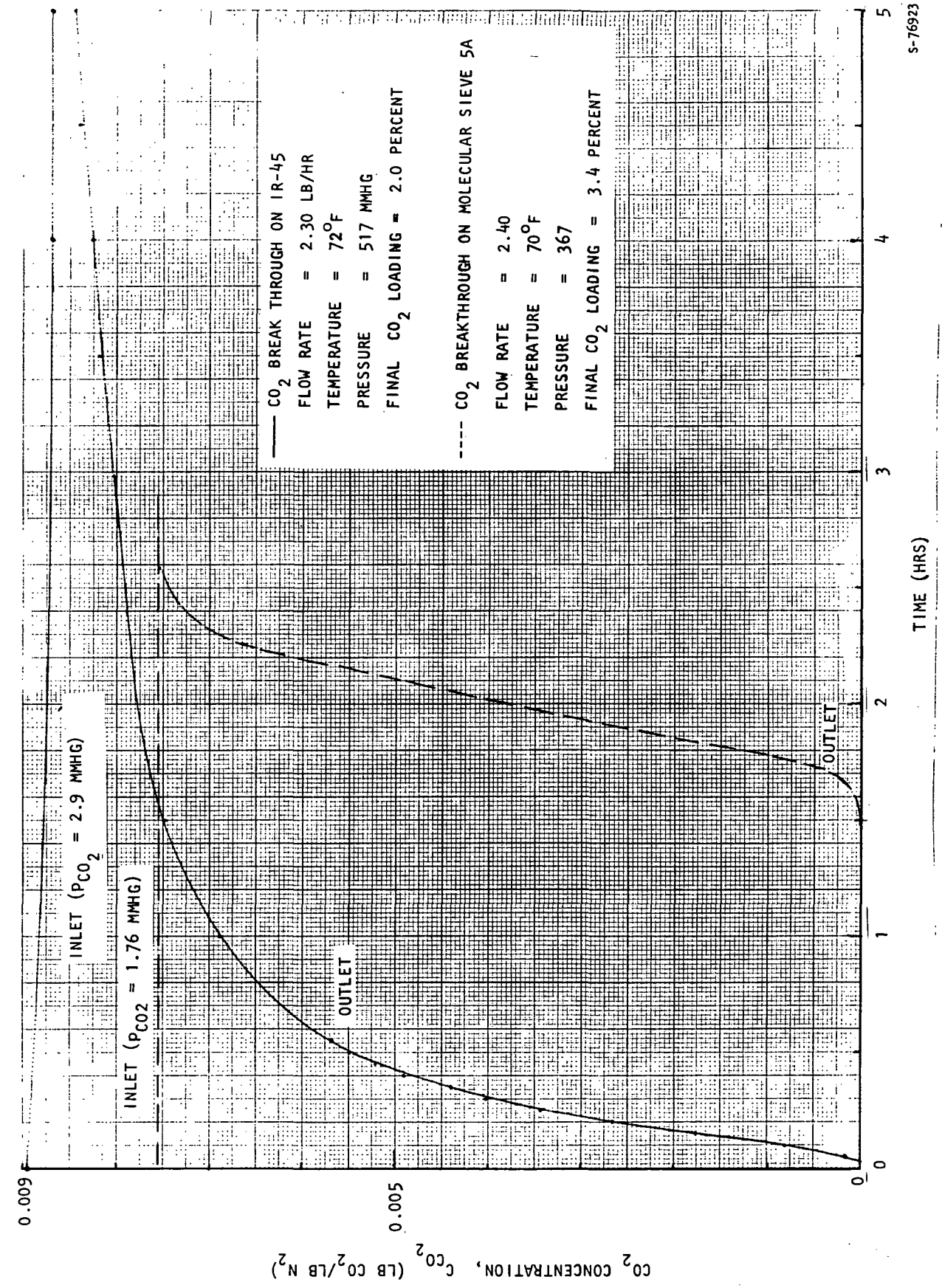

Figure 3-7. Isothermal CO_2 Absorption by IR-45 in 1/2-in.-Fin Bed; 2.9 mm Hg P_{CO_2}.

each test were 13.9 and 13.6 percent. These loadings have already been discussed and as shown in Figure 2-4 are somewhat below saturated values. By extrapolating the breakthrough curves to estimated points of completion, it was calculated that the saturated loadings would be 15.3 and 13.9 percent.

The CO_2 absorption breakthrough at 7 mm Hg p_{CO_2} and 7 psia (Figure 3-5) is also quite poor. For comparison, a CO_2 adsorption breakthrough on Linde molecular sieve 5A with similar conditions is also shown on the figure. At this p_{CO_2} level, molecular sieves would have higher capacity, and it can be argued that the figure does not provide a valid comparison. However, the general shape of the breakthrough on IR-45 indicates a difficult absorption process, probably limited by the rate of diffusion of CO_2 (or water in the preloading cases) into the pellet interior.

Figure 3-7 shows the CO_2 absorption breakthrough on IR-45 carried out at 10 psia, and much lower p_{CO_2}, 2.9 mm Hg. Here, too the breakthrough performance is poor. No exact comparison to a molecular-sieve breakthrough is available. However, one molecular sieve test at 7 psia was run for more difficult sorption conditions: inlet CO_2 concentration of 0.48 volume percent (0.0076 lb CO_2/lb N_2) vs 0.56 volume percent (0.0088 lb CO_2/lb N_2). This breakthrough is also given in Figure 3-7. In this range of partial pressure, the type 5A molecular-sieve equilibrium is not as favorable as that for IR-45. However, the molecular-sieve performance is clearly superior, with no measurable outlet CO_2 concentration in 1.5 hrs. The breakthrough was complete in 2.6 hours, with a total of 0.037 lb CO_2 absorbed. Even after 5 hours, the breakthrough on IR-45 was incomplete with only 0.017 lb CO_2 absorbed. Note that with the same test bed for both sets of runs, the bed volumes are the same.

Pressure drop in the IR-45 tests is higher than experienced with 1/16-inch molecular-sieve pellets. This is as expected since the IR-45 beads (20 to 50 mesh) are much smaller. At 2.3 lb/hr, the pressure drop with 1/16-inch molecular-sieve pellets would be about 0.7 mm Hg. For the water absorptions on IR-45, pressure drop varied with time from 5.5 to 8.3 mm Hg; as the bed picked up water and swelling occurred, the bed pressure increased.

After the two CO_2 absorption tests were completed, the bed was removed for unpacking. The first observation was that the resin beads were not the brilliant yellow color as when packed. Instead, they were duller, with a distinct yellow-green to bluish cast. This color change is probably due to copper ions complexed with ammonia. It was decided that for subsequent tests, the resin would be more thoroughly water washed before packing.

These tests cannot be considered conclusive with respect to which sorbent is better for spacecraft applications. There are several design variables to

be considered, and neither test series is actually representative of the conditions that would be seen in a CO_2-removal system. For instance, the molecular-sieve tests were performed on sorbent with absolutely no preload of CO_2 or water. In a flight system, there would be some residual loadings of both CO_2 and water on the bed. More important, the IR-45 tests did not have the same pretreatment--a steam desorption--that would be used in a spacecraft system. It would be expected that a steam desorption would be more thorough in removing CO_2 than the rather low temperature (100°F) vacuum bakeout used here.

ADIABATIC CO_2 ABSORPTION BREAKTHROUGH TESTS ON STEAM-DESORBED IR-45

Steam Desorption Procedures

Since absorption breakthrough tests were being conducted at 10 psia, it was initially decided to conduct steam desorptions at this pressure. This would correspond to 193°F desorption temperature. The procedure devised to conduct the steam desorptions was quite simple. Steam was introduced to the bed inlet. The effluent stream from the bed was directed to the vacuum system through a needle valve, which was adjusted manually to achieve a bed pressure of 10 psia. Even though the steam generation rate could be well controlled, the effluent flow rate continuously changed. This was due to condensation of steam in the bed and in the outlet flow section. Because of this variable outlet flow rate, which initially was quite low, and because of the very large pressure drop across the needle valve, it was very difficult to control the bed pressure. As a result, even over periods of several hours, bed temperatures were uneven and were continuously changing. Usually, maximum bed temperatures were much lower than the desired 193°F; for example, 140°F.

A number of CO_2-absorption breakthroughs were conducted after steam desorptions of this type. The quality of the data from these breakthroughs was not good, and reproducibility was poor. It was strongly suspected that the desorptions were not uniform, nor complete, and this was the primary cause of the poor data. In addition, there was always a problem of liquid water in the sample lines which are connected to the outlet flow section. Even when shutoff valves were installed at the sample line inlets, water which condensed in the outlet section would migrate into sample lines when the absorption breakthrough was started. Even attempts to blow out condensed water to the vacuum system before starting a test were not very successful. Consequently, there was always some doubt whether CO_2 concentration readings were valid; that is, whether liquid water had saturated the water traps in the CO_2 sample lines.

As a result of all these difficulties, a new desorption procedure was devised. The quality of all previous absorptions was considered so poor that none of those tests are presented in this report. The new procedure simply involved opening the outlet flow section to ambient through a small needle valve, and conducting the desorption at 14.7 psia. The needle valve was located on the bottom of the outlet flow section so that all condensed water not absorbed by the resin would be vented. All sample lines were closed off.

The revised desorption procedure worked very smoothly, since no pressure control was required. The bed outlet thermocouple usually indicated over 200°F within approximately a one-hour period. The steam generation rate was standardized at 1.5 lb/hr. On a theoretical basis, if there were no heat losses to ambient and all steam was condensed within the bed, a flow rate of about 0.25 lb/hr would be required. This includes an allowance for heating the metal of the bed. The difference between the calculated and actual is due to heat leak and the considerable bypassing of steam through the bed.

It was considered that these atmospheric desorptions provided very adequate clean up of the bed. Desorptions at 10 psia (that is, at 193°F) are expected to be equally adequate, but they might require a longer time period. For laboratory purposes, atmospheric-pressure desorptions are simpler, faster, and no real simulation accuracy is lost. If 10 psia desorptions were to be undertaken in the laboratory, the procedure would now be to vent the bed effluent stream into the bed-inlet bypass system which would be maintained at 10 psia with a flowing stream of nitrogen. This would simulate the desorption into a 10 psia (cabin pressure) reservoir, and it would also allow easy control of the desorption back pressure.

Adiabatic CO_2 Absorption Breakthrough Following Steam Desorptions

Figures 3-8 through 3-12 show CO_2 breakthroughs conducted immediately after steam desorptions at 14.7 psia. The flow rate range of these tests is 0.4 to 3.2 lb/hr. In all tests, inlet process gas temperature is approximately 70°F; inlet dew point was controlled at 50°F. The CO_2 partial pressure was essentially 3 mm Hg.

All of these absorption runs show very early, almost immediate, breakthrough of CO_2 followed by a prolonged period where a significant fraction of the CO_2 is absorbed out of the gas stream. These breakthroughs are much better than those obtained earlier with isothermal beds (Figures 3-5 and 3-7). It is considered that the presence of more water was the primary reason for the better breakthrough results. For example, after steam desorption, the bed would have approximately 40 percent water; this is compared to the 13 percent water preloads of the isothermal tests. Possibly another contributing factor is that steam desorptions could be more thorough than the 100°F vacuum-bakeouts that preceded the earlier tests. Also, the tests of Figures 3-8 through 3-11 should look somewhat better as they were conducted for lower flow rates (0.43, 0.80, and 1.60 lb/hr as compared to 2.3 lb/hr).

Even though the adiabatic, steam-desorbed breakthroughs are better, data from the breakthroughs leads to the conclusion that the sorption process is severely limited by diffusion of CO_2 into the interior of the sorbent pellet. The characteristics of the early portion of the breakthrough curve give this indication. Even more, the sorption behavior after a period of shutdown substantiates the conclusion. In the absorption run of Figure 3-8, the testing was terminated for 66 minutes to check for a leak. When it was verified there was no leak, the absorption test was reinitiated. As seen in the figure, the outlet concentration upon restart was nearly zero, but rose rapidly to the level

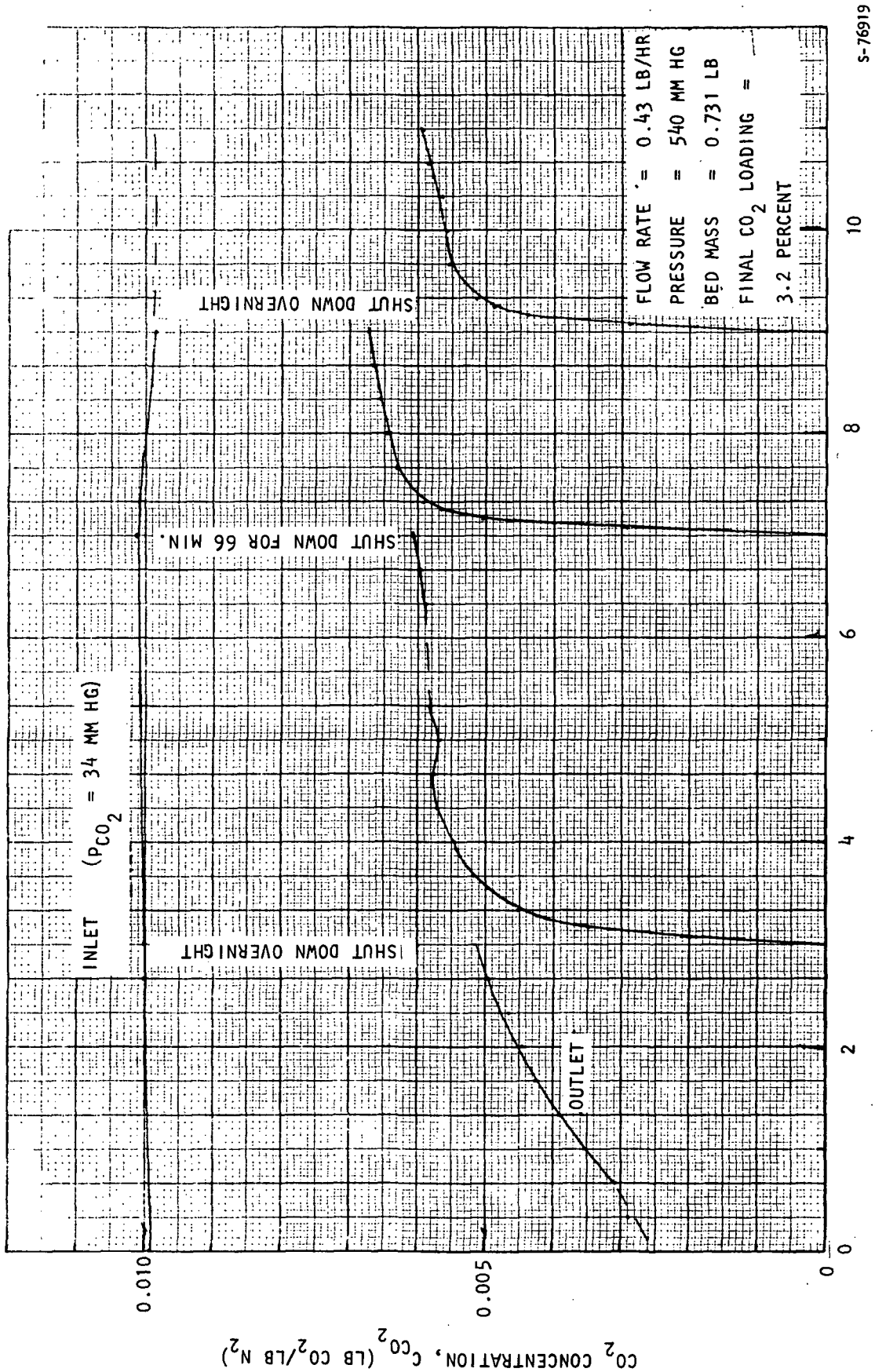

Figure 3-8. CO_2 Breakthrough on Steam Desorbed IR-45, 0.43 lb/hr Flow Rate.

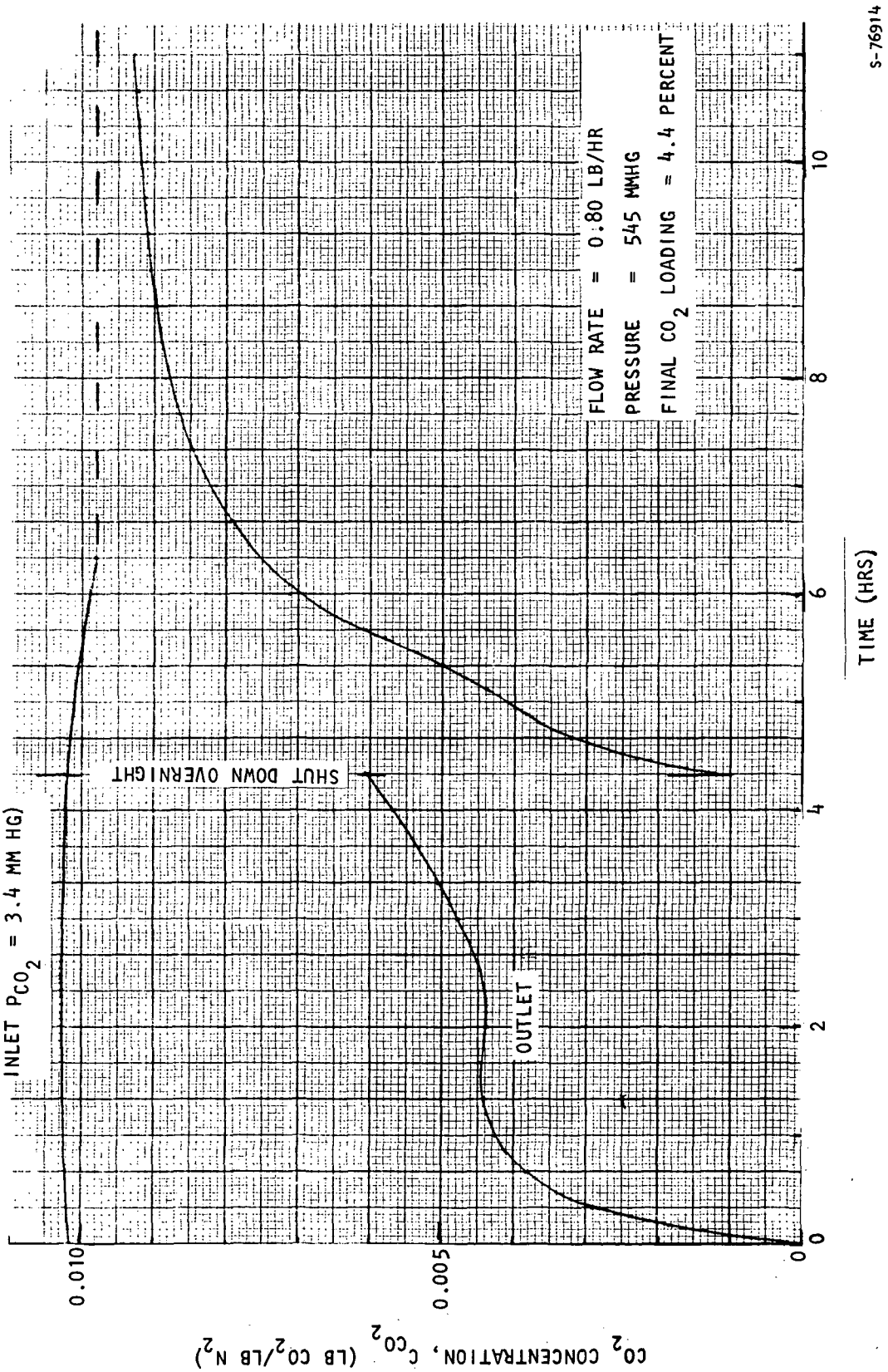

Figure 3-9. CO_2 Breakthrough on Steam Desorbed IR-45, 0.80 lb/hr Flow Rate.

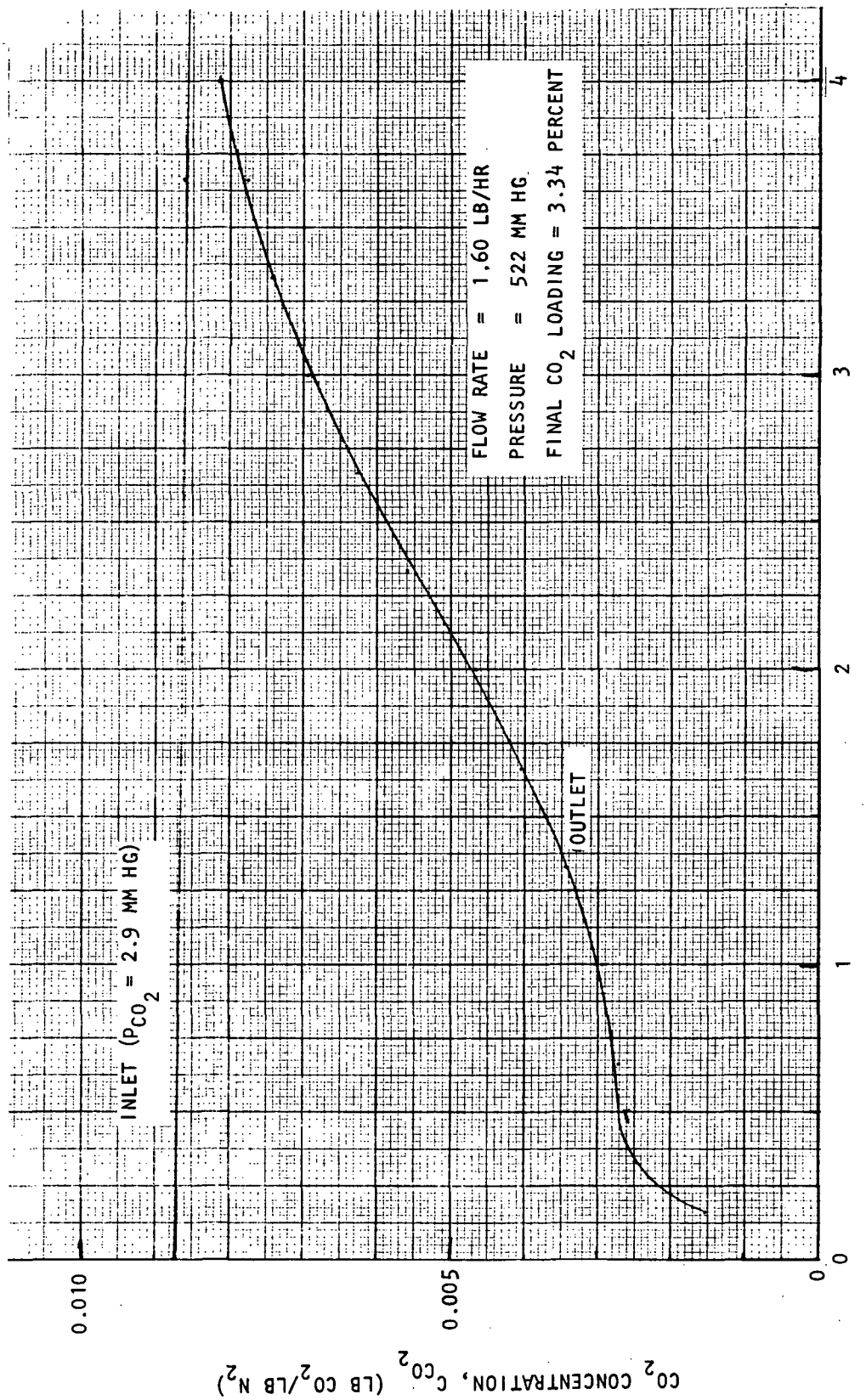

Figure 3-10. CO_2 Breakthrough on Steam Desorbed IR-45, 1.60 lb/hr Flow Rate.

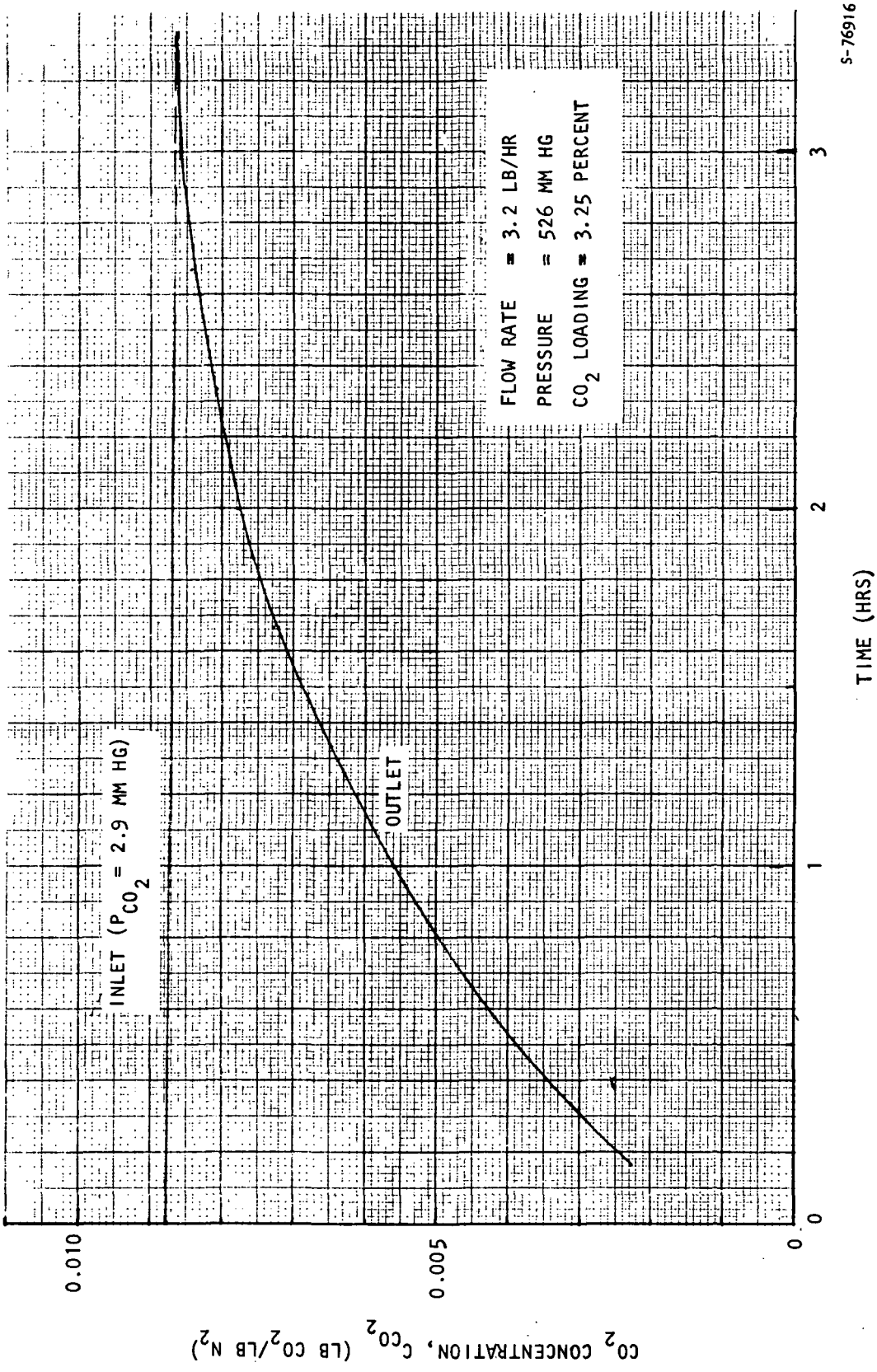

Figure 3-11. CO_2 Breakthrough on Steam Desorbed 1R-45, 3.2 lb/hr Flow Rate.

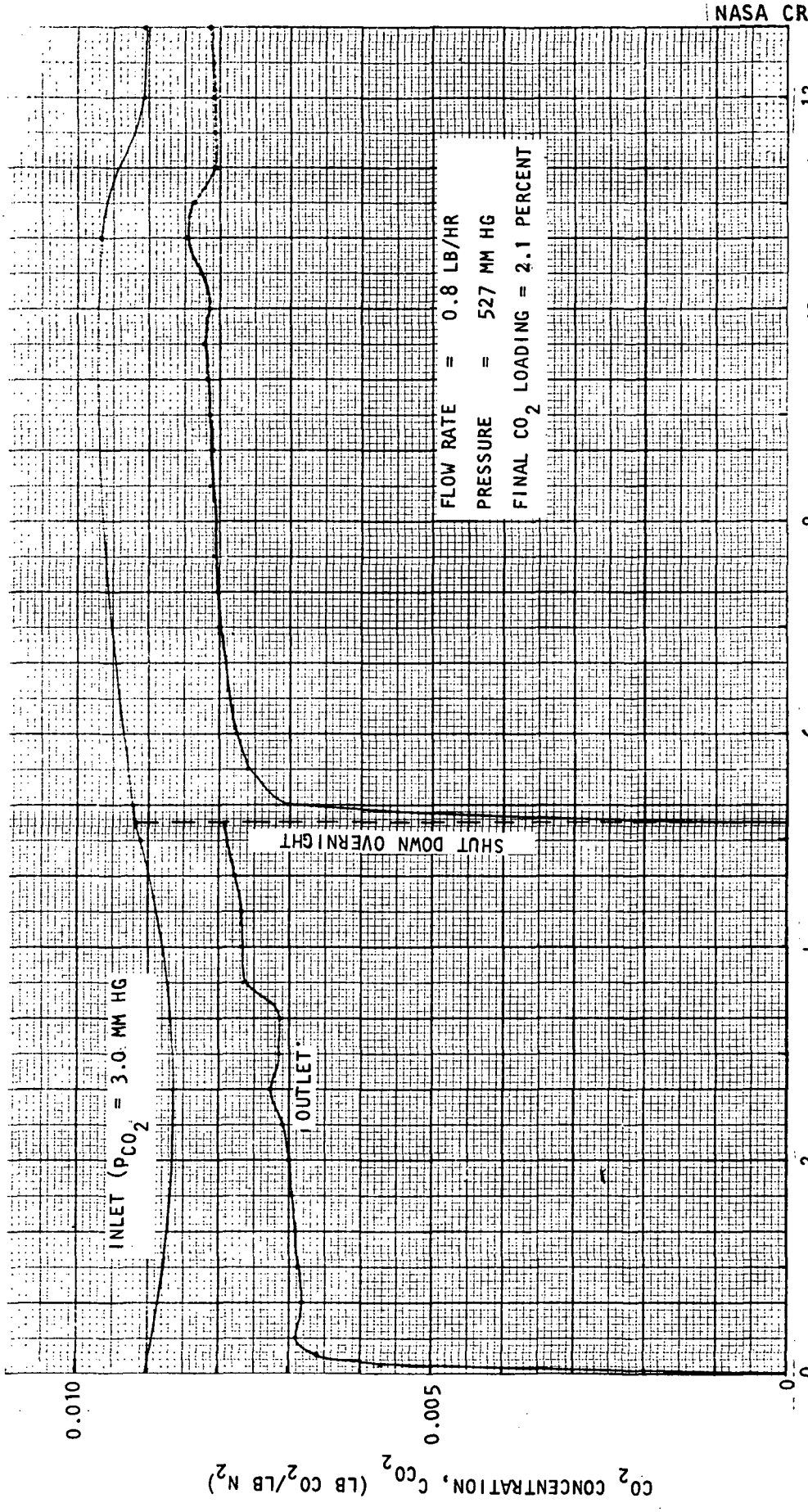

Figure 3-12. CO_2 Breakthrough on Steam Desorbed IR-45, Bed Cooling Before Absorption.

it had been at before shutdown. This furnishes clear evidence of the slow intraparticle diffusion process: during shutdown, previously absorbed CO_2 could diffuse into the particle interior, providing nearly fresh resin at the pellet exterior, and momentarily upon restart giving a high absorption rate. This is also shown after the overnight shutdown (Figure 3-9).

The tests for 0.80 lb/hr and 1.6 lb/hr both show a droop or saddle portion to the breakthrough after the initial rise of the curve. It is thought that this is due to cooling of the bed and removal of some of the water condensed during the previous desorption. It is considered that the flow rate (3.2 lb/hr) of the breakthrough shown in Figure 3-11 is too large to show the droop in the outlet concentration curve. That is, the rather fast, constantly rising breakthrough is as expected.

Figure 3-12 shows a breakthrough for a test in which the bed was allowed to cool to room temperature after steam desorption and before starting the absorption. All of the other breakthroughs for steam-desorbed resin were conducted as soon as possible (usually within a minute) after completion of the desorption. The breakthrough of Figure 3-12 is much poorer than that of the same conditions with a warm bed as given in Figure 3-9. This test was conducted to see if the reason for the immediate CO_2 breakthrough was due to low equilibrium sorption capacity of the resin at the high-temperature initial conditions of the test. Apparently, the high temperature is not the cause of the immediate breakthrough. It appears that the poorer cool-bed breakthrough is due to the high moisture content of the resin. With an initially hot bed, a great deal of water is removed early in the test, whereas moisture removal with the cool bed is much slower.

SECTION 4

SUMMARY AND CONCLUSIONS

The efforts under Task 3.1 have produced equilibrium data for water on IR-45 at 75°F, and for CO_2 on IR-45 with various preloads of water at 75°F. During the course of experimentation, two significant characteristics of the sorbent were observed. First, the material is very slow in absorbing water and CO_2. Second, prolonged exposure to vacuum and low-pressure degrades the capacity of the sorbent for CO_2.

Because of the extremely slow absorption behavior of the resin, the equilibrium data that is presented in the report represents only a fraction of the data that was originally desired. Unfortunately, it was not possible to extend testing into the range of high water loadings where the high CO_2 capacities were expected.

On the subject of degradation, a study was performed on the effect of various sorbent cleanup procedures. It is considered that there is negligible degradation if the sorbent is subjected to only one vacuum bakeout at moderate temperature and to low pressure for only the period of time necessary to obtain one equilibrium isotherm. Both 150°F and 100°F vacuum bakeout temperatures are acceptable. It appears that the higher temperature, with respect to lower temperature bakeouts, slightly promotes CO_2 absorption capacity and slightly diminishes the capacity for water.

CO_2 absorption breakthrough tests were conducted on packed beds of IR-45. Both isothermal and adiabatic tests were conducted. The principle observation from all of these tests was that absorption is quite slow and is limited almost entirely by internal diffusion. There seems to be little possibility of improvement of this characteristic with regard to using smaller particles. Pressure drop in the test beds is already quite high, roughly ten times that experienced for 1/16-in. molecular-sieve pellets.

The tests showed that there is definitely an effect of water loading on the absorption rate. However, not enough tests were performed to properly describe this phenomena. It seems definite that after a steam desorption, where the bed has absorbed a great deal of water, better performance is obtained if the absorption is started immediately without allowing any cooling of the bed. It is considered that the cause for the better performance is not higher CO_2 mass-transfer rates at higher temperature. Rather, it is due to the faster removal of water due to the bed being hot, and thus a faster approach to the level of water loading where CO_2 capacity is largest.

The shapes of all breakthrough curves indicated poor absorption performance for IR-45. Removal efficiency was low, even for very low flow rates. It is apparent that with IR-45, larger beds would be required than with molecular sieves--at least as far as the CO_2-removal bed is concerned. This is due to the very poor mass-transfer performance of IR-45 and its lower packed density (29 lb/ft^3 vs 47 lb/ft^3 for molecular sieves). Flow rate per unit face area

must be much lower than with molecular-sieve beds in order to have reasonable pressure drops.

With all of the various penalties that are involved, it is not possible without competitive design/tradeoff studies to conclusively determine the merit of CO_2-removal systems based upon amine resin IR-45. However, due to the disappointing mass-transfer performance of the material, its potential for degradation, the high pressure drop associated with it, and the large volumetric expansion of the material with water content, it is difficult to believe that the material would be a more ideal sorbent for long-term space flights than the inorganic molecular sieves.

For the design of IR-45 systems, additional basic data is desirable. Water equilibrium for sorbent temperatures above 75°F would be necessary. CO_2 equilibrium data for a wide range of water content and for sorbent temperatures from 75°F to 200°F should be obtained. These data will be difficult to obtain due to the tremendous amount of time that would be involved. Numerical information on mass-transfer coefficients would be needed. Estimates of these quantities could be obtained from the breakthrough curves at hand with the use of the computer program (Appendix A)--this effort would require valid equilibrium data maps over all conditions to be encountered.

APPENDIX A

COMPUTER PROGRAM FOR PREDICTING THE TRANSIENT PERFORMANCE OF SOLID AMINE SORBENTS FOR CO_2 REMOVAL

Dr. K. C. Hwang

APPENDIX A

This appendix describes the computer program AMINE which has been developed by the AiResearch Manufacturing Company of Los Angeles for the prediction of the transient performance of CO_2-removal systems employing solid absorbent materials such as amine resins. Specifically, the program contains data relative to CO_2 and water sorption by an aminated ion exchanger resin, Amberlite IR-45, manufactured by Rohm and Haas. The original intent of the program was to aid in the design and evaluation of CO_2-removal systems for manned spacecraft applications. However, the program is sufficiently general that it can be used for other applications. The expected means of desorption is by steam stripping; dry gas stripping can also be handled by the program.

This appendix includes the following information: a description of program capabilities and computations; an explanation of how the program is used, including definitions of required input data; an example of program output; and Fortran listings of all programs.

The computer program is the result of Task 3.2, Analytical Model Development, of contract NAS1-8559 "Development of Regenerative-CO_2-Removal-System Design Techniques" from NASA Langley Research Center.

Two previous computer programs dealing with the prediction of the transient response of spacecraft CO_2-removal systems were developed by AiResearch under this contract. These programs, intended primarily for systems employing inorganic molecular-sieve adsorbents, are documented in Reference 1.

CONTENTS

	Page
NOMENCLATURE	A-4
INTRODUCTION	A-10
GENERAL DESCRIPTION	A-12
TECHNICAL DESCRIPTION	A-12
Momentum Balance	A-12
Total Pressure Equation	A-14
Material Balance Equations	A-14
Energy Equations	A-14
Equilibrium Isotherms	A-14
Diffusion Model for the Interior of Sorbent	A-18
Method of Solution	A-19
PROGRAM INPUT	A-19
PROGRAM OUTPUT	A-21
EXAMPLE RUN	A-21

ILLUSTRATIONS

Figure		Page
A-1	An Amine System for CO_2 Removal	A-11
A-2	Logic Program for Amine Transient Absorption Performance Prediction Program	A-13
A-3	Equilibrium Absorption Capacity of IR-45 for CO_2 Parametric with Preload, 75°F Sorbent Temperature	A-15
A-4	IR-45/H_2O Equilibria (75°F)	A-16
A-5	Effects of Water on Saturation Capacity for CO_2	A-17
A-6	Model for Internal Diffusion	A-18
A-7	Comparison of Computed Breakthrough Curve with Test Data	A-28

TABLES

Table		Page
A-1	Input Data	A-22
A-2	Absorption Cycle Print Out	A-27
A-3	Desorption Cycle Print Out	A-27

NOMENCLATURE

FORTRAN	Algebraic	Definition
ADT		Temporary storage for DT
ADT2		Same as ADT
AO	A_o	Surface area of each sorbent particle, sq ft
AS	A_s	Cross-sectional area of sorbent bed, sq ft
ASG	a_{sg}	External surface area of sorbent, sq ft/cu ft of bed
$AVGCO_2$		Average CO_2 loading, lb CO_2/lb sorbent
$AVGH_2O$		Average H_2O loading, lb H_2O/lb sorbent
$AVRCO_2$		Average CO_2 removal rate, lb/hr
AI		Interface area between the exhausted and unused parts of a sorbent pellent, as shown in Figure 6, sq ft
B, C		Coefficients in the quadratic equation (1) for solving G_o
CAPT1, CAPT2		Variables for storing caption required in print-out
CPK		Molar heat capacity of sorbates, Btu/(lb-mole)-^oF
CPL		Heat capacity of each component in liquid state, Btu/lb-^oF
CPS		Heat capacity of loaded sorbent, Btu/lb-^oF
CPSDRY		Heat capacity of dry sorbent, Btu/lb-^oF
CP1, CS1, CS2, CS3, CS4, CS5, CS6, CS7, C1, CIP, CIPK		Temporary variables used in solving various differential equations

FORTRAN	Algebraic	Definition
C1TG C1WK C2 C2P C2PK C2TG C2WK C3 C3P C3TG C2WK C4		Temporary variables used in solving various differential equations
DH	H	Heat of absorption/desorption, Btu/lb
DIF	D	Internal diffusivity, (lb-mole)/hr-Ft-(mm Hg)
DP	D_p	Particle diameter, ft
DPKDTS	$\frac{\partial P_k^*}{\partial T_s}$	Derivative of equilibrium pressure with respect to temperature, (mm Hg)/^oF
DPKDWK	$\frac{\partial P_k^*}{\partial W_k}$	Derivative of equilibrium pressure with respect to loading, (mm Hg)/lb/lb
DT	Δt	Time step size, hr
DTI		0.5×10^{-5} x DTMAX, hr
DTMAX		Maximum Δt allowable, hr
DW		Loading change since the beginning of cycle, lb/lb
DWK		Approximate loading change in one absorption/desorption cycle, lb/lb
DX	Δx	Axial increment, ft
D4P		Temporary variable
EQAMN		Name of subroutine which computes equilibrium pressure
F	F	A flow resistance factor
FCON		$= a_s . e/(x . F)$
FDEQIM		A subroutine which solves finite-difference equations

FORTRAN	Algebraic	Definitions
FVOID	e	Void fraction
GKF		Mass-transfer coefficient representing the sorbent surface film resistance, (lb-moles)/hr-(sq ft)-(mm Hg)
GO	G_o	Superficial mass velocity, lb/hr-(sq ft)
HL		Temporary storage variable
HSG	h_{sg}	Heat-transfer coefficient between sorbent and gas, lb/hr-(sq ft)-^oF
INPUT		Namelist in which all input variables belong
K	k	Index denoting sorbate, k = 1 to k_{max}
KAB		Integer denoting absorption/desorption, 1 for the former, 2 for the latter
KG	K	Effective overall mass transfer coefficient, (lb-moles)/hr-(sq ft)-(mm Hg)
KMA	k_{max}	Total number of sorbates in the system
KP		A dummy index
THS		Thickness of the layer of exhausted sorbent, ft
MW		Molecular weight of sorbates
MWG		Average molecular weight of gas mixture
N	N	Axial node index
NCYCLE		Number of complete absorption/desorption cycles elapsed from the beginning
NCYCLT		Total number of complete cycles desired
NMAX		Total number of axial nodes to be used
NMAX1		= NMAX + 1
NMAX2		= NMAX + 2

FORTRAN	Algebraic	Definitions
NODE		Axial node index
NPR		Number of time steps elapsed since the last printout
NPRINT		Desired number of time steps between printouts
P		Equilibrium pressure of sorbate based on initial loading and temperature, mm Hg
PG	P	Total pressure, mm Hg
PGAV		Same as PG
PGC		Bed outlet pressures during absorption and desorption periods, mm Hg
PGI		$= \sum_{k=1}^{kmax} PKI\ (K, KAB)$
PGS		Temporary storage variable for PG
PG1		PG at time = time - (Δt)
PG2		PG at time = time - 2 (Δt)
PK	p_k	Partial pressure of sorbates, mm Hg
PKI		Inlet partial pressures of sorbates, mm Hg
PKS	p_k^*	Equilibrium pressure at WK and TS, mm Hg
PKS1		PKS at time = time - (Δt)
PKS2		PKS at time - time - 2 (Δt)
PKS4, PKS5, PKS6		Temporary variables for calculating $\frac{\partial p^*}{\partial w_k}$ and $\frac{\partial p^*}{\partial T_s}$
PK1		PK at time = time - (Δt)
PK2		PK at time = time - 2 (Δt)
PRBED		Name of subroutine which prints bed size
PRINT		Name of subroutine which prints bed performance

FORTRAN	Algebraic	Definitions
PTN		$= \sum_{k=1}^{k_{max}} PK\ (K, N)$, mm Hg
R	R	Universal gas constant
RH		Temporary storage variable
RHOG		Gas density, lb/(cu ft)
RHOS		Sorbent density (lb/cu ft)
RHOSB		Bulk density of sorbent, lb/(cu ft)
RN		Radius of the sphere of unused sorbent, ft
RO		Radius of sorbent particle, ft
R1		Film resistence, $= \frac{1}{GFK}$
R2		Resistance due to the layer of exhausted sorbent, $= \frac{1}{D_k} \left(\frac{A_o}{A_1}\right)$
SCON		Temporary variable used in accounting for axial conduction of heat
TG	T_g	Gas temperature, ^oF
TGI		Inlet gas temperature, ^oF
TG1		TG at time = time - (Δt)
TG2		TG at time = time - 2 (Δt)
THS	ℓ	Thickness of the layer of exhausted sorbent, ft
TI		Maximum temperature change allowable per time step, ^oF
TIME	t	Time from beginning of absorption/desorption cycle, hr
TIMEN		TIME in minutes
TOTCO2		Total amount of CO_2 removed since the beginning of cycle, lb

FORTRAN	Algebraic	Definitions
TS	T_s	Sorbent temperature, ^{o}F
TS1		TS at time = time - (Δt)
TS2		TS at time = time - 2 (Δt)
U		Gas velocity, ft/hr
V		Volume of unused sorbent in each sorbent particle, cu ft
VF	V	Volumetric flow of gas, (cu ft)/hr
VFI		Inlet volumetric flow rate at TGI and PGI, (cu ft)/hr
VFIA		Variable to store VFI during each cycle
VFRT		Coefficients used in solving total pressure equations
VISCG		Gas viscosity, lbm/hr-ft
VO		Volume of each sorbent particle, cu ft
WI		Maximum allowable loading change per time step, lb/lb
WK	W_k	Loading, lb/lb
WKO		Loading at the beginning of a cycle, lb/lb
WK1		WK at time = time - (Δt)
WK2		WK at time = time - 2 (Δt)
WTAB		Total weight of sorbent, lb
WTSORB		Same at WTAB
X		Mole fraction of each sorbate in gas stream
XS X1		Temporary storage for X

INTRODUCTION

Solid/amine polymer materials are potentially attractive as regenerative sorbents for spacecraft CO_2-removal systems. There have been a number of experimental investigations dealing with these materials for spacecraft applications, including those investigations carried out under this contract. These investigations have provided some basic mass-transfer data and certain indications of the merit of solid-amine CO_2 absorbents. However, the experiments cannot be used alone to assess the merits of CO_2-removal systems which employ such absorbents. The accurate assessment of such systems can only be provided by detailed design/trade-off studies. The computer program AMINE developed by AiResearch and described in this report provides a tool for such studies. The program predicts the transient, cyclic behavior of beds which alternately undergo absorption and desorption processes.

In a system employing solid-amine absorbents, cabin gas is passed through a bed of moist amine pellets with CO_2 being removed to some extent from the stream. Depending upon the bed's initial conditions, water can be absorbed from the gas stream or water can be evaporated from the bed into the stream. After a certain period of time, the CO_2-laden bed is regenerated by directing a flow of steam through it--the steam in effect stripping off and concentrating the CO_2. The absorb/desorb cycles are depicted in Figure A-1. At all times the bed or (beds) of a system are operating in a transient condition, and a true steady-state condition is never reached. However, after a long period of operation (neglecting any degradation of the sorbent), a repeating, cyclic condition will occur.

To properly predict the performance of such a system, the true transient nature of the operation must be considered. This leads to the use of large-scale computer programs. A number of programs are available which predict the cyclic sorption performance of systems which employ adsorbent materials such as molecular sieves. Two such programs have been developed by AiResearch (Reference 1). However, there are certain differences in the sorption behavior between solid amines and adsorbents; these differences do not permit the use of the existing programs in analyzing amine absorbent systems. One of the differences is the manner in which sorbate molecules enter the sorbent material. In adsorption, the sorbate may flow deep into the pellet interior before being adsorbed. With absorption, it is most likely that sorbate molecules are absorbed by chemical reaction first at the pellet outer surface; later, additional absorption occurs within the pellet after sorbate molecules have diffused through the spent sorbent material.

Another difference between amine CO_2 absorption processes and those of adsorption is the simultaneous coabsorption of CO_2, water, and possibly some minor quantities of O_2 and N_2. With solid amines, the coabsorption of CO_2 and water is very pronounced and must be accounted for quite accurately. In adsorption processes, (e.g. molecular sieves) there is of course coadsorption, but it is of such a nature that certain simplifying approximations are allowable.

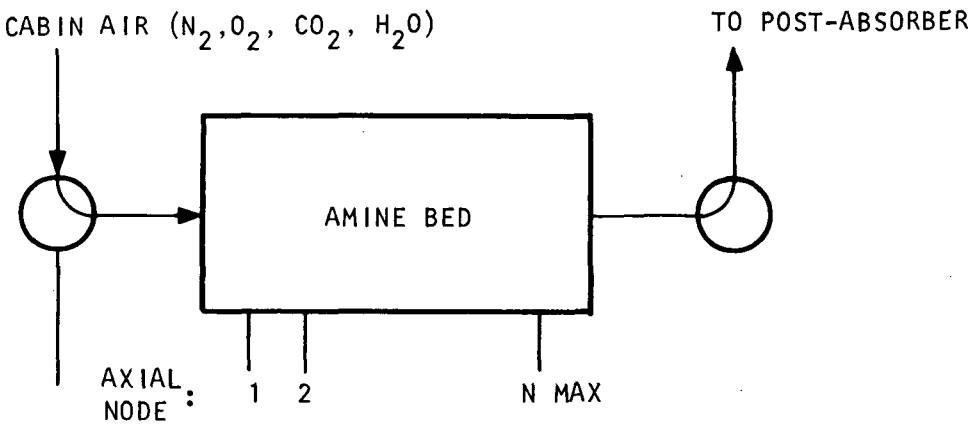

(a) ABSORPTION PERIOD

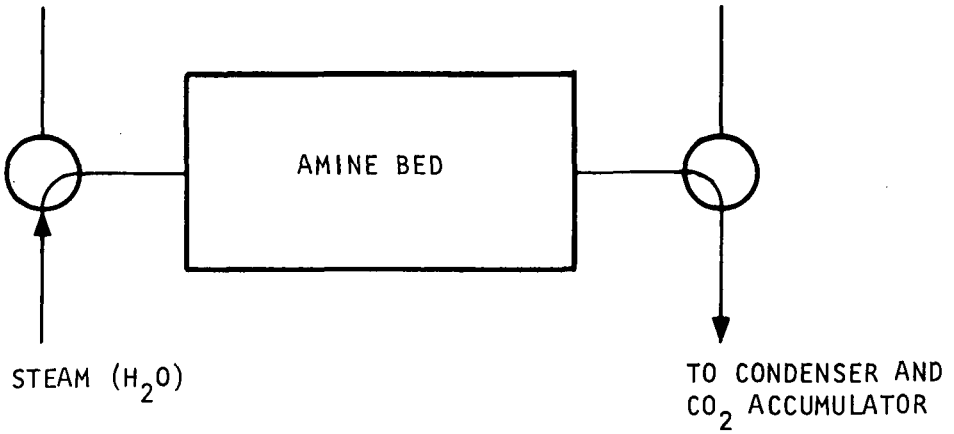

(b) DESORPTION PERIOD

S-77223

Figure A-1. An Amine System for CO_2-Removal

There is another quite significant difference in amine CO_2-removal systems. This involves the regeneration of the material by steam stripping. The stripping operation actually resembles a chromatographic separation process, with steam acting as the eluent. During the regeneration, flow rates and chemical composition of gas streams vary greatly in time throughout the bed. This requires an accurate detailed analytical technique.

The program as presented in this report is set up explicitly for the amine resin, Amberlite IR-45. Data describing this material was derived from the studies of Task 3.1 of this contract. Other sorbent materials can be used with the entry of the appropriate data.

The program has been checked out on a Univac 1108 system which employs Fortran V.

GENERAL DESCRIPTION

The overall structure of the program is shown by the logic diagram given as Figure A-2. As is shown by the diagram, the only input data read in by the program are those belonging to the NAMELIST INPUT. It should be noted that equilibrium isotherms of CO_2, H_2O, and N_2 over IR-45, which are required by the program are already in subroutine EQAMN; these data must be changed if a different sorbent is to be considered.

A subroutine called ABSORB is used for both absorption and desorption cycles, as the steam stripping operation is simply a reverse of an absorption process. The implicit solution method used in the subroutine can handle either case equally well.

The subroutine ABSORB computes volumetric flow rate at each time step and integrates energy and material balance equations simultaneously to advance one time step. An implicit scheme is used to keep the time step size reasonably large without developing numerical instabilities.

TECHNICAL DESCRIPTION

Differential equations describing absorber behavior are given below. These equations are numerically solved by the program.

Momentum Balance

Mass flow rate is calculated by solving the Ergun equation for G_o:

$$G_o^2 + \frac{150}{1.75}\frac{(1-e)\mu}{D_p}G_o - \frac{\rho D_p}{1.75}\left(\frac{-\Delta P}{\Delta x}\right)\left(\frac{e^3}{1-e}\right) = 0 \qquad (1)$$

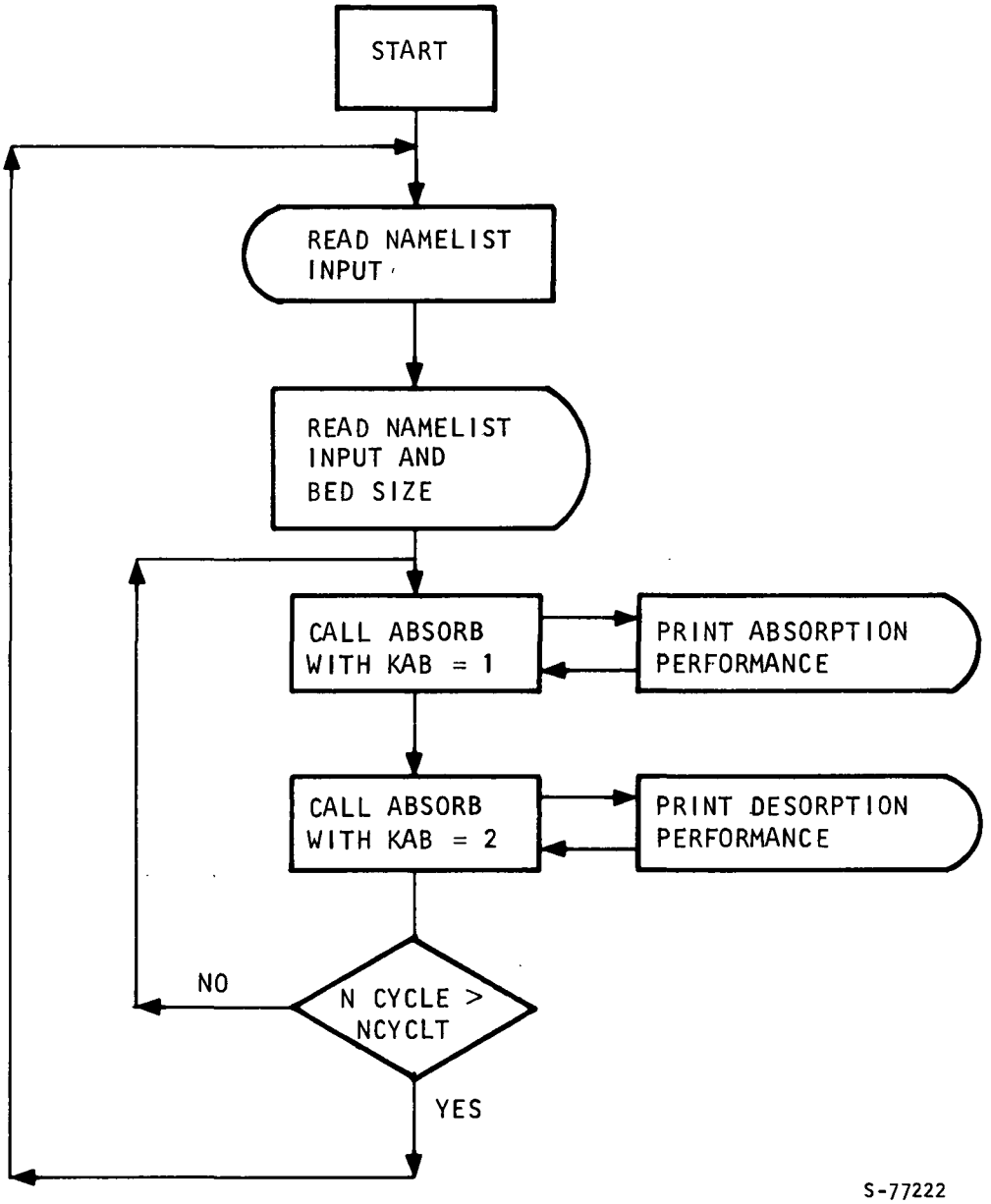

Figure A-2. Logic Diagram for AMINE Transient Absorption Performance Prediction Program

Total Pressure Equation

As pressure response is much more rapid than temperature or concentration changes, a quasi-steady state approach is taken for pressure computation. At steady state, the pressure equation is

$$\frac{e\ P_N}{a_{sg}\ (\Delta x)^2\ F\ R\ T_g} \left\{ P_{N-1} - 2\ P_N + P_{N+1} \right\} = \sum_k K_{n,k} \left\{ P_N X_{N,k} - p^*_{N,k} \right\} \quad (2)$$

subject to the boundary conditions that the inlet flow rate and the outlet pressure are specified.

Material Balance Equations

For the sorbent phase, the equation is

$$\rho_{sb} \cdot \frac{\partial W_k}{\partial t} = K_k\ a_{sg}\ (p_k - p_k^*) \quad (3)$$

For the gas phase, a quasi-steady-state equation shown below is used:

$$\frac{V}{R\ T_g}\ \frac{dp_k}{dx} = a_s\ a_{sg}\ K_k\ (p_k^* - p_k)\ ,\ k = 1 \text{ to } k_{max} \quad (4)$$

Energy Equations

For the sorbent:

$$\rho sb\ C_{p,s}\ \frac{\partial T_s}{\partial t} = a_{sg} \cdot h_{sg}\ (T_g - T_s) + a_{sg} \cdot \sum_k K_k\ (p_k - p_k^*)\ (\Delta H)_k + \frac{\partial}{\partial x} \left(a_s\ K_s\ \frac{\partial T_s}{\partial x} \right) \quad (5)$$

For the process gas stream

$$\frac{-V}{R \cdot T_g} \cdot \frac{dT_g}{dx} = a_s \cdot a_{sg} \cdot h_{sg} \cdot (T_s - T_g) \quad (6)$$

Equilibrium Isotherms

The equilibrium data shown in Figure A-3 for IR-45/CO_2 and Figure A-4 for IR-45/H_2O are built into subroutine EQAMN. Effects of water on the CO_2 absorption capacity of IR-45 were obtained from Figure A-3 and plotted as Figure A-5; those data are also stored in the subroutine.

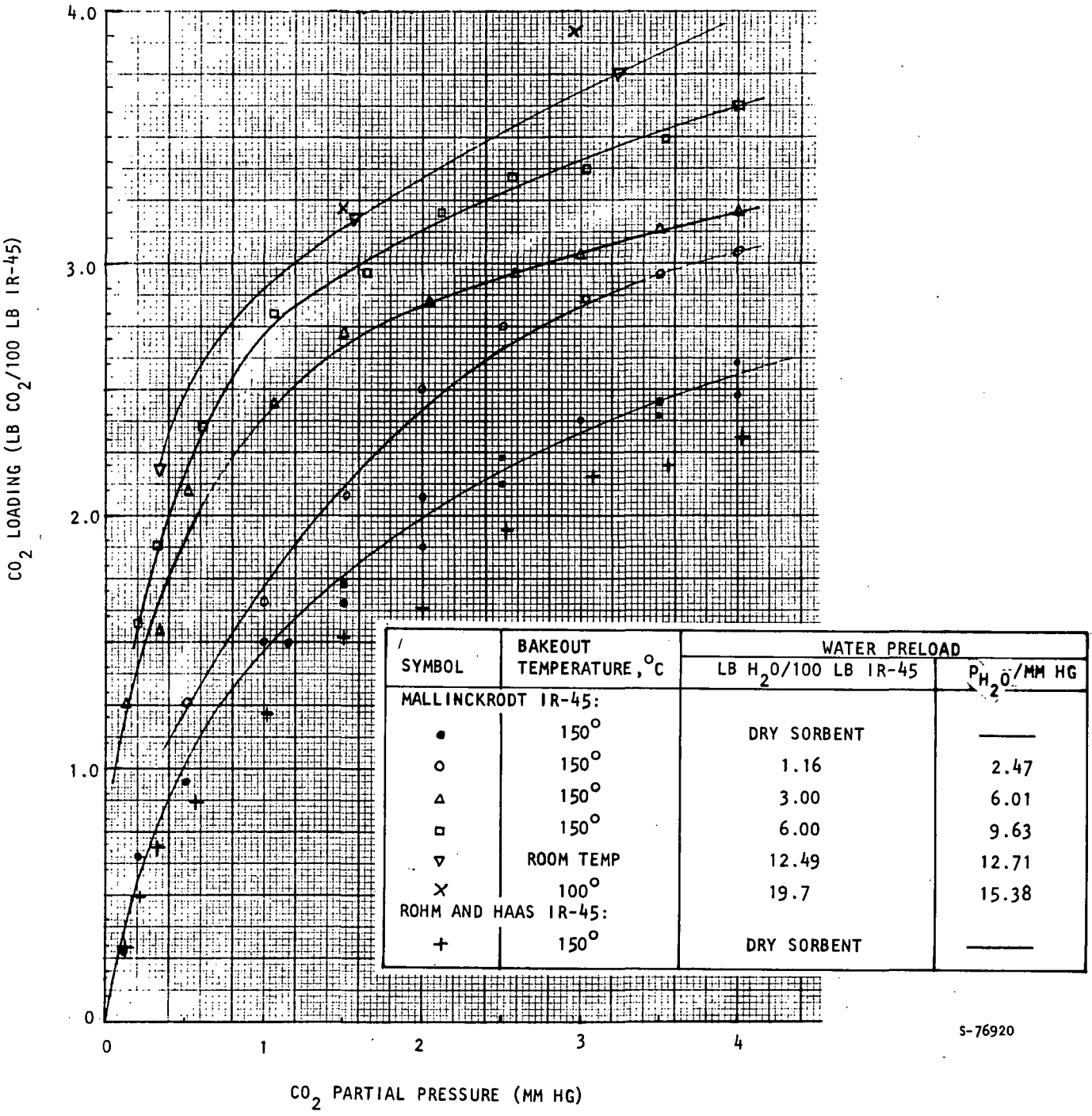

SYMBOL	BAKEOUT TEMPERATURE, °C	WATER PRELOAD LB H_2O/100 LB IR-45	WATER PRELOAD P_{H_2O}/MM HG
MALLINCKRODT IR-45:			
●	150°	DRY SORBENT	——
○	150°	1.16	2.47
△	150°	3.00	6.01
□	150°	6.00	9.63
▽	ROOM TEMP	12.49	12.71
×	100°	19.7	15.38
ROHM AND HAAS IR-45:			
+	150°	DRY SORBENT	——

Figure A-3. Equilibrium Absorption Capacity of IR-45 for CO_2, Parametric with Water Preload, 75°F Sorbent Temperature.

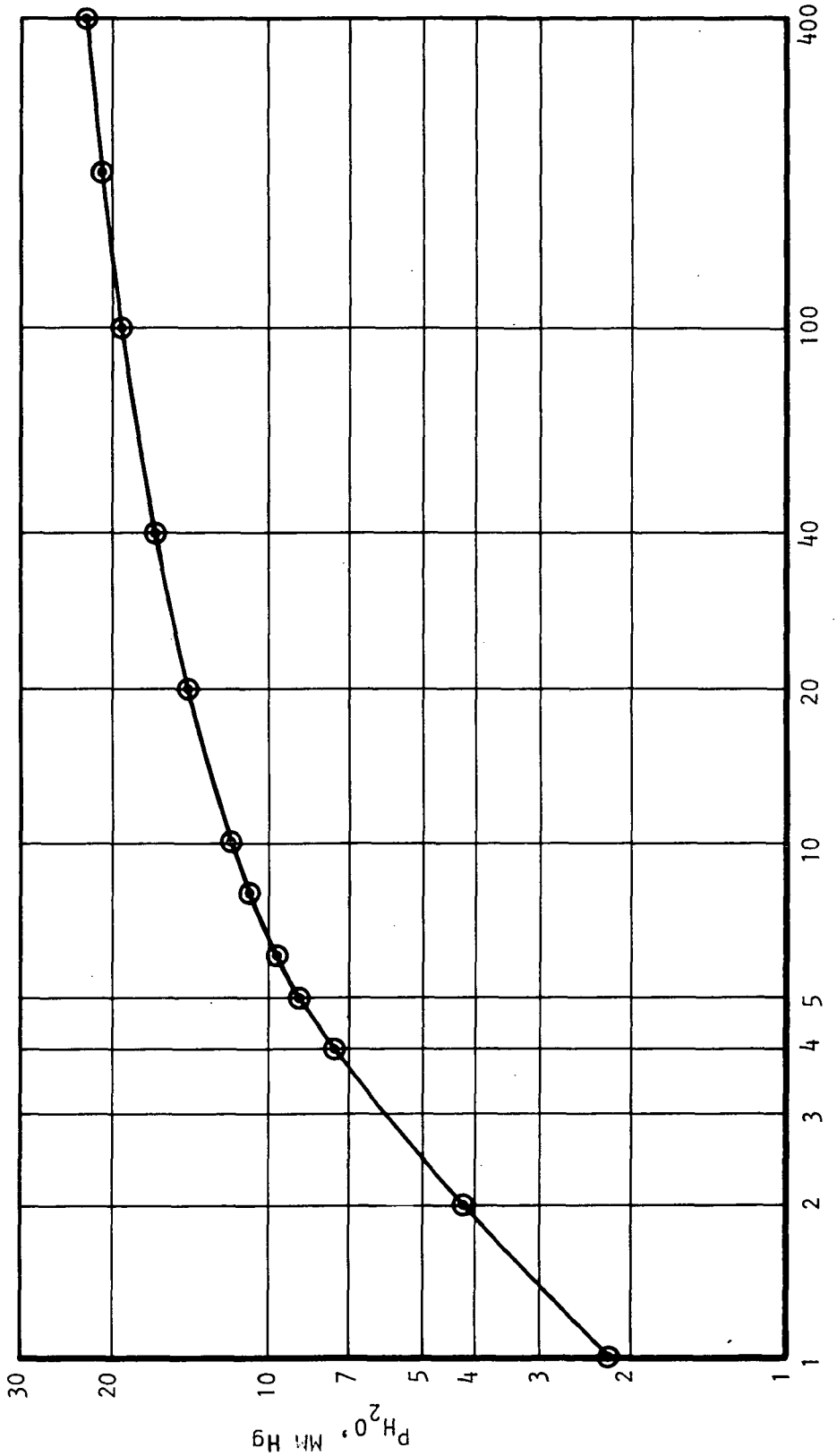

Figure A-4. IR-45/H_2O Equilibria (75°F)

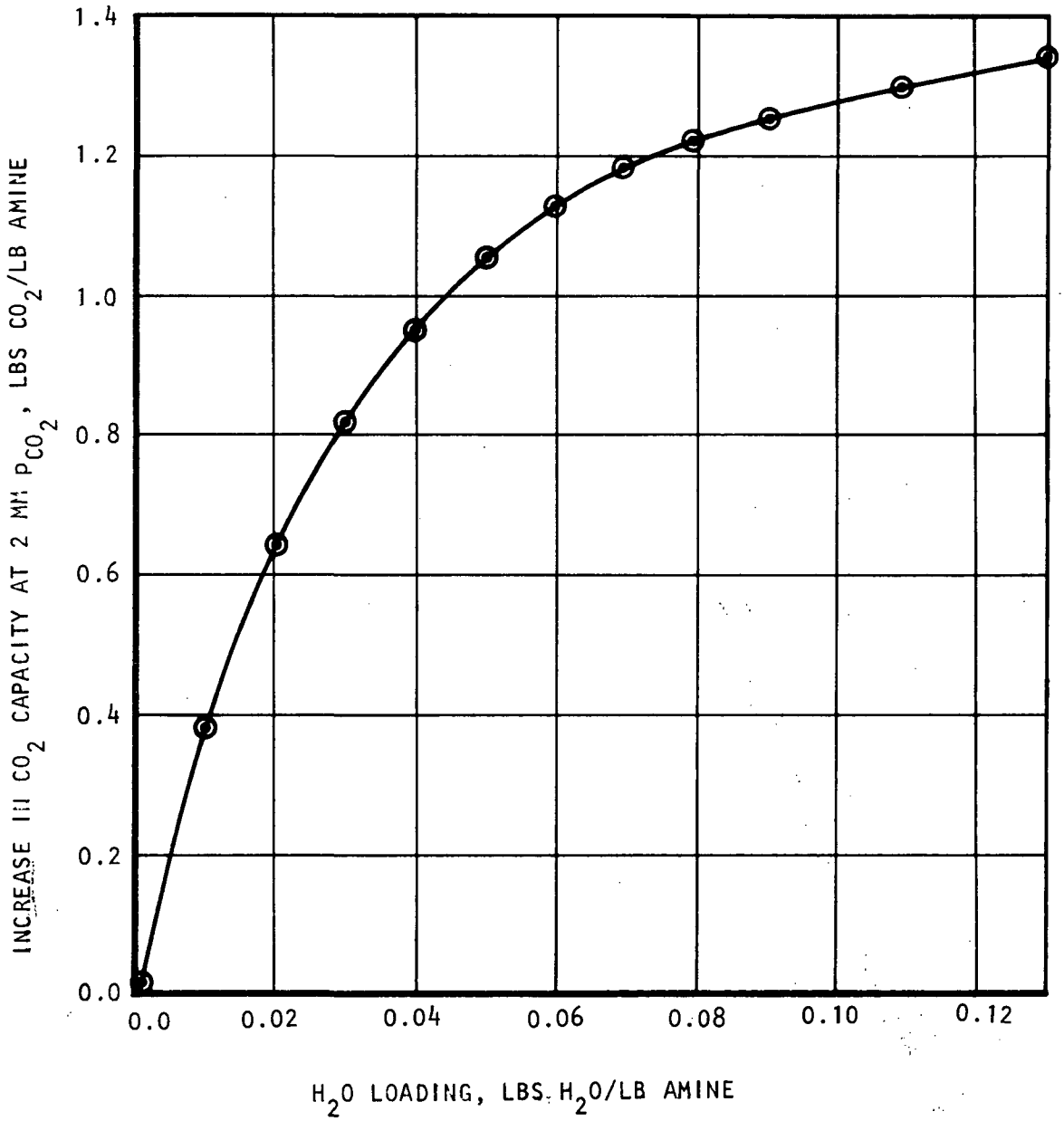

Figure A-5. Effects of Water on Saturation Capacity for CO_2

S-77219

Data for IR-45/N_2 were made up arbitrarily, as no experimental data were available.

Diffusion Model for the Interior of Sorbent

For the diffusion of sorbates through the interior of the sorbent particles, a simplified approach is employed. In this approach, an effective mass-transfer coefficient is used to represent the overall resistance between the process gas stream and the sorbent. The coefficient is allowed to vary, depending on how far each sorbate has to diffuse through the solid phase. This distance is determined from the fractional saturation of the sorbate of interest at the moment. The mass-transfer coefficient is, therefore, expressed as

$$K_k = \frac{1}{R_1 + R_2}$$

where R_1 is the resistance due to the stagnant surface film, and R_2 is due to the fact that at the moment, a layer of thickness ℓ, has been exhausted as far as sorbate k is concerned. The model is depicted in Figure A-6. The fraction of the total volume of sorbent still unused is assumed to be the same as the fraction of the initial capacity still remaining at the moment.

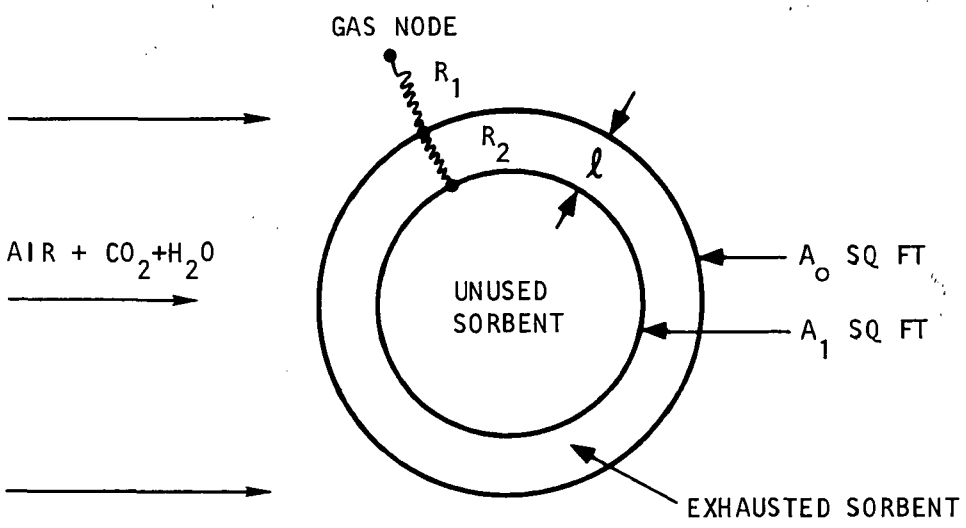

Figure A-6. Model for Internal Diffusion

Method of Solution

As all of the equations listed above are coupled, any implicit method of solution should solve all the equations simultaneously. Otherwise the solution may not be stable. No scheme has yet been found which solves all the equations simultaneously and implicitly. However, a method was devised whereby equations (3) to (6) are simultaneously and implicitly solved. This is achieved by expressing ΔW_k, Δp_k, ΔT_g, (k=1 to k_{max}) as functions of ΔT_s and first solving for T_s, then substituting back to obtain W_k, p_k and T_g.

PROGRAM INPUT

All input data are contained in one NAMELIST called INPUT, which are read in at the beginning of a run. These input variables are listed and defined below.

Symbol	Max. No. of Elements	Definition
AS	20	Cross-sectional area of packed bed for each axial node, sq ft
DX	20	Length of each axial increment, ft
CPL	10	Heat capacity of each component (10 components allowed) in liquid state, Btu/lb-^{o}F
CPSDRY	20	Heat capacity of dry sorbent at each node, Btu/lb-^{o}F
DH	10	Heat of absorption of each component, Btu/lb
DP	20	Effective particle diameter at each node, ft
HSG	20	Heat-transfer coefficient between sorbent and gas at each node, Btu/hr-(sq ft)-^{o}F
KMAX	1	Total number of components in the gas mixture
KS	20	Effective thermal conductivity of sorbent bed, Btu/hr-ft-^{o}F
NMAX	1	No. of axial nodes
RHOG	20	Initial gas density at each node, which are modified later by the program, lb/(cu ft)
RHOSB	20	Packed density of sorbent, lb(cu ft)
TS	20	Initial sorbent temperature, ^{o}F

Symbol	Max. No. of Elements	Definition
VISCG	20	Gas viscosity, lbm/hr-ft
WK	20,10	Initial loading of various sorbates on sorbent, the first subscript being axial index, the second being sorbate index, (lb sorbate)/(lb sorbent)
MW	10	Molecular weights of sorbates
RHOS	20	Sorbent particle density, lb/(cu ft)
PGC	2	Bed outlet pressures during absorption and desorption periods, mm Hg
TGI	2	Inlet gas temperature for absorption and desorption periods, ^{o}F
DTMAX	1	Maximum time increment size, hr
CYCLE	2	Lengths of absorption and desorption periods, hr
NPRINT	1	No. of time steps between printouts
CPK	10	Molal heat capacities of sorbates, Btu/(lb-mole)-^{o}F
PKI	10, 2	Inlet partial pressures of sorbates, the first index identifying the sorbate, the second one indicating the period, mm Hg
NCYCLT	1	No. of absorption and desorption cycles for which performance of the bed is desired
VFI	2	Inlet gas flow rate for the absorption and the desorption period, (cu ft)/hr
DWK	10	Approximate loading change of each sorbate in one absorption/desorption period, (lb sorbate)/(lb sorbent)
DIF	10	Mass diffusivity of sorbate through the interior of sorbent, (lb-mole)/hr-ft-(mm Hg)
GFK	1	Mass-transfer coefficient for sorbent surface film, (lb mole)/hr-(sq ft) (mm Hg)
WI	1	Maximum loading change allowable per time step in selecting time increment sizes, (lb sorbate)/(lb sorbent)
TI	1	Maximum temperature change allowable per time step in selecting time increment sizes, ^{o}F

Component Index	Component
1	CO_2
2	water
3	N_2

PROGRAM OUTPUT

The first output from the program is the input data, which have been read in under the NAMELIST INPUT. The standard format setup by the computer system for a NAMELIST output is used. All the input variables are, therefore, printed for checkout purposes. The list of data is of course identical to that given in the previous section. After the input data, the program gives total weight of the sorbent in the bed as computed from the input data.

Absorption bed performance data are printed next, followed by the data for the desorption period. The same formats are used for both cases. Cycle number is first printed, then the time from the start of the cycle, and the current time step size are printed. For each axial node, p_{CO_2}, p_{H_2O}, gas temperature, sorbent temperature, CO_2 loading, H_2O loading, volumetric gas flow rate and the total pressure are printed. Inlet gas conditions precede the above data, and the average CO_2 and H_2O loadings on the sorbent are also printed. Finally, a time average CO_2 absorption/desorption rate is given.

EXAMPLE RUN

As an example of program usage, the program was run to simulate actual breakthrough data which were presented as Figure 3-8 of this report. The bed used in the test contained 379 gms of dry IR-45, and the operating conditions were: total pressure 363 mm Hg, temperature 75°F, inlet dew point 50°F, and process gas flow rate 2.3 lb/hr (or 67 cfh).

The input data used in making the run are shown in Table A-1. Printouts of absorption and desorption periods are shown in Tables A-2 and A-3. Figure A-7 compares the breakthrough curve obtained by the program with the one obtained experimentally. The fit is generally excellent.

TABLE A-1

INPUT DATA

```
$INPUT
AS     = .62500000-01, .62500000-01, .62500000-01, .62500000-01,
         .62500000-01, .62500000-01, .62500000-01, .62500000-01,
         .62500000-01, .62500000-01, .62500000-01, .62500000-01,
         .62500000-01, .62500000-01, .62500000-01, .62500000-01,
         .62500000-01, .62500000-01, .62500000-01, .62500000-01,
ASX    = .00000000+00, .00000000+00, .00000000+00, .00000000+00,
         .00000000+00, .00000000+00, .00000000+00, .00000000+00,
         .00000000+00, .00000000+00, .00000000+00, .00000000+00,
         .00000000+00, .00000000+00, .00000000+00, .00000000+00,
         .00000000+00, .00000000+00, .00000000+00, .00000000+00,
AX     = .00000000+00, .00000000+00, .00000000+00, .00000000+00,
         .00000000+00, .00000000+00, .00000000+00, .00000000+00,
         .00000000+00, .00000000+00, .00000000+00, .00000000+00,
         .00000000+00, .00000000+00, .00000000+00, .00000000+00,
         .00000000+00, .00000000+00, .00000000+00, .00000000+00,
AXG    = .00000000+00, .00000000+00, .00000000+00, .00000000+00,
         .00000000+00, .00000000+00, .00000000+00, .00000000+00,
         .00000000+00, .00000000+00, .00000000+00, .00000000+00,
         .00000000+00, .00000000+00, .00000000+00, .00000000+00,
         .00000000+00, .00000000+00, .00000000+00, .00000000+00,
CPGM   = .24000000+00, .24000000+00, .24000000+00, .24000000+00,
         .24000000+00, .24000000+00, .24000000+00, .24000000+00,
         .24000000+00, .24000000+00, .24000000+00, .24000000+00,
         .24000000+00, .24000000+00, .24000000+00, .24000000+00,
         .24000000+00, .24000000+00, .24000000+00, .24000000+00,
CPS    = .10000000+11, .10000000+11, .10000000+11, .10000000+11,
         .10000000+11, .10000000+11, .10000000+11, .10000000+11,
         .10000000+11, .10000000+11, .10000000+11, .10000000+11,
         .10000000+11, .10000000+11, .10000000+11, .10000000+11,
         .10000000+11, .10000000+11, .10000000+11, .10000000+11,
CPX    = .00000000+00, .00000000+00, .00000000+00, .00000000+00,
         .00000000+00, .00000000+00, .00000000+00, .00000000+00,
         .00000000+00, .00000000+00, .00000000+00, .00000000+00,
         .00000000+00, .00000000+00, .00000000+00, .00000000+00,
         .00000000+00, .00000000+00, .00000000+00, .00000000+00,
DH     = .40000000+03, .10500000+04, .10000000-02, .10000000-02,
         .10000000-02, .10000000-02, .10000000-02, .10000000-02,
         .10000000-02, .10000000-02,
DP     = .22900000-02, .22900000-02, .22900000-02, .22900000-02,
         .22900000-02, .22900000-02, .22900000-02, .22900000-02,
         .22900000-02, .22900000-02, .22900000-02, .22900000-02,
         .22900000-02, .22900000-02, .22900000-02, .22900000-02,
         .22900000-02, .22900000-02, .22900000-02, .22900000-02,
DX     = .49999999-01, .49999999-01, .49999999-01, .49999999-01,
         .49999999-01, .49999999-01, .49999999-01, .49999999-01,
         .49999999-01, .49999999-01, .49999999-01, .49999999-01,
         .49999999-01, .49999999-01, .49999999-01, .49999999-01,
         .49999999-01, .49999999-01, .49999999-01, .49999999-01,
FVUID  = .00000000+00, .00000000+00, .00000000+00, .00000000+00,
         .00000000+00, .00000000+00, .00000000+00, .00000000+00,
         .00000000+00, .00000000+00, .00000000+00, .00000000+00,
         .00000000+00, .00000000+00, .00000000+00, .00000000+00,
         .00000000+00, .00000000+00, .00000000+00, .00000000+00,
HSG    = .20000000+02, .20000000+02, .20000000+02, .20000000+02,
         .20000000+02, .20000000+02, .20000000+02, .20000000+02,
         .20000000+02, .20000000+02, .20000000+02, .20000000+02,
         .20000000+02, .20000000+02, .20000000+02, .20000000+02,
         .20000000+02, .20000000+02, .20000000+02, .20000000+02,
HSX    = .00000000+00, .00000000+00, .00000000+00, .00000000+00,
```

TABLE A-1 (Continued)

		.00000000+00,	.00000000+00,	.00000000+00,	.00000000+00,
		.00000000+00,	.00000000+00,	.00000000+00,	.00000000+00,
		.00000000+00,	.00000000+00,	.00000000+00,	.00000000+00,
		.00000000+00,	.00000000+00,	.00000000+00,	.00000000+00,
HXG	=	.00000000+00,	.00000000+00,	.00000000+00,	.00000000+00,
		.00000000+00,	.00000000+00,	.00000000+00,	.00000000+00,
		.00000000+00,	.00000000+00,	.00000000+00,	.00000000+00,
		.00000000+00,	.00000000+00,	.00000000+00,	.00000000+00,
		.00000000+00,	.00000000+00,	.00000000+00,	.00000000+00,
KG	=	.20000000-03,	.20000000-03,	.20000000-03,	.20000000-03,
		.20000000-03,	.20000000-03,	.20000000-03,	.20000000-03,
		.20000000-03,	.20000000-03,	.20000000-03,	.20000000-03,
		.20000000-03,	.20000000-03,	.20000000-03,	.20000000-03,
		.20000000-03,	.20000000-03,	.20000000-03,	.20000000-03,
		.10000000-02,	.10000000-02,	.10000000-02,	.10000000-02,
		.10000000-02,	.10000000-02,	.10000000-02,	.10000000-02,
		.10000000-02,	.10000000-02,	.10000000-02,	.10000000-02,
		.10000000-02,	.10000000-02,	.10000000-02,	.10000000-02,
		.10000000-02,	.10000000-02,	.10000000-02,	.10000000-02,
		.20000000-03,	.20000000-03,	.20000000-03,	.20000000-03,
		.20000000-03,	.20000000-03,	.20000000-03,	.20000000-03,
		.20000000-03,	.20000000-03,	.20000000-03,	.20000000-03,
		.20000000-03,	.20000000-03,	.20000000-03,	.20000000-03,
		.20000000-03,	.20000000-03,	.20000000-03,	.20000000-03,
		.00000000+00,	.00000000+00,	.00000000+00,	.00000000+00,
		.00000000+00,	.00000000+00,	.00000000+00,	.00000000+00,
		.00000000+00,	.00000000+00,	.00000000+00,	.00000000+00,
		.00000000+00,	.00000000+00,	.00000000+00,	.00000000+00,
		.00000000+00,	.00000000+00,	.00000000+00,	.00000000+00,
		.00000000+00,	.00000000+00,	.00000000+00,	.00000000+00,
		.00000000+00,	.00000000+00,	.00000000+00,	.00000000+00,
		.00000000+00,	.00000000+00,	.00000000+00,	.00000000+00,
		.00000000+00,	.00000000+00,	.00000000+00,	.00000000+00,
		.00000000+00,	.00000000+00,	.00000000+00,	.00000000+00,
		.00000000+00,	.00000000+00,	.00000000+00,	.00000000+00,
		.00000000+00,	.00000000+00,	.00000000+00,	.00000000+00,
		.00000000+00,	.00000000+00,	.00000000+00,	.00000000+00,
		.00000000+00,	.00000000+00,	.00000000+00,	.00000000+00,
		.00000000+00,	.00000000+00,	.00000000+00,	.00000000+00,
		.00000000+00,	.00000000+00,	.00000000+00,	.00000000+00,
		.00000000+00,	.00000000+00,	.00000000+00,	.00000000+00,
		.00000000+00,	.00000000+00,	.00000000+00,	.00000000+00,
		.00000000+00,	.00000000+00,	.00000000+00,	.00000000+00,
		.00000000+00,	.00000000+00,	.00000000+00,	.00000000+00,
		.00000000+00,	.00000000+00,	.00000000+00,	.00000000+00,
		.00000000+00,	.00000000+00,	.00000000+00,	.00000000+00,
		.00000000+00,	.00000000+00,	.00000000+00,	.00000000+00,
		.00000000+00,	.00000000+00,	.00000000+00,	.00000000+00,
		.00000000+00,	.00000000+00,	.00000000+00,	.00000000+00,
		.00000000+00,	.00000000+00,	.00000000+00,	.00000000+00,
		.00000000+00,	.00000000+00,	.00000000+00,	.00000000+00,
		.00000000+00,	.00000000+00,	.00000000+00,	.00000000+00,
		.00000000+00,	.00000000+00,	.00000000+00,	.00000000+00,
		.00000000+00,	.00000000+00,	.00000000+00,	.00000000+00,
		.00000000+00,	.00000000+00,	.00000000+00,	.00000000+00,
		.00000000+00,	.00000000+00,	.00000000+00,	.00000000+00,
		.00000000+00,	.00000000+00,	.00000000+00,	.00000000+00,
		.00000000+00,	.00000000+00,	.00000000+00,	.00000000+00,
		.00000000+00,	.00000000+00,	.00000000+00,	.00000000+00,
KMAX	=	3,			

TABLE A-1 (Continued)

```
KS     =  .99999998-01,  .99999998-01,  .99999998-01,  .99999998-01,
          .99999998-01,  .99999998-01,  .99999998-01,  .99999998-01,
          .99999998-01,  .99999998-01,  .99999998-01,  .99999998-01,
          .99999998-01,  .99999998-01,  .99999998-01,  .99999998-01,
          .99999998-01,  .99999998-01,  .99999998-01,  .99999998-01,
KY     =  .00000000+00,  .00000000+00,  .00000000+00,  .00000000+00,
          .00000000+00,  .00000000+00,  .00000000+00,  .00000000+00,
          .00000000+00,  .00000000+00,  .00000000+00,  .00000000+00,
          .00000000+00,  .00000000+00,  .00000000+00,  .00000000+00,
          .00000000+00,  .00000000+00,  .00000000+00,  .00000000+00,
NMAX   =                10.
PG     =  .35000000+03,  .35000000+03,  .35000000+03,  .35000000+03,
          .35000000+03,  .35000000+03,  .35000000+03,  .35000000+03,
          .35000000+03,  .35000000+03,  .35000000+03,  .35000000+03,
          .35000000+03,  .35000000+03,  .35000000+03,  .35000000+03,
          .35000000+03,  .35000000+03,  .35000000+03,  .35000000+03,
RHOG   =  .27000000-01,  .27000000-01,  .27000000-01,  .27000000-01,
          .27000000-01,  .27000000-01,  .27000000-01,  .27000000-01,
          .27000000-01,  .27000000-01,  .27000000-01,  .27000000-01,
          .27000000-01,  .27000000-01,  .27000000-01,  .27000000-01,
          .27000000-01,  .27000000-01,  .27000000-01,  .27000000-01,
RHOSB  =  .26700000+02,  .26700000+02,  .26700000+02,  .26700000+02,
          .26700000+02,  .26700000+02,  .26700000+02,  .26700000+02,
          .26700000+02,  .26700000+02,  .26700000+02,  .26700000+02,
          .26700000+02,  .26700000+02,  .26700000+02,  .26700000+02,
          .26700000+02,  .26700000+02,  .26700000+02,  .26700000+02,
RHOX   =  .00000000+00,  .00000000+00,  .00000000+00,  .00000000+00,
          .00000000+00,  .00000000+00,  .00000000+00,  .00000000+00,
          .00000000+00,  .00000000+00,  .00000000+00,  .00000000+00,
          .00000000+00,  .00000000+00,  .00000000+00,  .00000000+00,
          .00000000+00,  .00000000+00,  .00000000+00,  .00000000+00,
TG     =  .00000000+00,  .00000000+00,  .00000000+00,  .00000000+00,
          .00000000+00,  .00000000+00,  .00000000+00,  .00000000+00,
          .00000000+00,  .00000000+00,  .00000000+00,  .00000000+00,
          .00000000+00,  .00000000+00,  .00000000+00,  .00000000+00,
          .00000000+00,  .00000000+00,  .00000000+00,  .00000000+00,
TS     =  .75000000+02,  .75000000+02,  .75000000+02,  .75000000+02,
          .75000000+02,  .75000000+02,  .75000000+02,  .75000000+02,
          .75000000+02,  .75000000+02,  .75000000+02,  .75000000+02,
          .75000000+02,  .75000000+02,  .75000000+02,  .75000000+02,
          .75000000+02,  .75000000+02,  .75000000+02,  .75000000+02,
TX     =  .00000000+00,  .00000000+00,  .00000000+00,  .00000000+00,
          .00000000+00,  .00000000+00,  .00000000+00,  .00000000+00,
          .00000000+00,  .00000000+00,  .00000000+00,  .00000000+00,
          .00000000+00,  .00000000+00,  .00000000+00,  .00000000+00,
          .00000000+00,  .00000000+00,  .00000000+00,  .00000000+00,
VISCG  =  .40000000+00,  .40000000+00,  .40000000+00,  .40000000+00,
          .40000000+00,  .40000000+00,  .40000000+00,  .40000000+00,
          .40000000+00,  .40000000+00,  .40000000+00,  .40000000+00,
          .40000000+00,  .40000000+00,  .40000000+00,  .40000000+00,
          .40000000+00,  .40000000+00,  .40000000+00,  .40000000+00,
WK     =  .99999998-04,  .99999998-04,  .99999998-04,  .99999998-04,
          .99999998-04,  .99999998-04,  .99999998-04,  .99999998-04,
          .99999998-04,  .99999998-04,  .99999998-04,  .99999998-04,
          .99999998-04,  .99999998-04,  .99999998-04,  .99999998-04,
          .13900000+00,  .13900000+00,  .13900000+00,  .13900000+00,
          .13900000+00,  .13900000+00,  .13900000+00,  .13900000+00,
          .13900000+00,  .13900000+00,  .13900000+00,  .13900000+00,
```

TABLE A-1 (Continued)

		.13900000+00,	.13900000+00,	.13900000+00,	.13900000+00,
		.99999998-04,	.99999998-04,	.99999998-04,	.99999998-04,
		.99999998-04,	.99999998-04,	.99999998-04,	.99999998-04,
		.99999998-04,	.99999998-04,	.99999998-04,	.99999998-04,
		.99999998-04,	.99999998-04,	.99999998-04,	.99999998-04,
		.99999998-04,	.99999998-04,	.99999998-04,	.99999998-04,
		.49999999-03,	.49999999-03,	.49999999-03,	.49999999-03,
		.49999999-03,	.49999999-03,	.49999999-03,	.49999999-03,
		.49999999-03,	.49999999-03,	.49999999-03,	.49999999-03,
		.49999999-03,	.49999999-03,	.49999999-03,	.49999999-03,
		.49999999-03,	.49999999-03,	.49999999-03,	.49999999-03,
		.49999999-03,	.49999999-03,	.49999999-03,	.49999999-03,
		.49999999-03,	.49999999-03,	.49999999-03,	.49999999-03,
		.49999999-03,	.49999999-03,	.49999999-03,	.49999999-03,
		.49999999-03,	.49999999-03,	.49999999-03,	.49999999-03,
		.49999999-03,	.49999999-03,	.49999999-03,	.49999999-03,
		.49999999-03,	.49999999-03,	.49999999-03,	.49999999-03,
		.49999999-03,	.49999999-03,	.49999999-03,	.49999999-03,
		.49999999-03,	.49999999-03,	.49999999-03,	.49999999-03,
		.49999999-03,	.49999999-03,	.49999999-03,	.49999999-03,
		.49999999-03,	.49999999-03,	.49999999-03,	.49999999-03,
		.49999999-03,	.49999999-03,	.49999999-03,	.49999999-03,
		.49999999-03,	.49999999-03,	.49999999-03,	.49999999-03,
		.49999999-03,	.49999999-03,	.49999999-03,	.49999999-03,
		.49999999-03,	.49999999-03,	.49999999-03,	.49999999-03,
		.49999999-03,	.49999999-03,	.49999999-03,	.49999999-03,
		.49999999-03,	.49999999-03,	.49999999-03,	.49999999-03,
		.49999999-03,	.49999999-03,	.49999999-03,	.49999999-03,
		.49999999-03,	.49999999-03,	.49999999-03,	.49999999-03,
		.49999999-03,	.49999999-03,	.49999999-03,	.49999999-03,
		.49999999-03,	.49999999-03,	.49999999-03,	.49999999-03,
		.49999999-03,	.49999999-03,	.49999999-03,	.49999999-03,
		.49999999-03,	.49999999-03,	.49999999-03,	.49999999-03,
		.49999999-03,	.49999999-03,	.49999999-03,	.49999999-03,
		.49999999-03,	.49999999-03,	.49999999-03,	.49999999-03,
		.49999999-03,	.49999999-03,	.49999999-03,	.49999999-03,
		.49999999-03,	.49999999-03,	.49999999-03,	.49999999-03,
		.49999999-03,	.49999999-03,	.49999999-03,	.49999999-03,
		.49999999-03,	.49999999-03,	.49999999-03,	.49999999-03,
		.49999999-03,	.49999999-03,	.49999999-03,	.49999999-03,
		.49999999-03,	.49999999-03,	.49999999-03,	.49999999-03,
MW	=	.44000000+02,	.18000000+02,	.29000000+02,	.00000000+00,
		.00000000+00,	.00000000+00,	.00000000+00,	.00000000+00,
		.00000000+00,	.00000000+00,		
RHOS	=	.64000000+02,	.64000000+02,	.64000000+02,	.64000000+02,
		.64000000+02,	.64000000+02,	.64000000+02,	.64000000+02,
		.64000000+02,	.64000000+02,	.64000000+02,	.64000000+02,
		.64000000+02,	.64000000+02,	.64000000+02,	.64000000+02,
		.64000000+02,	.64000000+02,	.64000000+02,	.64000000+02,
PGC	=	.36000000+03,			
VFIA	=	.50000000+02,			
PCO2I	=	.56000000+01,			
PH2OI	=	.76000000+03,			
TGI	=	.70000000+02,	.21200000+03,		
DTMAX	=	.25000000-02,			
CYCLE	=	.20000000+01,	.20000000+00,		
NPRINT	=	50,			
CPK	=	.10100000+02,	.90000000+01,	.71999999+01,	.00000000+00,
		.00000000+00,	.00000000+00,	.00000000+00,	.00000000+00,
		.00000000+00,	.00000000+00,		

TABLE A-1 (Continued)

```
 PRI     =    .68999999+01,    .92000000+01,    .34700000+03,    .00000000+00,
              .00000000+00,    .00000000+00,    .00000000+00,    .00000000+00,
              .00000000+00,    .00000000+00,    .00000000+00,    .76000000+03,
              .00000000+00,    .00000000+00,    .00000000+00,    .00000000+00,
              .00000000+00,    .00000000+00,    .00000000+00,    .00000000+00,
 NCYCLT  =                ,
 VFI     =    .67000000+02,    .20000000+02,
 TIME    =    .00000000+00,
 DT      =    .00000000+00,
 TOTCO2  =    .00000000+00,
 DWR     =    .25000000-01,    .11999999+00,    .10000000-02,    .00000000+00,
              .00000000+00,    .00000000+00,    .00000000+00,    .00000000+00,
              .00000000+00,    .00000000+00,
 DIF     =    .74999998-09,    .25000000-08,    .74999998-09,    .69999998-09,
              .69999996-09,    .69999998-09,    .69999998-09,    .69999998-09,
              .69999998-09,    .69999998-09,
 GKF     =    .20000000-04,
 WI      =    .99999998-04,
 II      =    .50000000+00,
 $END
```

TOTAL WEIGHT OF ABSORBER IN LBS = .8344

TABLE A-2

ABSORPTION CYCLE PRINT OUT

ABSORPTION CYCLE 1
TIME = .143 HR OR 9.6 MIN DT = .00250

AXIAL NODE	PCO2,MM	PH2O,MM	GAS TEMP DEG F	SORBENT TEMP,F	CO2 LOADING,LB/LB	H2O LOADING,LB/LB	VOL FLOW RATE,CFH	TOT PRESS MM
INLET	6.90	9.20	70.0				67.00	365.10
1	6.65	9.94	75.0	75.0	.0103	.1328	67.41	364.73
2	6.37	10.51	75.0	75.0	.0099	.1340	67.56	364.26
3	6.06	10.97	75.0	75.0	.0095	.1350	67.68	363.79
4	5.79	11.34	75.0	75.0	.0091	.1358	67.79	363.32
5	5.50	11.64	75.0	75.0	.0086	.1365	67.88	362.84
6	5.21	11.88	75.0	75.0	.0082	.1370	67.97	362.37
7	4.92	12.08	75.0	75.0	.0078	.1374	68.04	361.90
8	4.63	12.23	75.0	75.0	.0073	.1377	68.11	361.42
9	4.34	12.35	75.0	75.0	.0069	.1380	68.17	360.95
10	4.05	12.45	75.0	75.0	.0065	.1382	68.22	360.48
AVG					.0084	.1362		

TIME AVG CO2 ABSORPTION = .0425 LB/HR (NODE 10 IS OUTLET)

TABLE A-3

DESORPTION CYCLE PRINT OUT

DESORPTION CYCLE 1
TIME = .022 HR OR 1.3 MIN DT = .00004

AXIAL NODE	PCO2,MM	PH2O,MM	GAS TEMP DEG F	SORBENT TEMP,F	CO2 LOADING,LB/LB	H2O LOADING,LB/LB	VOL FLOW RATE,CFH	TOT PRESS MM
INLET	.00	760.00	212.0				20.00	760.00
1	.19	352.44	75.8	75.0	.0238	.1516	28.98	360.38
2	.35	345.82	75.1	75.0	.0239	.1538	23.95	360.18
3	.50	339.81	75.1	75.0	.0239	.1465	17.28	360.01
4	.67	319.74	75.1	75.0	.0239	.1360	8.70	359.89
5	.68	141.86	75.0	75.0	.0238	.1185	.46	359.83
6	.55	35.45	75.0	75.0	.0237	.1135	.20	359.83
7	.69	22.46	75.0	75.0	.0236	.1153	.20	359.87
8	.54	12.54	75.0	75.0	.0236	.1178	.20	359.91
9	.47	11.17	75.0	75.0	.0235	.1203	.20	359.91
10	.55	13.53	75.0	75.0	.0234	.1225	.20	359.95
AVG					.0237	.1296		

TIME AVG CO2 DESORPTION = -.0011 LB/HR (NODE 10 IS OUTLET)

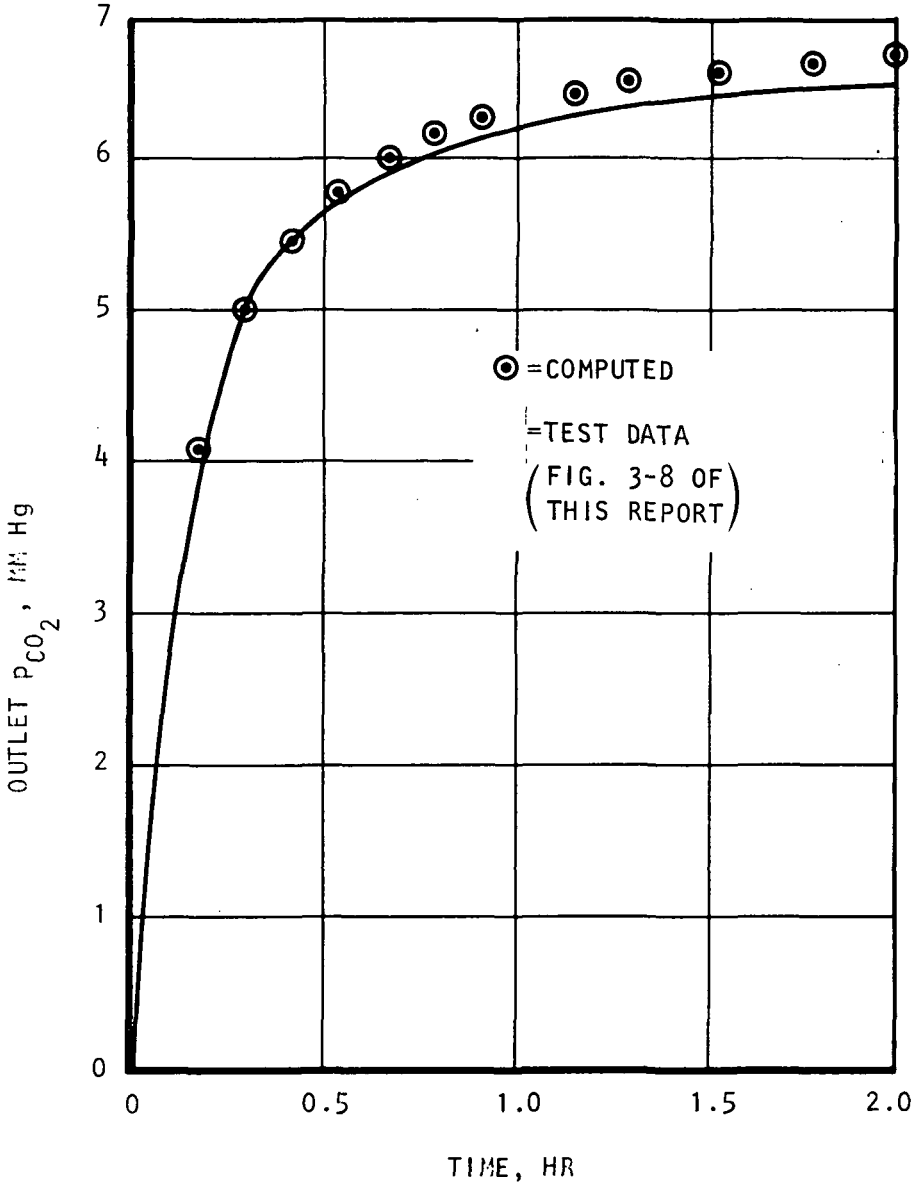

Figure A-7. Comparison of Computed Breakthrough Curve with Test Data

S-77218

APPENDIX B

AMINE FORTRAN V LISTINGS

```
@ FLT AMTNF,1,721117, 33083     , 1

000001                  COMMON /AMD/
000002                 1AS(20),AX(20),ASG(20),PGI,     AXG(20),TGT(2),PKI(10,2),CYCLE(2),
000003                 2DY(20),PG(20),PG1(20),PG2(20),PS(20),VFI(2), FS(20),
000004                 3PS1(20),PS2(20),PK(20,10),PK1(20,10),
000005                 4PK2(20,10),PKS(20,10),PKS1(20,10),PKS2(20,10),
000006                 5TS(20),TS1(20),TS2(20),TX(20),TX1(20),
000007                 6TX2(20),TG(20),CPSDRY(20),CPL(10),
000008                 7TG1(20),TG2(20),         RHOS(20),
000009                 8RHOSB(20),RHOX(20),KS(20),KX(20),
000010                 9DH(10),CPS(20),CPX(20),CPGM(20),
000011                 1KG(20,10),F(20),FVOID(20),MW(10),WK(20,10), XS(20,10), MWG(20),
000012                 2HSG(20),         HXG(20),
000013                 3SCON(20),XCON(20),         VF(20),
000014                 4DP(20),VISCG(20),ASX(20),HSX(20),                  WK1(20,10),
000015                 5WK2(20,10),FCON(20),RHOG(20),X(20,10)
000016                 1,VFRT(20),         CPK(10),C1P(20),C2P(20),C3P(20),D4P(20),VFS(20)
000017                 2,C1PK(10),C2PK(10),C1WK(10),C2WK(10),C3WK(10),DWK(10),DTF(10)
000018                 3,WKO(20,10),PGC(2),VFTA,TIME,DT,TOTCO2
000019                  DOUBLE PRECISION C1P,C2P,C3P,D4P
000020           C
000021                  REAL KG,KS,   MW,MWG
000022                  EQUIVALENCE(WTSORB, WTAB)
000023                  NAMELIST/INPUT/     AS,DX,         CPL,         CPGM,CPSDRY, DH,
000024                 1DP,          HSG,                KMAX,KS,    NMAX,
000025                 2RHOG,RHOSB,                  TS,   VISCG,   WK,MW,RHOS,
000026                 3PGC ,                  TGI,DTMAX,CYCLE,NPRINT,CPK,PKI,NCYCLT,VFI
000027                 4                ,DWK,DTF,GKF,WT,TI
000028           C
000029           C
000030                  DATA R/554.0/
000031            9999 CONTINUE
000032                  READ(5,INPUT)
000033                  WRITE(6,INPUT)
000034                  NMAX1=NMAX+1
000035                  NMAX2=NMAX+2
000036                  DO 2 N=1,20
000037                2 ASG(N)=6.*RHOSB(N)/RHOS(N)/DP(N)
000038           C
000039           C      TOTAL ABSORBENT WEIGHT
000040                  WTAB=0.000
000041                  DO 500 N=2,NMAX1
000042              500 WTAB=WTAB+AS(N)*DY(N)*RHOSB(N)
000043                  CALL PRSED
000044                  NCYCLE=1
000045              510 CONTINUE
000046                  KAB=1
000047                  CALL ABSORB
000048                  KAB=2
000049                  CALL ABSORB
000050                  NCYCLE=NCYCLE+1
000051                  IF(NCYCLE.GT.NCYCLT) GO TO 9999
000052                  GO TO 510
000053                  SUBROUTINE ABSORB
000054           C
000055           C          INITIALIZATION
000056           C
000057                  TIME = 0.0
000058                  DTI=DTMAX*0.50E-5
```

```
000059                DT=DTI
000060                NPR =0
000061                TOTCO2=0.0000
000062                DO 1 N=1, NMAX2
000063                EVOID(N)=1. - RHOSB(N)/RHOS(N)
000064                F(N)=.1E-3
000065                FS(N)=.1E-3
000066                TG(N)=TS(N)
000067                PG(N)=PGC(KAB)
000068                PG1(N)=PG(N)
000069                PG2(N)=PG(N)
000070                PS(N)=PG(N)
000071                PS1(N)=PS(N)
000072                PS2(N)=PS(N)
000073                TS1(N)=TS(N)
000074                TS2(N)=TS(N)
000075                TX1(N)=TX(N)
000076                TX2(N)=TX(N)
000077                TG1(N)=TG(N)
000078                TG2(N)=TG(N)
000079
000080                DO 1 K=1, KMAX
000081                CALL EQAMN(K,P,WK(N,K),TS(N),WK(N,2))
000082                PK(N,K)=P
000083                PK1(N,K)=P
000084                PK2(N,K)=P
000085                PKS(N,K)=P
000086                PKS1(N,K)=P
000087                PKS2(N,K)=P
000088                WK1(N,K)=WK(N,K)
000089                WK2(N,K)=WK(N,K)
000090                WK0(N,K)=WK(N,K)
000091              1 CONTINUE
000092                DO 5 N=1,NMAX1
000093                SCON(N)= 2./(DX(N)/(AS(N)*KS(N))+DX(N+1)/(AS(N+1)*KS(N+1)))
000094              5 CONTINUE
000095                PGI=0.00000
000096                DO 6 K=1,KMAX
000097                PK(1,K)=PKI(K,KAB)
000098                PGI=PGI+PKI(K,KAB)
000099              6 CONTINUE
000100                TG(1)=TGI(KAB)
000101          C
000102          C
000103                GO TO 1000
000104           8000 CALL PRINT
000105                NPR =0
000106          C
000107           1000 CONTINUE
000108                IF(TIME .LT. 10.*DTT) GO TO 61
000109          C    TO COMPUTE DT
000110                ADT=DTMAX
000111                DO 60 N=1,NMAX,4
000112                DO 60 K=1,KMAX
000113                ADT2=WI/(ABS(WK(N,K)-WK2(N,K))+1.E-9)*DT*2.0
000114                IF(ADT2.LT.ADT) ADT=ADT2
000115                ADT2=TI/(ABS(TS(N)-TS2(N))+1.E-9)*DT*2.0
000116                IF(ADT2.LT.ADT) ADT=ADT2
000117             60 CONTINUE
000118                DT=ADT
```

```
000119              61 CONTINUE
000120                 IF(TIME.GE.CYCLE(KAB))RETURN
000121                 IF((TTME+DT).GT.CYCLE(KAB)) DT = CYCLE(KAB)-TTME
000122                 TTME = TIME+DT
000123                 DO 10 N=1, NMAX2
000124                 PG2(N)=PG1(N)
000125                 PG1(N)=PG(N)
000126                 TS2(N)=TS1(N)
000127                 TS1(N)=TS(N)
000128                 TX2(N)=TX1(N)
000129                 TX1(N)=TX(N)
000130                 TG2(N)=TG1(N)
000131                 TG1(N)=TG(N)
000132                 VFS(N)=VF(N)
000133                 DO 10 K=1,KMAX
000134                 PK2(N,K)=PK1(N,K)
000135                 PK1(N,K)=PK(N,K)
000136                 WK2(N,K)=WK1(N,K)
000137                 WK1(N,K)=WK(N,K)
000138                 PKS2(N,K)=PKS1(N,K)
000139                 PKS1(N,K)=PKS(N,K)
000140                 XS(N,K)=X(N,K)
000141              10 CONTINUE
000142                 DO 3 N=1,NMAX2
000143                 V0=1.0/6.*3.14*DP(N)**3
000144                 R0=DP(N)/2.0
000145                 A0=4.0*3.14*R0**2
000146                 DO 3 K=1,KMAX
000147                 DW=ABS(WK(N,K)-WK0(N,K))
000148                 V=V0*ABS(DWK(K)-DW)/DWK(K)
000149                 IF(V.LT.1.E-20) V=1.E-20
000150                 RN=
000151                1  R0*(V/V0)**0.3333333
000152                 A1=4.0*3.14*RN**2
000153                 THS=R0-RN
000154                 R1=1.0/GKF
000155                 R2=1.0/DIF(K)*THS*(A0/A1)
000156                 KG(N,K)=1.0/(R1+R2)
000157               3 CONTINUE
000158                 DO 618 N=1,NMAX1
000159                 CPS(N)=CPSDPY(N)
000160                 DO 618 K=1,KMAX
000161                 CPS(N)=CPS(N)+WK(N,K)*CPL(K)
000162             618 CONTINUE
000163           C
000164           C      SIMULTANEOUS SOLUTION FOR TS, WK, TG, AND PK
000165           C
000166                 DO 50 N=2,NMAX1
000167                 CS1=AS(N)*DX(N)*RHOSB(N)*CPS(N)/DT
000168                 CS2=AS(N)*DX(N)*RHOSB(N)/DT
000169                 CS3=AS(N)*DX(N)*ASG(N)*HSG(N)
000170                 CS4=AS(N-1)*KS(N-1)/(DX(N-1)+DX(N))*2.0
000171                 CS5=AS(N)*KS(N)/(DX(N)+DX(N+1))*2.0
000172                 CS6=0.000
000173                 CS7=0.000000
000174                 C1=VFRT(N-1)
000175                 C2=VFRT(N)
000176                 C3=AS(N)*DX(N)*ASG(N)
000177                 C1TG=0.00
000178                 C2TG=0.00
```

```
000179                C3TG=AS(N)*DX(N)*ASG(N)*HSG(N)
000180                DO 51 K=1,KMAX
000181                PKS4=PKS1(N,K)
000182                CALL EQAMN( K,PKS5,(WK1(N,K)+0.001),TS1(N),WK1(N,2))
000183                DPKDWK=(PKS5-PKS4)/0.001
000184                CALL EQAMN(K, PKS6,WK1(N,K),(TS1(N)+0.010),WK1(N,2))
000185                DPKDTS=(PKS6-PKS4)/0.01
000186                C1PK(K)=C1*PK(N-1,K)/(C2+C3*KG(N,K))
000187                C2PK(K)=C3*KG(N,K)/(C2+C3*KG(N,K))
000188                C1WK(K)=RHOSB(N)/DT-MW(K)*KG(N,K)*ASG(N)*(C2PK(K)-1.)*DPKDWK
000189                C2WK(K)=MW(K)*KG(N,K)*ASG(N)*(C1PK(K)+(C2PK(K)-1.0)*PKS1(N,K))
000190                C3WK(K)=MW(K)*KG(N,K)*ASG(N)*(C2PK(K)-1.)*DPKDTS
000191                CS6=CS6+CS2*DH(K)*C3WK(K)/C1WK(K)
000192                CS7=CS7+CS2*DH(K)*C2WK(K)/C1WK(K)
000193                C1TG=C1TG+VFRT(N-1)*PK(N-1,K)*CPK(K)
000194                C2TG=C2TG+VFRT(N)*PK(N,K)*CPK(K)
000195             51 CONTINUE
000196                RH=TS1(N)*(CS1-CS6)+CS7+CS3*((C1TG*TG(N-1))/(C2TG+C3TG)+CS4*(TS1(N-
000197               11)-TS1(N))+CS5*(TS1(N+1)-TS1(N))
000198                HL=CS1-CS6-CS3*(C3TG/(C2TG+C3TG)-1.0)
000199                TS(N)=RH/HL
000200          C
000201                TG(N)=(C1TG*TG(N-1)+C3TG*TS(N))/(C2TG+C3TG)
000202                DIMENSION PTN(20)
000203                PTN(N)=0.000
000204                DO 52  K=1,KMAX
000205                WK(N,K)=WK1(N,K)+C2WK(K)/C1WK(K)+C3WK(K)/C1WK(K)/C1WK(K)*(TS(N)-
000206               1TS1(N))
000207                CALL EQAMN(K,PKS(N,K),WK(N,K),TS(N),WK(N,2))
000208                PK(N,K)=C1PK(K)+C2PK(K)*PKS(N,K)
000209                IF(PK(N,K).LT.0.00) PK(N,K)=0.00000
000210                PTN(N)=PTN(N)+PK(N,K)
000211             52 CONTINUE
000212                DO 50 K=1,KMAX
000213                X1=PK(N,K)/PTN(N)
000214                XS(N,K)=X(N,K)
000215                X(N,K)=X1
000216                X(N,K)=0.50*(X(N,K)+XS(N,K))
000217             50 CONTINUE
000218          C
000219          C
000220          C          TOTAL PRESSURE
000221          C
000222                DIMENSION CP1(20)
000223                DIMENSION PGS(20)
000224                DO 19 N=1,NMAX1
000225                PGAV=PG(N)
000226                PGS(N)=PG(N)
000227                CP1(N)=FVOID(N)/(ASG(N)*DX(N)**2*F(N)*R*(TG(N)+460.))*PGAV
000228             19 CONTINUE
000229                CP1(1)=CP1(2)
000230                DO 20 N=2, NMAX1
000231                C2=0.0
000232                C4=0.0
000233                DO 21 K=1,KMAX
000234                C2=C2+KG(N,K)*X(N,K)
000235                C4=C4+KG(N,K)*PKS(N,K)
000236             21 CONTINUE
000237                C1P(N-1)=CP1(N-1)
000238                C3P(N-1)=CP1(N)
```

```
000239                C2P(N-1)=-C1P(N-1)-C3P(N-1)-C2
000240                D4P(N-1)=-C4
000241             20 CONTINUE
000242                C2P(1)=C2P(1)+C1P(1)
000243                VFIA=VFT(KAB)
000244                D4P(1)=D4P(1)-VFIA/FCON(2)*C1P(1)*(TG(2)+460.)/(TG(1)+460.)
000245               1*PGI/PG(2)
000246                C1P(1)=0.000
000247                D4P(NMAX)=D4P(NMAX)-C3P(NMAX)*PGC(KAB)
000248                C3P(NMAX)=0.000
000249                CALL FDEQIM(C1P,C2P,C3P,D4P,PG(2),NMAX)
000250                PG(NMAX2)=PGC(KAB)
000251                DO 22 N=1, NMAX1
000252             22 PG(N)=0.50*(PG(N)+PGS(N))
000253          C
000254          C
000255                DO 11 N=1,NMAX1
000256                MWG(N)=0.00000
000257                DO 12 K=1,KMAX
000258             12 MWG(N)=MWG(N)+MW(K)*X(N,K)
000259                RHOG(N) =PG(N)*MWG(N)/(R*(TG(N)+460.))
000260                B=(75./1.75)*(1.-FVOID(N))*VISCG(N)/DP(N)
000261                C=      (PG(N)-PG(N+1))*RHOG(N)*DP(N)*FVOID(N)**3/(1.75*DX(N)*(1.-
000262               1FVOID(N)))*32.2*14.7*144.*3600.*3600./760.
000263                IF(C.LT.0.) C=0.00000
000264                GO= -B+SQRT(B*B+C)
000265                VFS(N)=VF(N)
000266                VF(N)=GO/RHOG(N)*AS(N)
000267                IF(VF(N).LT. 0.000) VF(N)=VFI(KAB)*1.E-2
000268                U=VF(N)/AS(N)/FVOID(N)
000269                FS(N)=F(N)
000270                F(N)=760./(32.2*144.*14.7*3600.**2)/FVOID(N)**2
000271               1                                              *(1.-FVOID(N))/DP(N)*
000272               2(VISCG(N)*
000273               3 150.0*(1.-FVOID(N))/DP(N)+1.75*RHOG(N)*U*FVOID(N))
000274                FCON(N)= AS(N)*FVOID(N)/(DX(N)*F(N))
000275                IF(N.EQ.1) VF(1)=VFT(KAB)
000276             11 CONTINUE
000277                DO 70 N=1,NMAX1
000278                VFRT(N)=VF(N)/(R*(TG (N)+460.))
000279             70 CONTINUE
000280          C
000281          C
000282                TOTCO2=TOTCO2+DT*(VFRT(1)*PK(1,1)-VFRT(NMAX1)*PK(NMAX1,1))*44.000
000283                NPR=NPR+1
000284                IF(NPR.GE.NPRINT) GO TO 8000
000285                IF(TIME.GE. CYCLE(KAB)) GO TO 8000
000286                GO TO 1000
000287                SUBROUTINE PRINT
000288                TIMEM=60.*TIME
000289                DIMENSION CAPT1(3,2),CAPT2(5,2)
000290                DATA (CAPT1(L,1),L=1,3)/18H1ABSORPTION CYCLE                    /
000291                DATA (CAPT1(L,2),L=1,3)/18H1DESORPTION CYCLE                    /
000292                DATA (CAPT2(L,1),L=1,5)/30H0TIME AVG CO2 ABSORPTION =           /
000293                DATA (CAPT2(L,2),L=1,5)/30H0TIME AVG CO2 DESORPTION =           /
000294                WRITE(6,900)(CAPT1(KP,KAB),KP=1,3),NCYCLE,TIME,TIMEM,DT
000295             900 FORMAT(3A6,T5                          /' TIME ='F7.3,' HR    OR
000296               1'F7.1' MIN'7X'DT ='F7.5//' AXIAL'2X'PCO2,MM'2X'PH2O,MM'2X'GAS TEMP
000297               2'2X'SORBENT'2X'CO2 LOAD='2X'H2O LOAD='2X'VOL FLOW'2X'TOT PRESS'/
000298               3                                                  ' NODE'22X
```

```
000299                4)DEG F14X'TEMP,F13X'ING,LB/LB12X'ING,LB/LB12X'RATE,CFM14X'MM')
000300                 WRITE(6,901)PK(1,1),PK(1,2),TG(1),VFIA,PGT
000301               901 FORMAT(1H0'INLET'F8.2,F10.2,F8.1,30X,F12.2,F11.2/)
000302                 DO 902 N=2,NMAX1
000303                 NODE=N-1
000304               902 WRITE(6,903) NODE,
000305                1                PK(N,1),PK(N,2),TG(N),TS(N),WK(N,1),WK(N,2),VF(N)
000306                2,PG(N)
000307               903 FORMAT(I4,F10.2,F10.2,F8.1,F10.1,F10.4,F10.4,F12.2,F11.2)
000308                 AVGCO2=0.
000309                 AVGH2O=0.
000310                 DO 9031 N=2,NMAX1
000311                 AVGCO2=AVGCO2+AS(N)*DX(N)*RHOSB(N)*WK(N,1)
000312                 AVGH2O=AVGH2O+AS(N)*DX(N)*RHOSB(N)*WK(N,2)
000313              9031 CONTINUE
000314                 AVGCO2=AVGCO2/WTSORB
000315                 AVGH2O=AVGH2O/WTSORB
000316                 WRITE(6,904)AVGCO2,AVGH2O
000317               904 FORMAT(1H0'AVG'38X,2F10.4)
000318                 AVRCO2=TOTCO2/TIME
000319                 WRITE(6,905)(CAPT2(KP,KAB),KP=1,5),AVRCO2,NMAX
000320               905 FORMAT(5A6,                          F10.4' LB/HR',6X,
000321                1 16X,'(NODE'I3,' IS OUTLET)')
000322                 RETURN
000323                 SUBROUTINE PRBED
000324                 WRITE(6,906)WTAB
000325               906 FORMAT(1H1///' TOTAL WEIGHT OF ABSORBER IN LBS =' G10.4)
000326                 RETURN
000327                 END
```

```
      * FLT FQAMN,1,730213, 59417     , 1

000001                SUBROUTINE FQAMN(K,P,W,T,WH2O)
000002          C  K=1,  CO2
000003          C  K=2,  H2O
000004          C  K=3,  N2
000005                DIMENSION WTAB(12,10),PTAB(12,10), WH2OT(12), DWCO2T(12),DER(10)
000006               1,TTAB(10)
000007                DATA TTAB(1)/75.0/
000008                DATA (WTAB(I,1),I=1,12)/0.0, .00250,.005,.0075,.010,.0125,
000009               1.015,.0175,
000010               1.020,.0225, .025,.0275/
000011                DATA (PTAB(I,1),I=1,12)/0.0, .08,.17,.31,.49,.72,1.05,1.48,2.02,
000012               12.74,3.72,5.05/
000013                DATA TTAB(2)/75.0/
000014                DATA (WTAB(I,2),I=1,12)/.00, .02, .04, .05,.06, .08,.10,.20,.40,
000015               11.00,2.00,4.00/
000016                DATA (PTAB(I,2),I=1,12)/.000,4.16,6.72,8.69,9.60, 10.9,
000017               1                                                  11.9,14.3,16.5,
000018               119.1, 20.8, 22.5/
000019                DATA (WTAB(I,3),I=1,12)/.00000,.50E-4,.48E-4,.95E-4,1.3E-4,1.6E-4,
000020               12.1E-4,2.5E-4,3.0E-4,3.4E-4,4.0E-4,.40/
000021                DATA (PTAB(I,3),I=1,12)/0.0,50.,70.,100.,150.,200.,300.,400.,500.,
000022               1600.,750., 50000./
000023          C
000024                DATA WH2OT/0.0, .01, .02, .03, .04, .05, .06, .07, .08, .09, .11,
000025               1.13/
000026                DATA DWCO2T/0.0, .0038, .0064, .0082, .00955, .01055, .0113,
000027               1.0118, .0122, .0125, .0130, .0134/
000028                DATA (DER(I),I=1,3)/ 3*1.E4/
000029                IF(W.LT.1.E-10) W=1.E-10
000030                IF(K.EQ.1) CALL LAGIN2(116,WH2OT,12,2.WH2O,DWCO2,DWCO2T)
000031                WE=W
000032                IF(K.EQ.1) WE=W-DWCO2
000033                IF(WE.LT.1.E-10) WE=1.E-10                                    *NEW
000034                CALL LAGIN2(29,WTAB(1,K),12,2,WE,PLSET,PTAB(1,K))             **-1
000035                IF(PLSET.LT.1.E-6) PLSET=1.E-6
000036                PL=ALOG(PLSET)+DER(K)*(1./(TTAB(K)+460.0)-1./(T+460.0))
000037                P=EXP(PL)
000038                RETURN
000039                END
```

```
* FLT FDFQTM.1.721024, 55228    , 1

000001                  SUBROUTINE FDFQTM(C1,C2,C3,D,VAR,NN)
000002                  DIMENSION C1(1),C2(1),C3(1),D(1),VAR(1),B(30),Q(30)
000003                  DOUBLE PRECISION C1,C2,C3,D,B,Q
000004                  NN1=NN-1
000005                  B(1)=C3(1)/C2(1)
000006                  DO 41 J=2,NN1
000007               41 B(J)=C3(J)/(C2(J)-C1(J)*B(J-1))
000008                  Q(1)=D(1)/C2(1)
000009                  DO 42 J=2,NN
000010               42 Q(J)=(D(J)-C1(J)*Q(J-1))/(C2(J)-C1(J)*B(J-1))
000011                  VAR(NN)=Q(NN)
000012                  DO 43 J=2,NN
000013                  L=NN+1-J
000014               43 VAR(L)=Q(L)-B(L)*VAR(L+1)
000015                  RETURN
000016                  END
```

```
* FLT LAGIN2.1.721024, 55229    , 1

000001                  SUBROUTINE  LAGIN2(ID,X,NP,ND,XO,YO,Y)
000002            C     REVISED FOR FORTRAN IV 8-8-65  S. WONG
000003                  DIMENSION  X(2),  Y(2)
000004            C
000005                  ILO=1
000006                  IF(XO-X(1))10,16,4
000007                4 IF(XO-X(NP))19,13,7
000008                7 ILO=NP-1
000009               10 IHI=ILO+1
000010                  WRITE (6,1) ID,XO
000011                  GO TO 46
000012               13 ILO=NP
000013               16 YO=Y(ILO)
000014                  RETURN
000015               19 DO 22 ILO=2,NP
000016                  IF(XO-X(ILO))25,16,22
000017               22 CONTINUE
000018               25 IHI=ILO
000019                  ILO=IHI-1
000020                  IF(ND-2)46,46,28
000021               28 DO 43 I=3,ND
000022                  IF(ILO-1)40,40,31
000023               31 IF(IHI-NP)34,37,37
000024               34 IF (2.*XO-X(ILO-1)-X(IHI+1)) 37,37,40
000025               37 ILO=ILO-1
000026                  GO TO 43
000027               40 IHI=IHI+1
000028               43 CONTINUE
000029               46 YO=0.0
000030                  PN=1.0
000031                  DO 49 I=ILO,IHI
000032               49 PN=PN*(XO-X(I))
000033                  DO 58 I=ILO,IHI
000034                  P=PN/(XO-X(I))
000035                  DO 55 J=ILO,IHI
000036                  IF(J-I)52,55,52
000037               52 P=P/(Y(I)-X(J))
000038               55 CONTINUE
000039                  YO=YO+P*Y(I)
000040               58 CONTINUE
000041                  RETURN
000042                1 FORMAT (97X,7HLAGIN2 ,I4,E12.5)
000043                  END
```

REFERENCES

1. K. C. Hwang, A Transient Performance Method for CO_2 Removal with Regenerable Adsorbents, NASA CR-12098 (AiResearch Report 72-8786), October 1972, AiResearch Mfg. Co., Los Angeles, California.

2. R. M. Wright, J. M. Ruder, V. B. Dunn, K. C. Hwang, Development of Design Information for Molecular-Sieve Type Regenerative CO_2-Removal Systems, AiResearch Report 72-8417, December 1972, AiResearch Mfg. Co., Los Angeles, California (will be published as a low-numbered NASA CR-report).

3. F. Tepper, F. Vancheri, W. Samuel, R. Vdavcak, Development of a Regenerable Carbon Dioxide Removal System, MSA Research Corporation, NASA Contractor Report No. 66571, Contract NAS1-5277, January 1968.

4. R. B. Martin, H. F. Brose, An Amine Polymer CO_2 Concentrator for the 90-day LRC/MDAC Manned Chamber Test, presented at NASA Langley Research Center, 1971.

5. J. F. Bertrand, H. F. Brose, F. L. Kester, P. J. Lunde, Investigations to Improve Carbon Dioxide Control with Amine and Molecular Sieve Type Sorbers, NASA CR-112021, Hamilton Standard Division of United Aircraft Corp., March 1972.